MODEL OF AIRFLOW IN UN- STRATIFIED CROSS-VENTILATED RECTANGULAR DOMAIN WITH OPENINGS ON VERTICAL WALLS

By

Muhammad Auwal Lawan

SPS/10/PMT/00001

B.Sc., M.Sc. MATHEMATICS (B.U.K)

THESIS SUBMITTED TO MATHEMATICS DEPARTMENT, BAYERO UNIVERSITY, KANO, IN PARTIAL FULFILLMENT OF THE REQUIREMENTS FOR THE AWARD OF THE DEGREE OF DOCTOR OF PHILOSOPHY IN MATHEMATICS

December, 2016

DECLARATION

I hereby declare that this work is the product of my research efforts undertaken under the supervision of Dr. Abdullahi Bichi Baffa and has not been presented anywhere for the award of a degree in any other University. However, information from other sources is duly acknowledged.

_____

Muhammad Auwal Lawan

SPS/10/PMT/00001

CERTIFICATION

This is to certify that the research work for this thesis entitled "**MODEL OF AIRFLOW IN UN- STRATIFIED CROSS- VENTILATED RECTANGULAR DOMAIN WITH OPENINGS ON VERTICAL WALLS**" by Muhammad Auwal Lawan with registration number (SPS/10/PMT/00001) were carried out under my supervision.

_____

Dr. Abdullahi Bichi Baffa

Supervisor

_____

Dr. Bashir Ali

Head of Department

APPROVAL

This thesis has been examined and approved for the award of Ph.D in (Mathematics).

_____

Professor Akintelu Folake O.

External Examiner

_____

Dr. Saminu Ilyasu Bala

Internal Examiner

_____

Dr. Abdullahi Bichi Baffa

Supervisor

_____

Dr. Bashir Ali

Head of Department

ACKNOWLEDGEMENT

All Praise is due to Allah the Lord of the universe, who gave me the opportunity to study the degree of Doctor of philosophy in Mathematics. Peace and blessings of Allah be upon his beloved servant, the noble prophet, Muhammad (S.A.W), his family members, his companions and all those that follow their foot path with right deeds to the last day.

This thesis is a product of various individuals' effort in different capacities. I would like to express my profound gratitude to my supervisor Dr. Abdullahi Bichi Baffa for his painstaking and inspiring guides in improving the quality of this study. My special thanks goes to Dr. Saminu I. Bala and Dr. Ibrahim Idris who despite their enormous engagement were able to spare time and guide me to the successful completion of this study.

I am highly grateful and indebted to the following people for their various contributions towards the successful completion of the thesis: Chairman SKY Technical and Construction Company Alh. Kabir Sani Kwangila, the Director H & M Construction Company Alh. Magaji Shehu, Prof. Muhammad Yahuza Bello, Prof. Bashir Maifada Yakasai, Dr. Abdul Iguda, Dr. Bashir Ali, Prof. Aisha Halliru and Dr. Aliyu Kiri.

I sincerely wish to express my gratitude to all my family, relations, friends and colleagues, who gave me moral support at one point or the other for the successful completion of this work.

My words of appreciation goes to all academics and non- academics staff of Kano University of Science and Technology, Wudil.

I am most grateful to my beloved Wives: Khadija Abdulhamid Musa Fagge and Naja'atu Ibrahim Sagagi. And also to my children: Muhammad, Khadija, and Zahra'u Muhammad Auwal for their prayers, patience and endurance during my ups and downs for the study.

DEDICATION

This thesis is dedicated to the Alhaji Lawan Musa Lawan Panshekara Families, who have been giving me un- ending love and absolute support through life.

TABLE OF CONTENTS

CHAPTER TWO

LITERATURE REVIEW

CHAPTER THREE

MODEL FORMULATION AND SOLUTION METHODS

CHAPTER FOUR

ANALYSES, RESULTS, DISCUSSION AND KEY INTERVENTIONS

CHAPTER FIVE

SUMMARY, CONCLUSION AND RECOMMENDATIONS

ABSTRACT

Natural ventilation of building provides improvement of internal comfort and air quality conditions leading to a significant reduction of cooling energy consumption. Design of natural ventilation systems for many types of building is based on buoyancy forces. However, external wind flow can have significant effects on buoyancy- driven natural ventilation. In the proposed study, model of airflow process in un- stratified cross- ventilated rectangular domain with openings on vertical walls was presented. The study considered a uniform interior temperature, the assumption has enabled the simplification of the calculation of air flow process in the building. One dimensional Navier- Stokes equations was utilized to model the airflow process in the domain, which were then nondimensionalised using some dimensionless parameters to reduced the equation to ordinary differential equations and then solved analytically by method of variation of parameters to obtained the solutions. The behavior of parameters in the solutions were accurately predicts the velocity and temperature profiles together with volumetric airflow and mass transfer. MATLAB Codes were written to describe the asymptotic behavior of the results. Various parameters of airflow process; such as effective thermal coefficient (θ_0), Prandtl number (Pr), and discharge coefficient (c_d) were used to determine the effect of changes of parameters to the overall flow distributions, and ascertain the best one for optimal natural ventilation.

In conclusion, it was then described that in order to maintain the effect of buoyancy forces in the domain envelope, approximation of reduced gravity were take into account. Study gives the Architectures and designers a luxury to consider several design options in a minimum amount of time. The position/ or location of the openings in the study give a more homogeneous temperature profiles in the domain envelopes in order to avoid overheating

therefore, the temperature profiles in the domains are within comfortable conditions. Therefore, the expected aim and objectives in the study were achieved.

LIST OF FIGURES

LIST OF TABLES

NOMENCLATURE

These are some of the nomenclatures used in the study

A, A_M, A_Y, A_C, A_W Total area of vertical vent (m^2)

A_l, A_u Lower and upper opening surface area $(1.4\ and\ 0.7m^2)$

A_{eff} Effective area of the vertical vent (m^2)

A_w Area of window openings (m^2)

A_t, A_b Areas of top and bottom openings (m^2)

A_2^*, A_3^* Dimensionless total area of openings in domain with two and three openings $(-)$

A_l^*, A_u^* Dimensionless area of lower and upper openings $(-)$

$C_{20}, C_{21}, C_{22}, C_{23}, C_{24}, C_{25}$ Arbitrary constants $(-)$

C_d Discharge coefficients $(-)$

c_p, c_{p_i} and c_{Pe} Specific heat capacity of air $(1006J/kgK)$

D Diameter of the vertical vent (m)

dc_p Difference air specific heat capacity between interior and exterior $(1006J/kgK)$

dp Mean static pressure difference across the openings $(kg/(m.s^2))$

dT Temperature of air difference between interior and exterior (K)

$d_1, d_2, f_1, f_2, j_1, j_2, i_1, i_2$ Roots of equations $(-)$

f Surface friction coefficient $(-)$

g Gravity acceleration $(10m/s^2)$

g' Reduced gravity (m/s^2)

H Vertical distance between lower and upper openings (m)

H_w Height of window opening (m)

h, x, Y_x Height of openings (m)

k Floor air temperature ratio $(-)$

L, T, Θ Length scale of the height of openings, time and temperature $(-)$

m, m_C, m_Y, m_w, m_M Mass transfer of air (kg/s)

m_2^*, m_3^* Dimensionless mass transfers in domain with two- and three- openings $(-)$

p Pressure along the component of constant width of openings $(kg/(m.s^2))$

p_e, p_i External and internal air pressure $(kg/(m.s^2))$

q_w, q_M Air heat transfer $(m^2.kg/s^2)$

Q, Q_C, Q_Y, Q_w, Q_M Volumetric airflow (kg/s)

Q_2^*, Q_3^* Dimensional volumetric airflows in domain with two- and three- openings $(-)$

Q_s, Q_w Volumetric airflow induced by wind and stack- driven effect (kg/s)

s, n Dummy variables $(-)$

$T_i, T_0, T_{in}, T_{out}, T_e$ Inside and outside temperature of air (K)

T_1, T_2 Zone 1 and zone 2 temperature of air (K)

T_a Mean average temperature of air (K)

T_f Floor air temperature (K)

u, u_m Velocity distributions of air (m/s)

U, U_{ref} Mean and reference wind speed (m/s)

U Dimensional air velocity profiles (m/s)

U^* Dimensionless air velocity profiles in domain with openings on vertical walls $(-)$

U_2^*, U_3^* Dimensionless air velocity profiles in domain with two- and three- openings $(-)$

U_{c_2}, U_{c_3} Complimentary solution for air velocity profiles $(-)$

U_{p_2}, U_{p_3} Particular solution for air velocity profiles $(-)$

v_0 Indirect air velocity of opposing flow (m/s)

v_i, v_O Velocity of air in zone 1 and zone 2 (m/s)

v_W, v_M, v_Y, v_C Velocity distributions of air (m/s)

V_1, V_2, V_3, V_4 Functions obtained from particular solutions $(-)$

W Width of the openings (m)

$W(y_1, y_2), W_1(y_3, y_4)$ Wroskians $(-)$

x_{wl}^*, x_{wu}^* Dimensionless width between lower and upper openings $(-)$

x_l, x_u Dimensional width between lower and upper openings (m)

x_w Dimensional width of the openings (m)

y Dimensional height of the openings (m)

y^* Dimensionless height of the openings $(-)$

y_l^*, y_u^* Dimensionless height between lower and upper openings $(-)$

y_l, y_u Dimensional height between lower and upper openings (m)

y_1, y_2, y_3, y_4 Functions obtained from complimentary solutions $(-)$

Y_N, z Neutral height of the openings (m)

Greek Symbols

α Thermal diffusivity (m^2/s)

κ Thermal conductivity $(W/m.K)$

μ Dynamic air viscosity coefficient $(1.72 \times 10^{-5} kg/m.s)$

Φ_v Viscous dissipation m^2

$\emptyset = T$ Temperature distributions (K)

Γ Thermal diffusion coefficient $(Kg/m.s)$

ν Kinematic viscosity (m^2/s)

β Thermal expansion coefficient (K^{-1})

ΔT Air temperature differences (K)

θ_0 Effective thermal coefficient (K)

$\Delta\theta$ Dimensional change of air temperature (K)

θ Dimensional temperature profiles across the openings (K)

θ^* Dimensionless temperature profiles across the openings in domain with openings on vertical walls $(-)$

θ_2^*, θ_3^* Dimensionless temperature profiles across the openings in domain with two and three openings $(-)$

$\Delta\rho$ Density difference of the air (kg/m^3)

ρ Density of the air (kg/m^3)

$\bar{\rho}$ Average density of the air (kg/m^3)

ρ_0 Constant density of air $(1.1849 kg/m^3)$

Dimensionless parameter

Pr Prandtl number $(-)$

Pe Peclet number $(-)$

Abbreviations

M	M. Santamouris
Y	Yougo Li
C	C. L. Chow
W	W. G. Brown
L	Lower
u	Upper
eff	Effective
w	Window or width
t	Top
b	Bottom
2	Two
3	Three
d	Discharge
i	Interior
e	Exterior
s	Stack- driven effect

w	Wind- driven effect
in	Interior
out	Outside
f	Floor
m	Mean
ref	Reference
o	Outside
wl	Width of lower
wu	Width of upper
N	Neutral
v	Viscosity

PUBLISHED/ ACCEPTED PAPERS

The following Papers have been published as a result of this research.

1. **A. L. Muhammad** and A. B. Baffa 2015. Airflow process across vertical vents induced by stack- driven effect with an opposing flow in one of the upper openings. International Journal of Computer Application (IJCA). Volume 123(1). 1- 8.
2. **A. L. Muhammad** and A. B. Baffa and M. Z. Ringim 2016. Investigation of stack-driven airflow through rectangular cross- ventilated building with two openings using analytic technique. International Journal of Computer Application (IJCA). Volume 141(6). 5- 11.
3. **A. L. Muhammad** and A. B. Baffa, and U. M. Dauda 2016. Transient airflow process across vertical vents induced by Stack- driven effect inside un- stratified cross- ventilated rectangular with an opposing flow in one of the upper opening. International Journal of Computer Application (IJCA). Volume 148(1). 4- 11.

The following Paper is also accepted for publication as a result of this research.

1. **A. L. Muhammad** and A. B. Baffa, M. Z. Ringim, and U. M. Dauda 2016. Transient investigation of Stack- driven airflow process through rectangular cross- ventilated building with two vents in the absence of opposing flow in the upper opening. International Journal of Computer Application (IJCA). Volume *(*). July 2016.

CHAPTER ONE

INTRODUCTION

1.0 Preamble

Generally, the study of air flow distributions in buildings is considered to be as a result of the knowledge of the exact air supply to a building. This is necessary to determine its thermal performance and the concentration of the indoor pollutants. The exchange of air can be achieved either by mechanical or natural ventilation (See appendix A.1.2). Exchanges between external and interior space of buildings caused by flows that are driven by wind or by temperature differences (stack- driven or buoyancy effect) are the foundation of natural ventilation process. Natural ventilation uses the freely available resources of the wind and thermal energy that is a result of solar and incidental heating of the building. Although these resources are free, they are difficult to control. The challenge is to provide the necessary control mechanisms to develop the required indoor air quality. To achieve this, it is necessary to understand the physics of ventilation. The main factors controlling indoor air quality are the air movement responsible for transporting both heat and pollutants and the building fabric, which influence the perceived temperature by radiative effects and by heat exchanges with the air (Linden, 1999).

However, natural ventilation is being pursued by humans, who are increasingly spending more time indoors, to extend the possibilities of living in uncongenial or squally conditions etc. The improvements of the quality of the interior space both in its attractiveness, spaciousness, luminosity and more importantly its proper natural ventilation are major concerns for designers of modern structures.

People spend 90% of their time and work in buildings. Building ventilation provides the require amount of fresh air into a buildings under specified weather and environmental conditions. The process includes supplying air to and removing it from enclosures, disturbing and circulating the air therein, or preventing indoor contamination. Maintaining the indoor thermal comfort for occupants imposes an energy load on building as illustrated in Figure 1.1(Tong Yang, 2004).

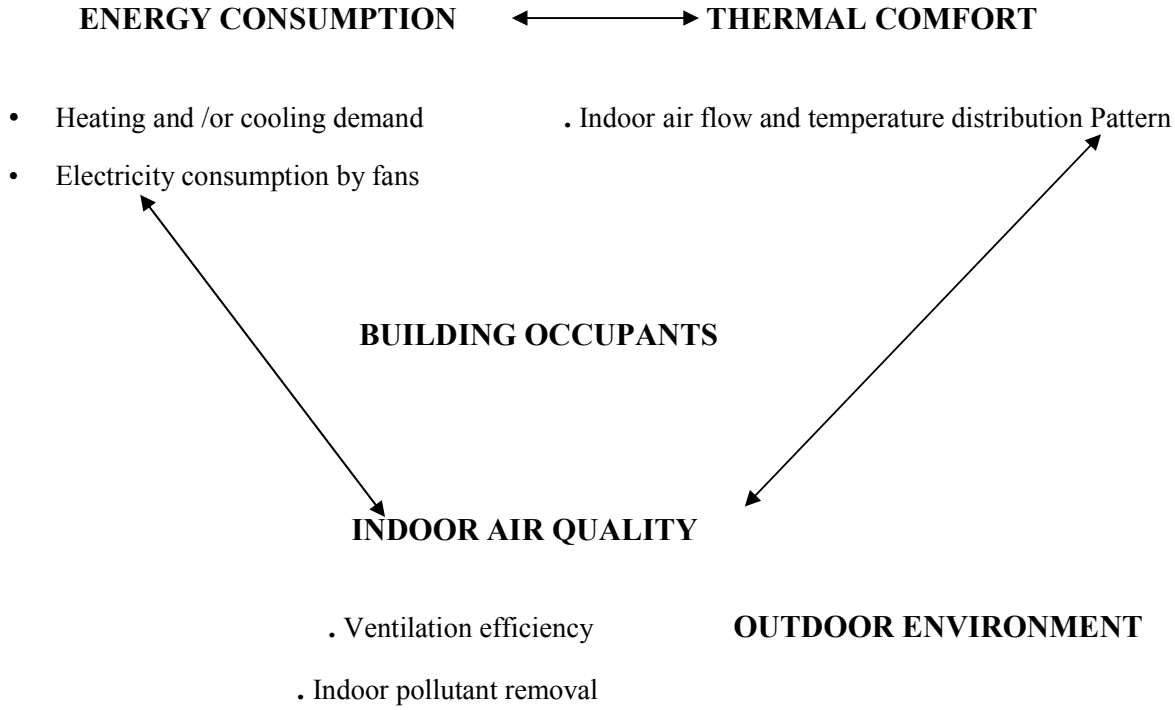

Figure 1.1: Pictorial representation of the relation between building occupants, building and the environment on natural ventilation process.

Knowledge of the physical laws describing natural convection through the multi-zones buildings is necessary to accurately predict the volumetric airflow (quantity of air supply/ in), mass-transfer (quantity of air removed/ out) and temperature distribution inside the various zones. The contribution of these considerations to the design of a domain is that knowing

these mechanisms, the dimensions and locations of the openings between the various zones can be designed in such away as to give a more homogeneous temperature distribution inside the building and therefore avoid overheating.

Air flow modeling gives Architectures and Engineers the luxury to consider several design options in the minimum amount of time. As a result, the final design is not based on a tentative approach but on a professional design process considering several options and selecting the best design. Air flow methods can be divided into two main categories, semi analytical and multi- zone methods. Semi analytical method is generally applied to simple geometry buildings, example, single- sided ventilation, including both wind- driven and stack- driven flows and one- zone buildings with two openings, including wind- driven, stack- driven and combined- driven flows, when the indoor temperature is known.

Air flow models are used to simulate the rates of incoming and outgoing air flows for a domain with known leakages under given weather and shielding conditions. In air flow two broad classes of models may be distinguished: macroscopic and microscopic models. Macroscopic models (e.g., multi- zone building methods) are based on physical idealizations of building systems as collections of control volumes whose behavior may be described by Bernoulli's equation or ordinary differential equations and microscopic models (e.g., computational fluid dynamics (CFD)) are based on numerically approximate solutions of systems of partial differential equations. The major application for macroscopic model type is on the single-family house with no internal partitions and for microscopic model type is normally applied to multi-zone structures, which also take internal partitions into account. Bernoulli's equation is mainly used by the simple analytic methods and the multi- zone methods.

In a recent study (Tong Yang, 2004) was presented that Gan Guohui (2010) described the approach with advantages and disadvantages of various methods for modeling air flow in the building, which are shown in Table 1.1,

Table 1.1 shows the advantages and disadvantages of various methods for modeling air flow in the building.

Approach		Advantages	Disadvantages
Theoretical	Macroscopic models (Multi-zone methods)	1. Simple, usually in formula or graphical form	1. Restricted to simple geometry 2. Assumptions are needed about the details of the flow to obtain simplified flow equations in the building.
	Microscopic models (e.g., computational fluid dynamics (CFD))	1. Predict flow field in details 2. Resolve flow future development with time	1. Numerical truncation error 2.Boundary condition problems 3. Assumptions about turbulence structure and near well treatment. 4. Computer cost. 5. Experience user costs.
Experiment		Capable of being most realistic.	1. Equipment required 2. Scaling problem 3. Tunnel correction. 4. Measuring difficulties. 5. Operating costs.

Considerable research efforts have been made on understanding the airflow process through openings in building envelopes. In the literature on airflow process, a wealth of information

is available and satisfactory means have been evolved for the estimation of the velocity distributions, volumetric airflow and mass transfer in buildings. Santamouris , Argiriou, Asimakopoulos, Klitsikas and Dounis 1995 studied heat and mass- transfer through an openings by natural convection in a single sided ventilated building, and Chow 2010 investigated volumetric airflow across vertical opening induced by room heat sources. The studies present an equation that predicts volumetric airflow in terms of stack- driven effect using Bernoulli's equation for an in viscid fluid.

In the developed study an effort will be make to present a new macroscopic model on steady airflow process. One dimensional Navier- Stokes equation with suitable boundary conditions will be use to develop the model that predicts temperature-, velocity profiles together with volumetric airflow and mass transfer in un- stratified cross- ventilated rectangular building with opening on a vertical wall.

The new model has advances over the previous studies reported by Santamouris *et al.* 1995 and Chow, 2010, in which the developed study are based on two domains: (1) Domain with one lower and two upper openings in the presence of opposing flow in each of the upper openings, (2) Special case of (1) with one lower and one upper openings in the absence of opposing flow. One dimensional Navier- Stokes equations with suitable boundary conditions are used to develop the model equations, the models predicts temperature, velocity profiles together with volumetric airflow and mass transfer, parameters such as, effective thermal coefficient and dimensionless group Prandtl number were also introduced. The study will tries to investigate temperature profiles across the openings in order to provide thermal comfort in the domain, effect of changes of parameters to overall flow distributions were also

investigated and ascertain the best for optimal natural ventilation, which were believed to have significant effects on natural ventilation process in buildings.

1.1 STATEMENT OF THE PROBLEMS

The study would seek to re-established, qualitatively, the factors that impact on natural ventilation. We anticipate that one-dimensional Navier-Stokes equation with appropriate boundary conditions would describe the problems that analytically determine the velocity and temperature profiles across the openings together with volumetric airflow and mass transfer in building.

1.2 AIM

To develop a Mathematical model that would appropriately describe airflow process in un-stratified cross ventilated rectangular domain with openings on vertical walls.

1.3 OBJECTIVES OF THE STUDY

- To develop a clear Mathematical understanding of natural ventilation process.
- To give an accurate representation of the physical phenomenon of airflow process in the domains.
- To provide the necessary control mechanisms to develop the required indoor air quality through mathematical model.
- To use one dimensional Navier- Stokes equations with appropriate boundary conditions to describe the problems.
- To obtain the solution of the model equations, by employing variation of parameters.
- To presents the analyses of the results by developing MATLAB codes.

- Effect of changes of key parameters to the overall flow distribution will be investigated to ascertain the best one for optimal ventilation.

- Qualitative comparison between proposed results and the existing results.

1.4 SCOPE AND LIMITATIONS

The flow of air through large openings in un-stratified cross- ventilated domain is a special case of single-sided ventilated domain. The possibility of un- stratified cross- ventilated domain leads to a new class of problem, the domain has its own time scale associated with the volume and the flow rate through the space and the detailed flow patterns depends on the connections between the openings. It may take the form of either mixing or displacement ventilation depending on the position of the openings (orifices). This leads to the mathematical interest of airflow in un-stratified cross ventilated rectangular domains. The study is only limited to the mathematical interest of airflow in un-stratified cross ventilated rectangular domains with openings at same height on vertical walls.

1.5 SIGNIFICANCE OF THE STUDY

Air flow around buildings is very useful in the field of applied mathematics, engineering and architectural design. The study would seek to re-established, qualitatively, the factors that impact on natural ventilation but especially determine the factors that effects ventilation process through modeling techniques. These are novel approaches which we believe will lead to better understanding of the phenomenon and help researchers to come up with better models on natural ventilation.

1.6 STRUCTURE OF THE THESIS

Thesis comprises of five (5) chapters in total. The structure of the thesis will be briefly introduced in the following.

Chapter one contains a comprehensive introduction of natural ventilation process including the advantages and disadvantages of various methods for modeling air flow process, statement of the problem, aim, objectives of the study, scope, significance of the study and limitations are presented.

Chapter two consists of review of the knowledge and techniques of modeling airflow process in natural ventilation process.

Chapter three present the model formulation and solution methods of the model equations for un- stratified cross- ventilated rectangular domain with openings on vertical walls.

Chapter four present the analyses and discussion of the results obtained from model equations and key interventions with the previous studies.

Finally Summary, conclusion and recommendations are included in Chapter five.

CHAPTER TWO

LITERATURE REVIEW

2.0 Preamble

This Chapter is a brief review of the knowledge and techniques of modeling airflow process in natural ventilation process. Of fundamental interest is the information that can be used to assist in the model and development of integrated design tools for naturally ventilated domains.

Many attempts to investigate this phenomenon have been made by some researchers. In the early work on natural ventilation Emswiler, (1926) investigated the case of multiple openings in a wall and obtained an expression for the rate of flow of air in terms of temperature differences using Bernoulli's Equation for ideal flow, and they did not consider the case of a single opening. A great deal of attention has been given in the studies of natural convection to problems of air flow process in buildings. The study of natural convection and their applications to practical situations, ranging from heating equipment to the cooling of turbine blades was conducted by (Schmidt, 1961). Displacement ventilation (where the interior is stratified**)** was presented by **(**Murakami and Kato, 1989), and the mixing ventilation (where the interior has uniform temperature) was presented by (Liddament, 1991). Gladstone, Woods, Philips and Caulfied (1998) considered airflow process that combined the ideas of displacement ventilation from (Linden, Lane- Serff and Smeed, 1990). Liang Chung James Lo (2012) Considered wind-driven cross- ventilation in building with small openings. Andrew Acred, Gary Hunt (2014) presented a simple mathematical model of stack ventilation flows in multi-compartment buildings with a view to providing an intuitive

understanding of the physical processes governing the movement of air and heat through naturally ventilated buildings.

Buchanan and Sherman, (2000) considered a simple macro-scale mathematical model for the prediction of a heat recovery factor in a cross ventilated building with two openings with air as the connecting fluid. The domain is separated by vertical rectangular openings of height x, which as illustrated in Figure 2.1. The temperature distribution of the air in the building envelope is maintained at T with $T_i = 298K, T_0 = 274K$ as inside and outside temperature, u as the velocity distributions, Γ as diffusion coefficient, Q_0 as infiltration rate, and Pe as Peclet number.

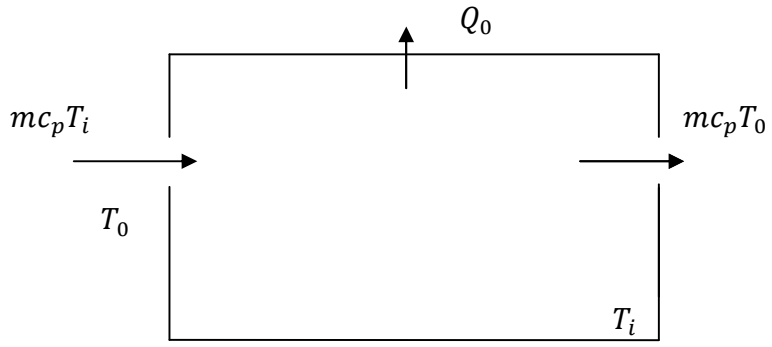

Figure 2.1: Diagram of cross ventilated building with two openings.

The model is based on the steady-state one dimensional convection-diffusion equation,

$$\frac{d}{dx}[\rho uT] = \frac{d}{dx}\Gamma\frac{dT}{dx}, \tag{2.1}$$

Equation (2.1) provides a simple analytical solution for the calculation of heat recovery as,

$$T(x) = T_0 + (T_i - T_0)\left[\frac{e^{Pe(\frac{x}{L})}-1}{e^{Pe}-1}\right]. \tag{2.2}$$

Allocca, Qingyan Chen, and Leon Glicksman (2003) investigated airflow process in single-sided natural ventilation, by using a computational fluid dynamics (CFD) model, together with analytical and empirical models. The CFD model was applied to determine the effects of buoyancy, wind or their combination on ventilation rates and indoor conditions. In order to study airflow parameters, various analytical methods have been developed. One such method involves applying simple equations from Bernoulli theory for buoyancy-driven flow, together with an empirical discharge coefficient, to single-sided ventilation. The most important parameter for natural ventilation design is the volumetric airflow through the opening(s). The building considered is single- sided ventilation in which, the lower and upper openings are located on the wall with A as an equal area of the openings and h, T_{in} and T_{out} maintained as height of the openings, outside and inside temperature of the air. Schematic diagram of airflow process through an upper and lower opening, and through a single opening are shown in Figure 2.2a, and 2.2b.

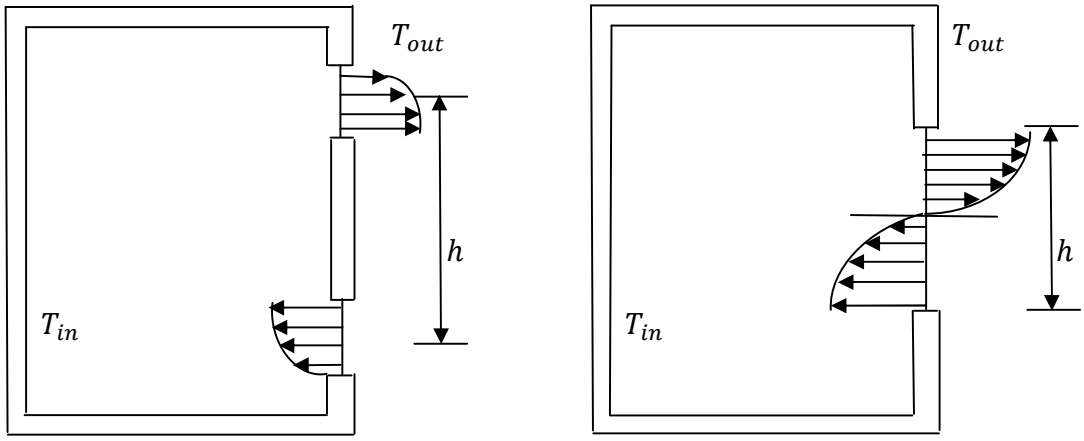

(2.2a) (2.2 b)

Figure 2.2a and 2.2b: Causing flow through an upper and lower opening, and through a single opening.

Duan Shuangping and Yuguo Li (2005) present an example of solution multiplicity in a building with bi-directional flow openings.

Mostafa Rahimi and Imam Arianmehr (2009) examine the combination of both natural ventilation methods. A test room of single-sided ventilation was equipped with a vertical vent which is illustrated in Figure 2.3. Ventilation rate through the openings was evaluated based on the air flow velocity measured at the surface area of the openings. The vertical vent was kept closed during the first run of the experiments then the same experiments repeated where the vent was in use. Based on the experimental results, the effects of the vertical vent on the ventilation rate was clarified and a model was suggested based on combination for the two ventilation methods.

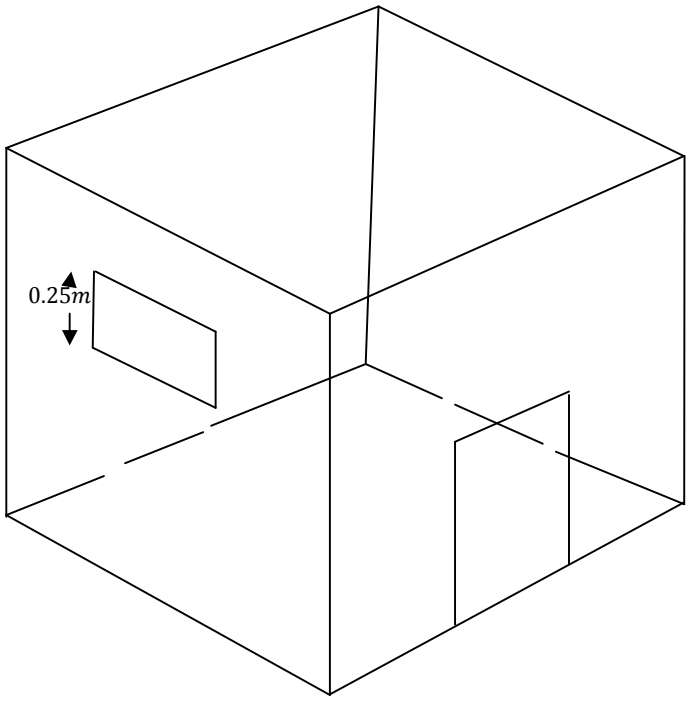

Figure 2.3: Diagram of a test room of single-sided vent.

The predicted results for volumetric airflow and mass transfer are as follows,

$$Q = C_d \left[\frac{A_u A_l}{(A_u^2 + A_l^2)^{\frac{1}{2}}} \right] \sqrt{\frac{2gHT_i - T_0}{T_0}}, \quad 2.3$$

$$m = \frac{\rho A \sqrt{2\beta g(T_i - T_0)L}}{\sqrt{K_i + K_0 + f(L/D)}}. \quad 2.4$$

where A cross section area of the vertical vent, A_l lower opening surface area, A_u upper opening surface area, C_d discharge coefficient D diameter of the vertical vent, f surface friction coefficient, g gravity acceleration, H vertical distance between lower and upper openings, m air mass flow rate, Q air volumetric flow rate, T_i temperature inside and T_0 temperature outside.

Mahajan (1987) measured the air flow velocity components by natural convection in inter-zonal building. Riffat (1989) made an experiment and found that the values of discharge coefficient in natural ventilated building with small and large openings ranges from 0.09 to 0.25. Davies and Linden (1992) studied the exchange flow rate through a full height doorway at the ends of a corridor (closed at the other end) in the presence of a head wind.

Sun, Stowell and Keener Michel Junior (2002) presented the Two- dinmensional computational fluid dynamics model of airflow velocity and ammonia distribution in a High-Rise ™ Hog building (HRHB).

Tine Larsen, (2003) considered $5.56 \times 5.56 \times 3.00m$ single-sided natural ventilated building which is illustrated in Figure 2.4. The study describes the results from the measurements evaluated on the basis of the air change rate, which has been measured both by use of tracer gas and by measured air velocities in the opening. Both the effect of wind velocity,

temperature difference and incidence angle of the wind are discussed together with future possibilities of developing new design methods for natural single-sided ventilation.

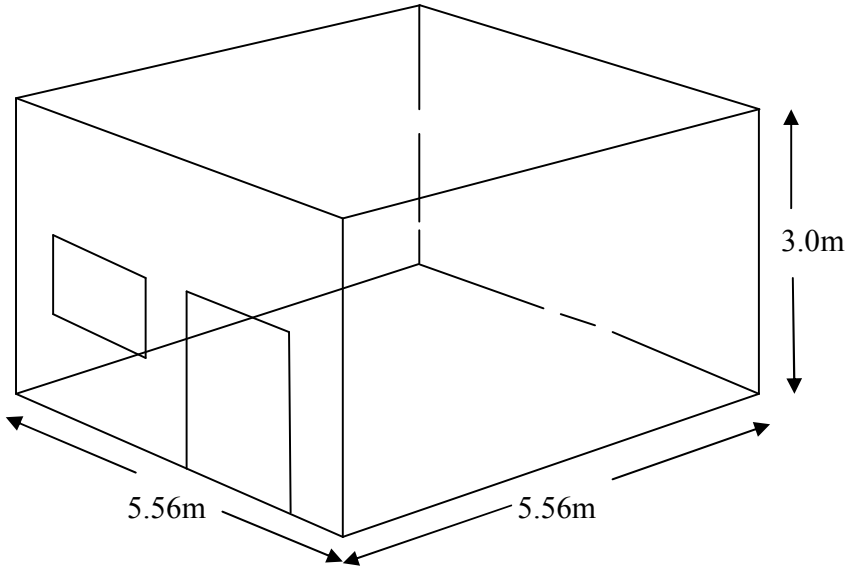

Figure 2.4: Diagram of single-sided vent.

The study obtained the following results for velocity and volumetric airflow as,

$$u_m = \sqrt{(0.001u_{10}^2 + 0.0035\Delta T + 0.01)}, \quad 2.5$$

$$Q = A_{eff}u_m = \tfrac{1}{2}Au_m. \quad 2.6$$

where, A_{eff} effective area of the vertical vent, u_m velocity of air, and Q volumetric airflow.

Cooper and Linden, (1995) presented the natural ventilation problems using the so- called salt bath methods in single sided ventilated system with two openings with linear vertical temperature profiles. Cooper and Linden, (1996) investigated natural ventilation in an enclosure containing two buoyancy forces. Iain Walker and Davies Wilson (1998) Designed an explicit algebraic equations for calculating of wind and stack driven ventilation in building envelopes.

Awbi and Nemri, (1990) Scale effect in room air-flow studies and later Awbi, (1996) investigated air movement on naturally-ventilated building, and Chow, (2010) reviewed the works of (Awbi, (1996)) which investigated the air flow rate across a vertical opening induced by thermal source in a room. Simple cross ventilated building with dimension of $5.3m \times 3.6m \times 2.8m$ height and window size of $0.7m \times 1.0m$ height has been considered as a test building which is illustrated in Figure 2.5. A Simple macro-scale mathematical model for the predictions of volumetric airflow and mass-transfer wsa derived using Bernoulli's equation.

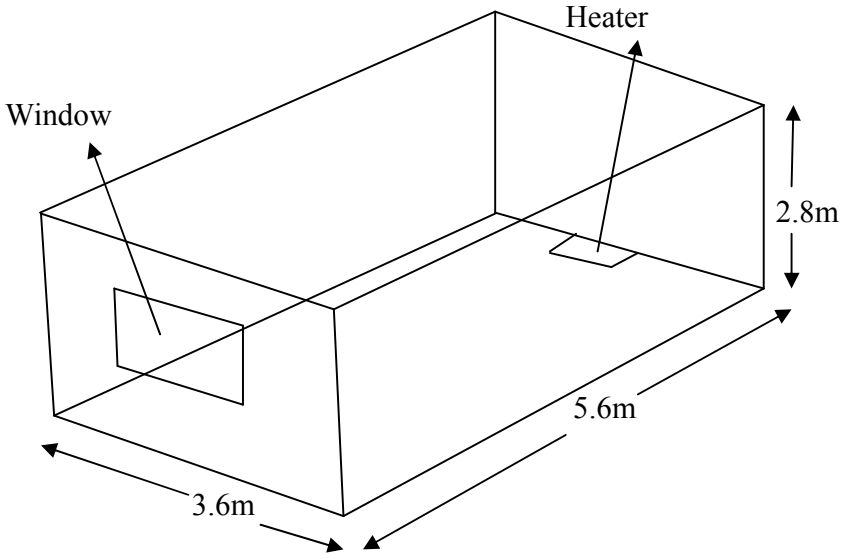

Figure 2.5: Diagram of single sided building.

The model equations that describing the problems in the study is given by Awbi (1996) is,

$$\Delta T g H_w = \frac{1}{2} T_O v_C^2 ,$$

with $v_i = v_O = 0$ at $z = 0$ and $v_O = 0$ at $z = 1, z = \frac{H_w}{2}$. 2.7

The predictions for velocity, volumetric airflow and mass transfer are,

$$v_C(H_w) = \sqrt{2gH_w\frac{\Delta T}{T_O}}, \quad 2.8$$

$$Q_C = \frac{1}{3}A_w c_d\sqrt{gH_w\frac{\Delta T}{T_O}}, \quad 2.9$$

$$m_C = \frac{1}{3}c_d A_w \rho_0\sqrt{\frac{gH_w\Delta T}{T_0}}. \quad 2.10$$

where, outside density of air is $,\rho_O$, inside and outside velocity of air is v_i, v_O, velocity distribution across the openings, volumetric airflow and mass transfer of air is v_C, Q_C, m_C, area of the window openings is A_w, acceleration due to gravity is g, height of window of the openings is H_w, interior, and outside air temperature are T_i, T_0, and the discharge coefficient is c_d.

Yugou Li, (1999) presenetd an analysis methods that described natural and hybrid ventilation(combined natural and mechanical ventilation), and Yugou Li and Deselte (2001) also considered Natural ventilation induced by combined wind and thermal forces The building considered is a simple building having two openings at different vertical level on opposite walls, the height of the two openings are relatively small, and the areas of the top and bottom openings are A_t and A_b respectively. The study obtained an equation that predicts volumetric airflow in terms of stack-effect or temperature differences when the indoor temperature is uniform using Bernoulli's equation for an in viscid fluid. And the floor air temperature ratio k is; $k = \frac{T_f - T_0}{T_i - T_0} = 0.35{\sim}1$ for fully mixed room air.

The model equations that describing the problems in the study is given by Yugou Li *et al.* (2001) is,

$$(T_i - T_0)gh = \frac{1}{2}T_O v_Y^2,$$

with $v_i = v_O = 0$ at $z = 0$ and $v_O = 0$ at $z = 1, z = \frac{h}{2}$. 2.11

The predictions for velocity, volumetric airflow and mass transfer are,

$$v_Y(h) = \sqrt{2g\frac{T_i - T_0}{T_0}h}, \quad 2.12$$

$$Q_Y = AC_d\sqrt{2gh\frac{T_i - T_0}{T_0}}, \quad 2.13$$

$$m_Y = A\rho_0 C_d\sqrt{2gh\frac{T_i - T_0}{T_0}}. \quad 2.14$$

where, inside and outside velocity of the air is $v_i, v_{O.}$ velocity distribution across the openings, volumetric airflow, and mass transfer of air is v_Y, Q_Y, m_Y, areas of the top and bottom openings are A_t, A_b. Total area of the openings is $A = \frac{A_t A_b}{\sqrt{A_t^2 + A_b^2}}$, acceleration due to gravity is g, height of the openings is h, the interior, outside and floor air temperature are T_i, T_0, T_f floor air temperature ratio (effective thermal coefficient) is k, and discharge coefficient is C_d.

Tong Yang (2004) investigated natural ventilation in a full-scale building induced by combined wind and buoyancy forces. The system under consideration is that of Figure 2.6, in which the openings are on the same vertical wall, having a rectangular opening of height h. The densities of the air remote from the wall are maintained at ρ_i and ρ_e, air temperatures at T_i and T_e, air pressure at p_i and p_e, air specific heat capacity at C_{p_i} and C_{Pe}, and air heat at q_i and q_e. The overall objectives were to verify and validate a CFD model for the naturally ventilated buildings, collect high quality full-scale experimental data for CFD validation and

formulate guidelines for modeling natural ventilation in design practice and a steady envelope flow model were applied to calculate the volumetric airflow induced by wind (Q_w) and stack- driven effect (Q_s) as,

$$Q_w = C_d A U_{ref} \sqrt{\frac{dC_p}{2}} = C_d A \sqrt{\frac{dp}{\rho}}, \quad 2.15$$

$$Q_s = C_d A \sqrt{\frac{(d\rho)gh}{\rho_a}} = C_d A \sqrt{\frac{(dT)gh}{T_a}}. \quad 2.16$$

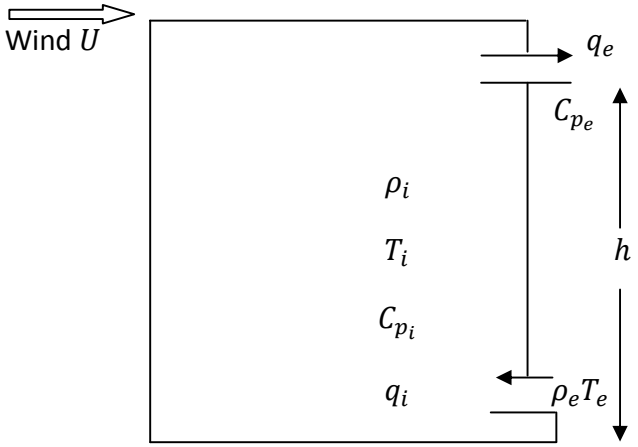

Figure 2.6: Schematic presentation of single sided ventilated building.

where U is mean wind speed, U_{ref} is reference wind speed, g is acceleration due to gravity, dp is mean static pressure difference across the openings, dC_p is air specific heat capacity difference between interior and exterior, $d\rho$ is air density difference between interior and exterior, dT is air temperature difference between interior and exterior, C_d is discharge coefficient, A is total area of the openings, ρ is air constant density in the building, ρ_a is mean average density of air and T_a is mean average temperature of air.

Angui, Phillip Jones, Pingge Zhao and Liping Wang (2004) investigated heat transfer and airflow rate in single sided heated solar chimney.

Brown and Solvason, (1962a,b) presented a macroscopic model that describes natural convection through rectangular openings in a single sided ventilated building. The study obtained an equation that predicts velocity distributions, volumetric airflow and mass transfer in terms of wind- driven effect using Bernoulli's equation for an in viscid fluid. The system under consideration is that of Figure 2.7 in which, two large sealed cavities are separated from one another by a vertical partition having a rectangular opening of height H and width W. The densities of the air remote from the wall are maintained at ρ_1 and ρ_2, the air temperatures at T_1 and T_2 and the air concentrations at c_1 and c_2.

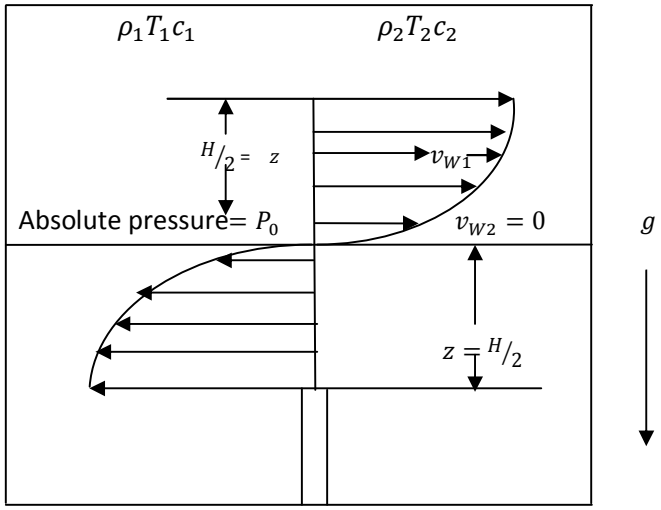

Figure 2.7: Schematic representation of natural convection across an opening in a vertical partition.

The model equations that describing the problems in the study is given by,

$\Delta\rho g z = \frac{1}{2}\bar{\rho} v_W^2$,

With $v_1 = v_2 = 0$ at $z = 0$ and $v_{W2} = 0$ at $z = 1, z = \frac{H}{2}$. 2.17

The predictions for velocity, volumetric airflow and mass transfer are,

$$v_W(z) = \sqrt{\frac{2\Delta\rho g z}{\bar{\rho}}}, \quad 2.18$$

$$Q_w = \frac{W c_d}{3}\sqrt{\frac{g\Delta\rho}{\bar{\rho}}}\, H^{\frac{3}{2}}, \quad 2.19$$

$$m_w = \frac{W\rho c_d}{3}\sqrt{\frac{g\Delta\rho}{\bar{\rho}}}\, H^{\frac{3}{2}}, \quad 2.20$$

$$q_w = \frac{W c_d \rho c_p \Delta T}{3}\sqrt{\frac{g\Delta\rho}{\bar{\rho}}}\, H^{\frac{3}{2}}. \quad 2.21$$

where $z = \frac{H}{2}$ is the neutral level of the openings c_d is the discharge coefficient, g is the acceleration due to gravity, v_{W2} is the exterior air velocity, ρ is the constant air density in the building, $\bar{\rho}$ is the average air density between interior and exterior, c_p is the air specific heat capacity, ΔT air temperature difference, and v_w, Q_w, m_w, q_w are the velocity distributions, volumetric airflow, mass- and heat- transfer.

Brown, Salvason and Wilson, (1963) investigated heat and moisture flow through openings by natural convection in building. Britter, Hunt and Mumford, (1979) shows the interaction of the wind with building by considering the wind-driven flow only.

Santamouris, Argiriou, Asimakopoulos, Klitsikas and Dounis (1995) presented a macroscopic model that describes heat and mass- transfer through an openings by natural convection in a single sided ventilated building. The study obtained an equation that predicts velocity distributions, volumetric airflow and mass transfer in terms of stack-effect using Bernoulli's equation for an in viscid fluid. The system under consideration is single- sided ventilated building in which, the schematic diagram of airflow process is illustrated in Figure 2.8. Zones are separated from one another by a rectangular opening of height Y_x. The

densities of the air remote from the wall are maintained at ρ_1 and ρ_2, and the air temperatures at $T_1$and T_2.

The study works with the following assumptions: The pressure variation is a function of the distance from the floor level; the fluid is in viscid and incompressible flow and the neutral height is at the middle of the opening $\left(Y_N = \frac{Y_x}{2}\right)$.

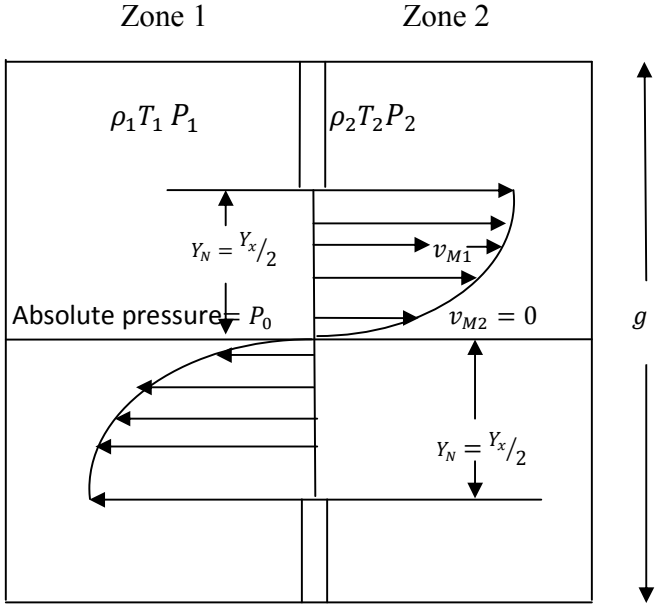

Figure 2.8: Schematic diagram of airflow process across opening in a single sided ventilated building.

Since, the flow is only induced by stack- driven effect then, According to (Linden, 1999) the reduced gravity is given by,

$$g\frac{\Delta\rho}{\bar{\rho}} = g\frac{\Delta T}{\bar{T}}, \qquad 2.22$$

The model equations that describing the problems is,

$$\Delta T g Y_N = \frac{1}{2}\bar{T} v_M^2,$$

With $v_1 = v_2 = 0$ at $Y_N = 0$ and $v_2 = 0$ at $Y_N = 1, Y_N = \frac{Y_x}{2}$. 2.23

Therefore, velocity distributions of air is,

$$v_M(Y_N) = \sqrt{2g\frac{\Delta T}{\bar{T}} Y_N}\,. \quad 2.24$$

For volumetric airflow, mass transfer and heat transfer are,

$$Q_M = \frac{1}{3} c_d W Y_x^{1.5} \sqrt{g\frac{\Delta T}{\bar{T}}}, \quad 2.25$$

$$m_M = \frac{2}{3} c_d\, \bar{\rho}\; W Y_x^{1.5} \sqrt{g\frac{\Delta T}{\bar{T}}} \quad 2.26$$

$$q_M = \frac{2}{3} c_d\, \bar{\rho}\, c_p \Delta T\; W Y_x^{1.5} \sqrt{g\frac{\Delta T}{\bar{T}}} \quad 2.27$$

Wilson and Kiel (1990) carried out an experiment on the exchange flow through a window in a heated, sealed room of a test house. The data give a smaller value of discharge coefficient $C_d = 0.044 + 0.004\Delta T$ and suggested that the reduction was coused by mixing of the incoming and outgoing air at the window, where $\Delta T, \Delta\rho$ is the temperature differences across the openings and density differences of air, c_d is the discharge coefficient, g is the acceleration due to gravity, v_{M1}, v_{M2} is the exterior air velocity, $\bar{\rho}$ is the average air density between interior and exterior, v_M is the air velocity, c_p is the air specific heat capacity, and Q_M, m_M, q_M are the volumetric airflow, mass- and heat- transfer of air.

Yunlong Liu, Alfred Moser, (2003) investigated air flow over Ahmed body by means of transient RANS turbulence models. Xin Wanga, Chen Huang, Weiwu Cao, (2009) experimentally studied a vertical temperature distribution of hybrid ventilation in an atrium building. Wei Yin, Guoqiang Zhang, Wei Yang, Xiao Wang, (2010) presented a two openings naturally ventilated building potential model considering solution multiplicity, window opening percentage, air velocity and humidity in China. Han Xing, Yang Jie, Zhang Xu, Wang Xiaozhi, Zhu Chun and Sui Xuemin, (2011) presented numerical study on natural ventilation in High- rise building. Fu Yuying, Huang Chen, Wang Xin, Luo Xing and Liu Sheng, (2009) considered a study on hybrid system in a large space building. Omar Asfour and Mohamed Gadi, (2008) investigated the potential of the vaulted roofs for improving wind- induced natural ventilation, using computational fluid dynamics three dimensional modeling. Cui Qin and Lihua Zhao (2010) presented a study on the energy efficient potential on natural ventilation for residential building in Guangzhou. Praphanpong Somsila, Umphisak Teeboonma and Wirapan Seehanam, (2009) investigated a buoyancy airflow inside solar chimney using computational fluid dynamics (CFD) technique. Yi Jiang and Qingyan Chen, (2003) full- scale experimental and CFD methods were used to investigate buoyancy- driven single sided natural ventilation with large openings. Roberto Fuliotto, (2010) presented an experimental and numerical analysis of heat- transfer and airflow on an interactive building façade (DSF). Saelens, Carmeliet and Hens, (2003) Analyzed the energy efficiency of different kinds of one- storey multiple skin façade with a dynamic building energy simulation program. The factors that influence the green house effect in a DSF were identified by Gratia and De Herde, (2007) use a one- dimensional approach under various operative Scenarios. A lumped variable procedure was used by Park, Augenbroe, Messadi,

Thitisawa and Sadegh, (2004), to provide on a real time basis, optimal setting for various DSF components. A non- dimensional analytical method was developed by Colombari and Bolocco (2005) to calculate the overall heat transfer coefficient and energy balance of a DSF. The literature on DSF contains only few experimental studies about flow and heat transfer issues in DSFs. Zollner, Winter and Viskanta (2002) performed an experimental analysis on a single full size ventilated box window without shading devices.

Ramesh Srikonda and Bala Ratnaker Dolkiparty, (2010) natural ventilation by thermal buoyancy in a building with a window and a small opening at ventilation level and periodic solar thermal model have been integrated to investigate the thermal behavior of a non- air conditioned building. Fan, (1995) presented a CFD model of airflow air indoor pollutant in rooms. Gan, (1995) investigated a room airflow distribution system using CFD. Harral and Boon, (1997) shows the comparison between predicted and measured airflow pattern in a mechanically ventilated livestock without animals. Van der maas (ed.), (1992) investigated airflow through large opening in natural ventilated building. Van der mass, Roulet and Hertig, (1989) presented some aspect of gravity driven airflow through large openings in building. Lee and Short, (2000) presented Two- dimensional numerical simulation of natural ventilated building. Vandaele and Wouters, (1990) presented a model that estimating airflow process and infiltration heat recovery in building. Luo Zhiwen, Zhao Jianing, Gao Jun and He Lixia, (2007) estimated natural ventilation potential by considering thermal comfort issues. Hunt and Linden (2001) examined ventilation driven by a point source of buoyancy on the floor of an enclosure in the presence of wind.

Henry and Leslie (2009) presented a flexible system- identification frame-work for linear thermal models that is well suited to accommodate the unique features of mixed-mode

buildings. The effectiveness of this framework was demonstrated on a multi-zone, mixed-mode building, with model-prediction accuracy shown to exceed that published for other naturally ventilated or mixed-mode buildings, none of which exhibited the complexity of this building. Isabel, Helena and Ricardo (2011) makes a review of the most recent patents on building solar air systems that make use of solar energy to induce the buoyancy effect for heating, cooling and ventilatingand demonstrate the increasing tendency in the development of building passive solutions that can satisfy, in just one system, more than one role: heating, cooling and ventilation. Yi Jiang, Camille Allocca and Qingyan Chen (2004) presented three computational fluid dynamics (CFD) models: steady Reynolds averaged Navier-Stokes equation (RANS) modeling, unsteady RANS modeling, and large eddy simulation (LES) to study both wind-driven and buoyancy-drive natural ventilation. The validation of the CFD models used the experimental data of wind-driven natural ventilation obtained from a wind tunnel with a scaled building model and the data of buoyancy-driven ventilation obtained from a full-scale chamber. LES results seem more accurate and informative than those obtained with the RANS modeling, but with severe penalty in computing time. This investigation has also analyzed turbulence energy spectra of natural ventilation. The peak turbulence energy for wind-driven natural ventilation is at frequencies higher than that for buoyancy driven natural ventilation. Thus, the fluctuating flowfield plays a more important role in determining ventilation rate for wind-driven natural ventilation than for buoyancy-driven natural ventilation. Van Hooff and Blocken (2013) presented 3D unsteady Reynolds-averaged Navier-Stokes (RANS) CFD simulations to reproduce the decay of CO_2 (Carbon dioxide) concentration in a large semi-enclosed stadium. The study focuses on the hours after a concert, when the indoor CO_2 concentration generated by the attendants has reached a

maximum. The wind flow, indoor airflow and dispersion of heat, water vapour and CO_2 are modelled on a high-resolution grid based on grid-sensitivity analysis. The simulations are validated with on-site measurements of wind velocity and CO_2 concentration decay.

CHAPTER THREE

MODEL FORMULATION AND SOLUTION METHODS

3.0 Preamble

This chapter consists of two sections which would seek to: (3.1) develop the mathematical models of: airflow process in un-stratified cross- ventilated rectangular domain with openings on vertical walls. The problem involve coupling of fluid flow and temperature flux via orifices. We anticipate that One-Dimensional Navier- Stokes Equations with appropriate boundary conditions would describe the problems, then, (3.2) solution of the model equations that predict the velocity, temperature profiles together with volumetric airflow and mass transfer. Graphical illustration of the research methodology for the study is illustrated in Figure 3.1 below,

3.1 MODEL FORMULATION OF AIRFLOW IN TWO RECTANGULAR OPENINGS

Section consists of two sub sections which would seek to develop the mathematical models of: (3.1.1) airflow process in un-stratified cross- ventilated rectangular domain with one lower and two upper openings in the presence of opposing flow in each of the upper openings, (3.1.2) Special case of (3.1.1) domain with one lower and one upper openings in the absence of opposing flow.

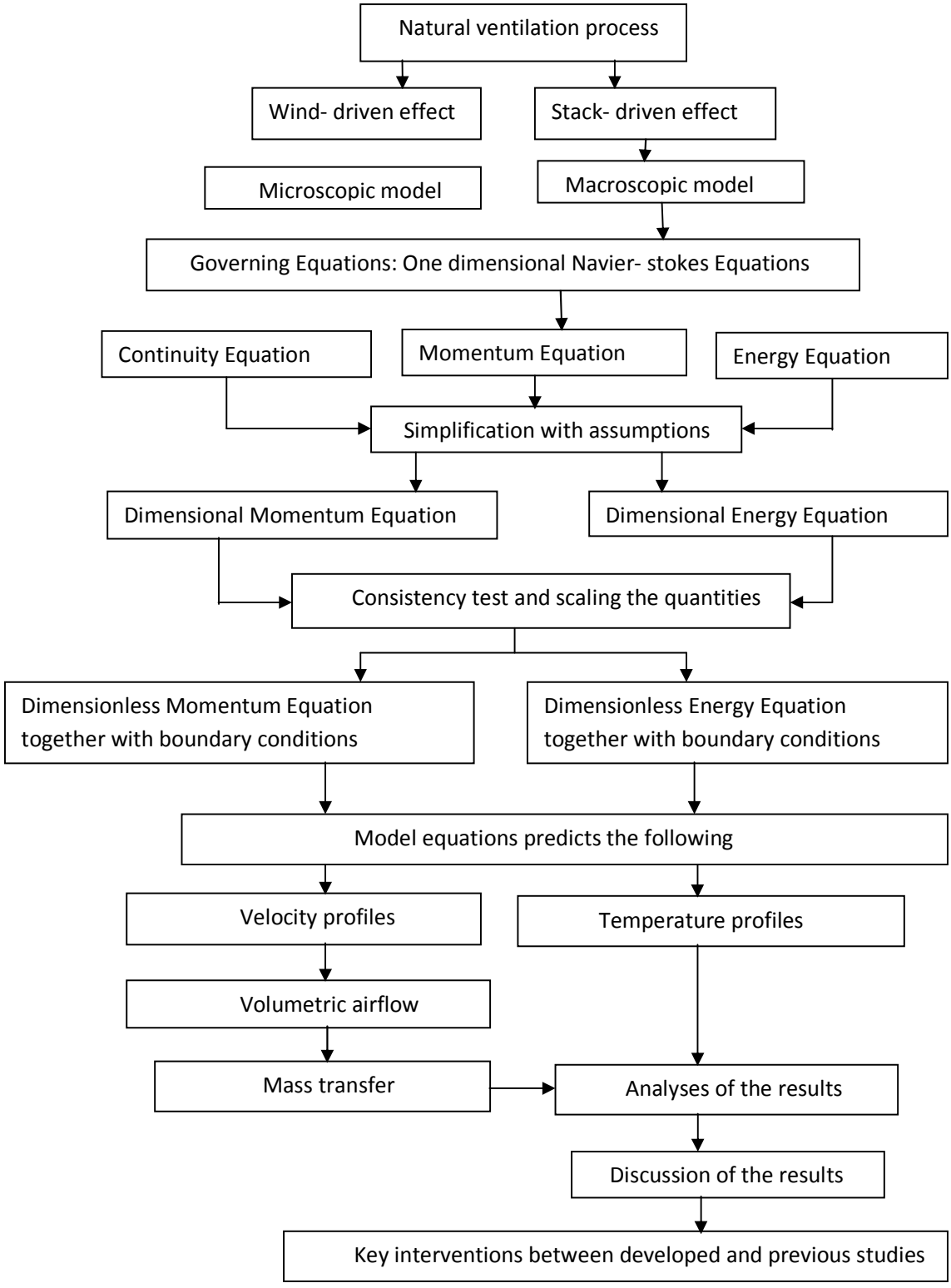

Figure 3.1: Graphical illustration of the research methodology.

3.1.1 Model formulation for rectangular with three openings

This sub section intends to describe the model of airflow process in rectangular domain with one lower and two upper openings in the presence of opposing flow in each of the upper openings.

3.1.1.5 Preliminary assumptions

Some approximations and simplifications are going to be made in modeling the entire domain. The most essentials and commonly made assumptions used in the study are as follows;

1. Airflow is at steady state condition ($\rho_i = Constant$), it behaves like incompressible by (Daniel, (2005)).
2. Uniform interior temperature in the domain.
3. Internal heat source and viscous dissipation (effect of viscous) is negligible that is $q \ll 1, \Phi_v \ll 1$).
4. There is an opposing flow in each of the upper openings in the domain (indirect velocity of air is v_0)
5. The flow is induced by stack- driven effect only (flow induced by temperature differences).
6. Velocity and temperature fields are independent of the distance parallel to the floor $U = u(y), \theta = T(y)$, $x_w =$ Constant width of openings.

3.1.1.2 Domain considerations for rectangular with three openings

Domains considered here is un-stratified cross- ventilated rectangular domain with Three-openings. The dimension of the domain is of $5.3m \times 3.6m \times 2.8m$ with two equal upper and one lower opening on the vertical walls. The area of two upper and one lower openings is $0.7m \times 1.0m, 0.7m \times 1.0m$ and $0.7m \times 2.0m$ with air as the connecting fluid. The

domains are separated by vertical rectangular openings of height y and width x_w, which is illustrated in Figure 3.2. The constant density of the air in the domain envelopes are maintained at ρ_i with temperature θ, and pressure $p(x_w)$.

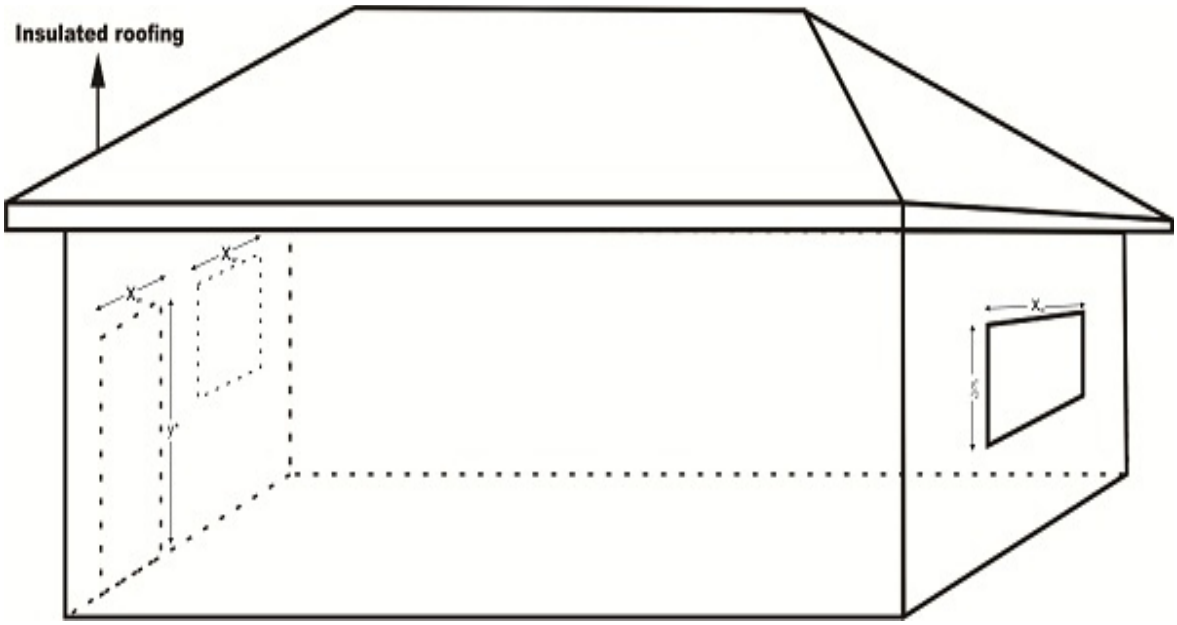

Figure 3.2: Cross section of a typical un- stratified cross- ventilated rectangular domain with three openings.

Temperature differences between the indoor (T_i) and outdoor (T_o) of a domain produce density differences and corresponding pressure differences that generate buoyancy- driven flow through the domain envelope. This flow depends not only on the indoor- outdoor temperature differences which is a function on the height between the openings. A special case of buoyancy- driven flow is set up for a domain that has two upper and one lower openings placed at equal heights above the floor. If a thermal difference between the indoor and outdoor environment exists, bidirectional or two- ways buoyancy- driven flow is obtained. In this case, the pressures gradient is a function of the constant width of the openings. Figure 3.3 depicts the schematic diagram of airflow process induced by buoyancy-

driven flow (stack effect) in rectangular domain with three openings in the presence of opposing flow in each of the upper openings (window) for an indoor temperature that is larger than the outdoor temperature. Cooler outdoor air enters through the lower opening (door) and warmer indoor air exist through the upper half of each upper openings (neutral height of the window). This exchange of air is a necessary consequence of the principle of mass conservation for an incompressible fluid.

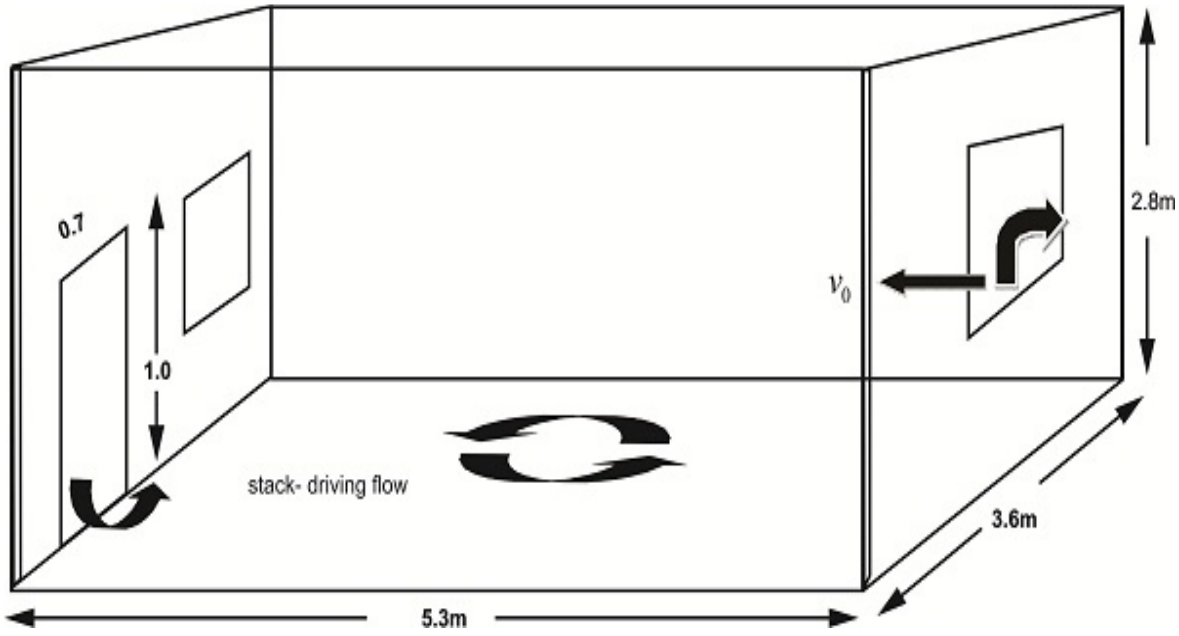

Figure 3.3 Schematic diagram of airflow process induced by stack effect in rectangular domain with three openings.

Since, the domain has three openings there is strong tendency for opposing flow in each of the upper opening with an indirect velocity v_0. Causing airflow through an upper opening with an opposing flow above the neutral height and the gravity opposing the flow is illustrated in Figure 3.4 and T_o, T_i maintained as outdoor and uniform indoor air temperatures.

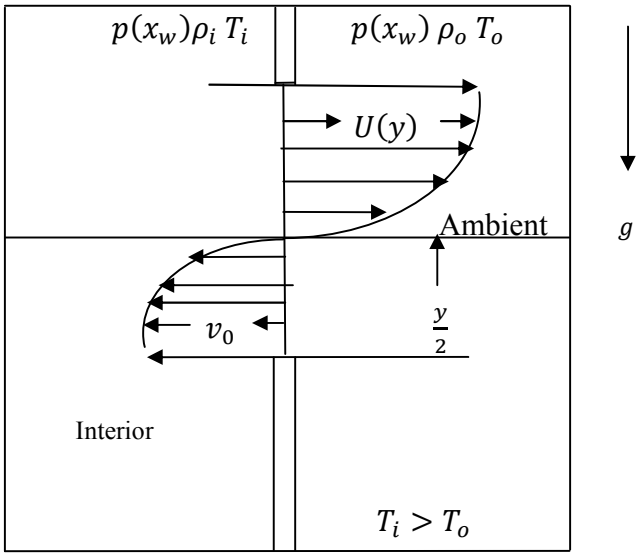

Figure 3.4: Causing airflow through one of the vertical upper vent in rectangular domain with three openings.

Convective motion induced by stack- driven effect as illustrated in Figure 3.3 is described by the conservation equations for continuity, momentum and energy (i.e. Navier- Stokes equation) is.

$$\frac{\partial u}{\partial x_w} + \frac{\partial v_0}{\partial y} = 0, \tag{3.1}$$

$$u\frac{\partial u}{\partial x_w} + v\frac{\partial u}{\partial y} = -\frac{1}{\rho_i}\frac{\partial p}{\partial x_w} - g\ + \nu\frac{\partial^2 u}{\partial y^2}, \tag{3.2}$$

$$u\frac{\partial T}{\partial x_w} + v\frac{\partial T}{\partial y} = \alpha\frac{\partial^2 T}{\partial y^2} + \frac{q}{\rho_i c_p}\Phi_v. \tag{3.3}$$

Pressure difference results from the weight of the air is,

$$\frac{\partial p}{\partial x_w} = -\rho g, \tag{3.4}$$

$$-\frac{1}{\rho_0}\frac{\partial p}{\partial x_w} - g = \frac{g}{\rho_i}(\rho - \rho_i). \tag{3.5}$$

The flow is induced by stack- driven effect, we need temperature difference. By employing an approximation of reduced gravity by (Linden, (1999)) is $g' = g\frac{\Delta\rho}{\rho_i} = g\frac{\Delta T}{T_i}, \Delta T = T - T_i$ and thermal expansion coefficient $\beta = \frac{1}{T_i}$.

$$-\frac{1}{\rho_i}\frac{\partial P}{\partial x_w} - g = g\frac{\Delta T}{T_i} = g\beta\Delta T, \quad 3.6$$

Momentum equation in (3.2) is now becomes,

$$u\frac{\partial u}{\partial x_w} + v\frac{\partial u}{\partial y} = g\beta\Delta T \ + \nu\frac{\partial^2 u}{\partial y^2}, \quad 3.7$$

together with the following matching conditions as,

$$U = u(y), v = v_0 = const.\ \theta = T(y),\ x = x_w = const., P = p(x_w). \quad 3.8$$

It assumed that the velocity and temperature fields are independent of the distance parallel to the floor, and the gravitational field is aligned with the direction of air motion the pressure will be a component along the constant width of the openings in the domain, and air as a non viscous fluid we can neglecting viscous dissipation as $\Phi_v \ll 1$, and $q \ll 1$.

Navier-Stokes equations are simplified by the above mentioned equation (3.8). In which mass conservation equation in (3.1) is satisfied identically then, Equations (3.3) and (3.7) can be reduced to one dimensional momentum and energy equation as,

$$v_0\frac{dU}{dy} = g\beta\Delta\theta \ + \nu\frac{d^2U}{dy^2}, \quad 3.9$$

$$v_0\frac{d\theta}{dy} = \alpha\frac{d^2\theta}{dy^2}, \quad 3.10$$

with the following boundary conditions as,

$0 \leq y \leq 2, U(y=0) = 0, U(y=1) = 0,\ \theta(y=0) = -\theta_0, \theta(y=1) = 1 - \theta_0, v_0 = const., x_w = const.$ 3.11

where, U, θ is velocity-, temperature- profiles of the air along the height of the openings (y), p is air pressure along the component of constant width of the openings (x_w), ν is kinematic viscosity of the air, and α is thermal diffusivity of air, θ_0 is effective thermal coefficient, and c_p is the specific heat capacity of air.

3.1.1.3 Consistency test

One needs to check equations (3.9) and (3.10) for consistency,

Let the dimension be Dim, L be the length scale of height, T be the length scale of time, and for temperature as supplementary quantity be Θ.

$Dim[U] = LT^{-1}, \quad Dim[v_0] = LT^{-1}, \quad Dim[\nu] = Dim[\alpha] = L^2T^{-1} \quad Dim[g] = LT^{-2}, Dim[y] = L$

$Dim[\Delta\theta] = \Theta, Dim[\beta] = \Theta^{-1},$ 3.12

Inserting equation (3.12) into (3.9),

$$LT^{-1}\frac{LT^{-1}}{L} = L^2T^{-1}\frac{LT^{-1}}{L^2},$$

$$LT^{-2} = LT^{-2}.$$ 3.13

Inserting equation (3.12) into (3.10), one obtain,

$$LT^{-1}\frac{\Theta}{L} = L^2T^{-1}\frac{\Theta}{L^2},$$

$$T^{-1} = T^{-1}. \quad 3.14$$

Therefore, equation (3.9) and (3.10) are consistent.

3.1.1.4 Non- dimensionalization

Non- dimensionalizing height, y^* with $\frac{y}{L}$, velocity, U^* with $\frac{\alpha U}{g\beta\Delta\theta L^2}$, ${v_0}^*$ with $\frac{v_0 L}{\nu}$ and θ^* with $\frac{\theta-\theta_0}{\Delta\theta}$.

In dimensionless form equations (3.9) and (3.10) may be expressed as,

$$Pr\frac{d^2U^*}{dy^{*2}} + C\frac{dU^*}{dy^*} + \theta^* = 0, \quad 3.15$$

$$\frac{d^2\theta^*}{dy^{*2}} + C\frac{d\theta^*}{dy^*} = 0, \quad 3.16$$

together with the following dimensionless boundary conditions as,

$$0 \le y^* \le 1, U^*(y^* = 0) = 0, U^*(y^* = 1) = 0, \theta^*(y^* = 0) = -\theta_0, \theta^*(y^* = 1) = 1 - \theta_0. \quad 3.17$$

where, $C = -{v_0}^* Pr$, the dimensionless group $Pr = \frac{\nu}{\alpha}$ is called Prandtl number, $U^*(y), \theta^*(y)$ is the velocity, and temperature profiles of the air, y^* is the dimensionless height of the openings.

3.1.2 Model formulation for rectangular domain with two openings

The sub section here is a special case of 3.1.1 which intends to describe the model of airflow process in rectangular domain with one lower and one upper opening in the absence of opposing flow in one of the upper openings.

3.1.2.1 Domain Considerations for rectangular domain with two openings

The domain considered here is a special case of domain in 3.1.1 in which, the domain has one upper and one lower opening on the vertical walls. The area of one upper and one lower opening is $0.7m \times 1.0m$, and $0.7m \times 2.0m$ (see Figure 3.5).

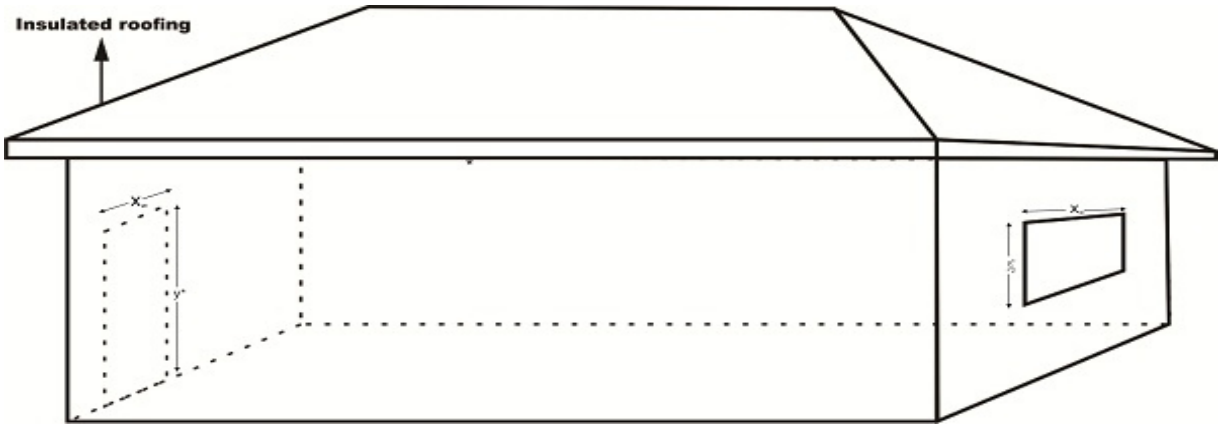

Figure 3.5: Cross section of a typical un- stratified cross- ventilated rectangular domain with two openings.

The schematic airflow process induced by stack- driven effect across the openings in the domain is illustrated in Figure 3.6 in which, the study did not considered an opposing flow in one of the upper openings.

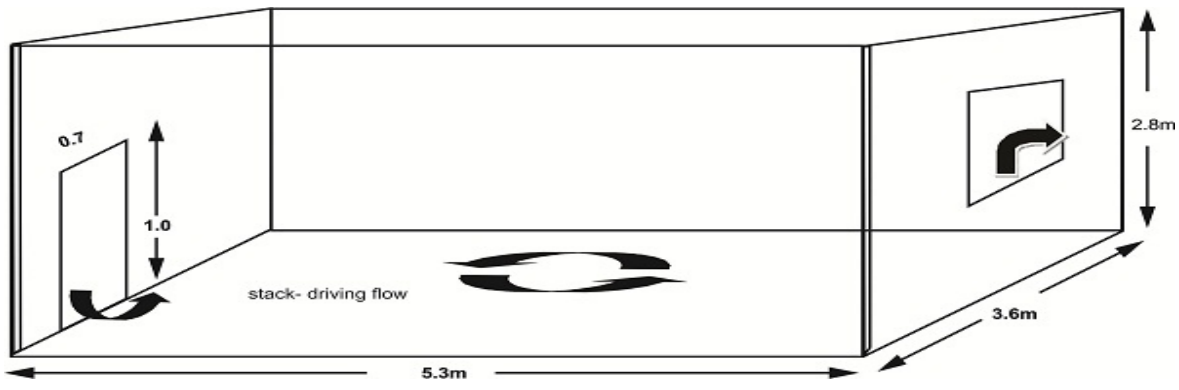

Figure 3.6: Schematic diagram of airflow process caused by stack effect in a rectangular domain with two openings.

Causing airflow through an upper opening in the absence of opposing flow above the neutral height and the gravity opposing the flow is illustrated in Figure 3.7, and also T_a, T_0 maintained as ambient and uniform room air temperature.

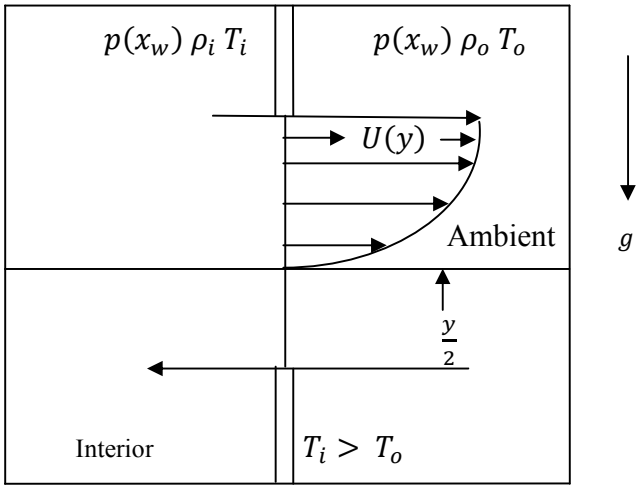

Figure 3.7: Causing airflow through the vertical upper vent in rectangular domain with two openings.

In the case where the domain has one lower and one upper opening on the vertical walls, the tendency effect for opposing flow in the upper openings is very negligible, so that the indirect velocity of the air is assumed to be $v_0 = 0$. The governing equations describing the problem are in equations (3.18), (3.19) which is a special case of equations (3.15) and (3.16) with indirect velocity $v_0 = 0$. Working with the above assumption in equations (3.15) and (3.16) yields to,

$$Pr\frac{d^2U^*}{dy^{*2}} + \theta^* = 0, \qquad 3.18$$

$$\frac{d^2\theta^*}{dy^{*2}} = 0, \qquad 3.19$$

together with the dimensionless boundary conditions as in equation (3.17).

3.2 SOLUTION METHODS OF THE DIMENSIONLESS MODEL EQUATIONS FOR UN- STRATIFIED CROSS- VENTILATED RECTANGULAR DOMAIN WITH OPENINGS ON VERTICAL WALLS

This section (3.2) consists of two sub- sections (3.2.1) and (3.2.2), which intends; to describe the solution methods of the dimensionless model equations (energy and momentum equations) in order to predict temperature, velocity profiles together with volumetric airflow and mass transfer in a cross ventilated rectangular domain with opening on vertical walls.

3.2.1 Solution of the dimensionless model equations for rectangular domain with three openings

This sub- section (3.2.1) consists of two sub- sub sections (3.2.1.1) and (3.2.1.2), which intends; to describe the solution methods of the dimensionless energy and momentum equations in order to predict temperature profiles and in other hands to predict the velocity profiles, volumetric airflow together with mass transfer across the openings in a cross ventilated rectangular domains with three openings.

3.2.1.1 Solution of the dimensionless energy equations for rectangular domain with three openings

This sub- sub section (3.2.1.1) intends to; describe the solution methods of the dimensionless energy in order to predict temperature profiles across the openings for rectangular domain with three openings.

The differential equation (D.E) in (3.16) is a homogeneous differential equation, one need to define the corresponding auxiliary Equation associated with the D.E as

$$j^2 + Cj = 0, \tag{3.20}$$

where, the roots of the equation (3.20) are $j_1 = 0, j_2 = -C$.

The solution to the D.E in Equation (3.15) is,

$$\theta^*(y^*) = C_1 + C_2 e^{-Cy^*}, \tag{3.21}$$

where, C_1 and C_2 are arbitrary constants in equation (3.21).

The two constant which appear in equation (3.21) can be determined by prescribing the boundary condition for the temperature profile in Equation (3.17), thus obtaining,

$$C_1 = \frac{1-\theta_0(1-e^{-C})}{1-e^{-C}}, C_2 = -\frac{1}{1-e^{-C}}, \tag{3.22}$$

Inserting equation (3.22) into (3.21), yield the temperature profile as,

$$\theta^*(y^*) = \theta_3^*(y^*) = \frac{1-\theta_0(1-e^{v_0 Pr})-e^{v_0 Pry^*}}{1-e^{v_0 Pr}}. \tag{3.23}$$

3.2.1.2 Solution of the dimensionless momentum equations for rectangular domain with three openings

This sub- sub section (3.2.1.2) also consists of three (3) sub- sub subsections (3.2.1.2.1), (3.2.1.2.2), and (3.2.1.2.3), which intends to describes the solution methods of the dimensionless momentum equation in order to predicts velocity profiles together with volumetric airflow and mass transfer across the openings for rectangular domain with three openings.

3.2.1.2.1 Velocity profiles across the opening for rectangular domain with three openings: This sub- sub subsection (3.2.1.2.1) intends to predict the velocity profiles using equation (3.15) in which, the D.E becomes.

$$\frac{d^2U^*}{dy^{*2}} + \frac{C}{Pr}\frac{dU^*}{dy^*} = -\frac{1}{Pr}\left(\frac{1-\theta_0(1-e^{v_0 Pr})-e^{v_0 Pry^*}}{1-e^{v_0 Pr}}\right). \quad 3.24$$

Since the D.E in (3.24) is non homogeneous, one need to start with the corresponding homogeneous D.E associated with equation (3.24) in order to obtain the complimentary solution,

$$\frac{d^2U^*}{dy^{*2}} + \frac{C}{Pr}\frac{dU^*}{dy^*} = 0, \quad 3.25$$

The corresponding auxiliary equation to equation (3.25) is given by,

$$i^2 + \frac{C}{Pr}i = 0, \quad 3.26$$

where, the roots of the Equation (4.26) are $i_1 = 0, i_2 = -\frac{C}{Pr}$.

The complementary solution $U_{C_1}(y^*)$ of the D.E (3.25) is given by,

$$U_{C_1}(y^*) = C_3 + C_4 e^{-\frac{C}{Pr}y^*}, \quad 3.27$$

where, C_3 and C_4 are arbitrary constant in equation (3.27).

By employing the variation of parameter methods, one can write the particular solution U_{P_1} of equation (3.24) as,

$$U_{P_1}(y^*) = V_1 y_1 + V_2 y_2 . \quad 3.28$$

where, $y_1 = 1\ y_2 = e^{-\frac{C}{Pr}y^*}$, are known functions obtained from equation (3.27) and V_1, V_2 are unknown functions of y^* which can be determined from equation (3.28). In which,

$V_1 = \int \frac{-R_1 y_2^*}{W_1(y_1,y_2)}\,dy^*$, and $V_2 = \int \frac{R_1 y_1^*}{W_1(y_1,y_2)}\,dy^*$,

$$V_1(y^*) = \int \frac{\left(\theta_0(1-e^{-C})+e^{-Cy^*}-1\right)}{C(1-e^{-C})}\,dy^*,$$

$$V_2(y^*) = \frac{1}{C(1-e^{-C})}\int \frac{1-\theta_0(1-e^{-C})-e^{-Cy^*}}{e^{-\frac{C}{Pr}y^*}}\,dy^*. \qquad 3.29$$

where, $R_1 = -\frac{1}{Pr}\left(\frac{1-\theta_0(1-e^{-C})-e^{-Cy^*}}{1-e^{-C}}\right)$, and Wroskian is $W_1(y_1, y_2) = -\frac{C}{Pr}e^{-\frac{C}{Pr}y^*}$.

By integrating equation (3.29), one obtains,

$$V_1(y^*) = \frac{1}{C(1-e^{-C})}\left(\theta_0(1-e^{-C})y^* - \frac{e^{-Cy^*}}{c} - y^*\right),$$

$$V_2(y^*) = \frac{Pre^{\frac{C}{Pr}y^*}}{C^2(1-e^{-C})}\left(1-\theta_0(1-e^{-C}) - \frac{e^{-Cy^*}}{1-Pr}\right). \qquad 3.30$$

Putting equation (3.30) into (3.28), one obtain the particular solution to the D.E (3.24) as,

$$U_{P_1} = \frac{1}{C^2(1-e^{-C})}\left[(\theta_0(1-e^{-C})-1)Cy^* - e^{-Cy^*}\left(1+\frac{Pr}{1-Pr}\right) + Pr\left(1-\theta_0(1-e^{-C})\right)\right]. \quad 3.31$$

The general solution of Equation (3.24) is,

$$U^*(y^*) = U_{P_1}(y^*) + U_{C_1}(y^*),$$

therefore, by inserting Equation (3.27) and (3.31) into $U^*(y^*)$, one obtains the general solution of Equation (3.24) as,

$$U^*(y^*) = C_3 + C_4 e^{-\frac{C}{Pr}y^*} + \frac{1}{C^2\left(1-e^{-C}\right)}\left[(\theta_0(1-e^{-C})-1)Cy^* - e^{-Cy^*}\left(1+\frac{Pr}{1-Pr}\right) + Pr\left(1-\theta_0(1-e^{-C})\right)\right], \quad 3.32$$

The two constant which appear in equation (3.32) can be determined by prescribing the boundary condition for the velocity field in equation (3.17), thus obtaining,

$$U^*(y^*) = U_3^*(y^*) = \frac{1}{C^2\left(1-e^{-C}\right)\left(1-e^{-\frac{C}{Pr}}\right)}\left[\left(1+\frac{Pr}{1-Pr}\right)\left(e^{-C} - e^{-\frac{C}{Pr}} - e^{-\frac{C}{Pr}y^*}(e^{-C}-1) - e^{-Cy^*}\left(1-e^{-\frac{C}{Pr}}\right)\right) + \left(1-\theta_0(1-e^{-C})\right)\left(C - Pr\left(1-e^{-\frac{C}{Pr}}\right) - Ce^{-\frac{C}{Pr}y^*} + \left(1-e^{-\frac{C}{Pr}}\right)(Pr - Cy^*)\right)\right]. \quad 3.33$$

where, $C_3 = \frac{\left(1+\frac{Pr}{1-Pr}\right)\left(e^{-C}-e^{-\frac{C}{Pr}}\right)+\left(1-\theta_0(1-e^{-C})\right)\left(C-Pr\left(1-e^{-\frac{C}{Pr}}\right)\right)}{C^2\left(1-e^{-C}\right)\left(1-e^{-\frac{C}{Pr}}\right)}$, $C_4 = -\frac{1}{C^2\left(1-e^{-C}\right)\left(1-e^{-\frac{C}{Pr}}\right)}\left[\left(1+\frac{Pr}{1-Pr}\right)(e^{-C}-1) + C\left(1-\theta_0(1-e^{-C})\right)\right]$.

3.2.1.2.2 Volumetric airflow in rectangular domain with three openings

This sub- sub subsection (4.2.2.2) intends to predict the volumetric airflow given by (W. G. Brown et al. (1962)),

$$\text{Volumetric airflow} = Q_3^* = A_3^* c_d \int_{n=0}^{n=\frac{y^*}{2}} U_3^*(n)dn. \quad 3.34$$

where, n is any dummy variable.

Integrating equation (3.34), yields to volume airflow as,

$$Q_3^*(y^*) = \frac{A_3^* c_d}{C^2\left(1-e^{-C}\right)\left(1-e^{-\frac{C}{Pr}}\right)}\left[\left(1+\frac{Pr}{1-Pr}\right)\left[\left(e^{-C}-e^{-\frac{C}{Pr}}\right)\frac{y^*}{2}+Pr(e^{-C}-1)\frac{e^{-\frac{C}{2Pr}y^*}}{C}+\right.\right.$$

$$\left.\left(1-e^{-\frac{C}{Pr}}\right)\frac{e^{-C\frac{y^*}{2}}}{C}-Pr\frac{\left(e^{-C}-1\right)}{C}-\frac{\left(1-e^{Pr}\right)}{C}\right]+\left(1-\theta_0(1-e^{-C})\right)\left[-Pr\left(-\frac{C}{Pr}+\left(1-\right.\right.\right.$$

$$\left.\left.\left.e^{-\frac{C}{Pr}}\right)\right)\frac{y^*}{2}+Pre^{-\frac{C}{2Pr}y^*}+\left(1-e^{-\frac{C}{Pr}}\right)\left(Pr\frac{y^*}{2}-C\frac{y^{*2}}{8}\right)-Pr\right]\right]. \quad 3.35$$

3.2.1.2.3 Mass transfer in rectangular domain with three openings

This sub- sub subsection (3.2.1.2.3) intends to predict the mass transfer in rectangular domain with three openings.

Recall, from elementary physics,

$$\text{Density} = \frac{\text{Mass transfer of air}}{\text{Volumetric airflow}}, \quad 3.36$$

$$\text{Mass transfer} = \text{Density of air} \times \text{Volumetric airflow}. \quad 3.37$$

According to **(**Santamouris et al. (1995)) mass transfer is given by,

$$m^*{}_3(y^*) = \rho_0 Q_3^*(y^*). \quad 3.38$$

Putting Equation (3.35) into (3.38), yield the mass transfer as,

$$m_3^*(y^*) = \frac{A_3^* \rho_0 c_d}{C^2\left(1-e^{-C}\right)\left(1-e^{-\frac{C}{Pr}}\right)}\left[\left(1+\frac{Pr}{1-Pr}\right)\left[\left(e^{-C}-e^{-\frac{C}{Pr}}\right)\frac{y^*}{2}+Pr(e^{-C}-1)\frac{e^{-\frac{C}{2Pr}y^*}}{C}+\right.\right.$$

$$\left.\left(1-e^{-\frac{C}{Pr}}\right)\frac{e^{-C\frac{y^*}{2}}}{C}-Pr\frac{\left(e^{-C}-1\right)}{C}-\frac{\left(1-e^{Pr}\right)}{C}\right]+\left(1-\theta_0(1-e^{-C})\right)\left[\left(C-Pr\left(1-e^{-\frac{C}{Pr}}\right)\right)\frac{y^*}{2}+\right.$$

$$\left.Pre^{-\frac{C}{2Pr}y^*}+\left(1-e^{-\frac{C}{Pr}}\right)\left(Pr\frac{y^*}{2}-C\frac{y^{*2}}{8}\right)-Pr\right]\right]. \quad 3.39$$

where, A_3^* is the dimensionless total area of the openings, $\theta^* = \theta_3^*, U^* = U_3^*, Q_3^*, m_3^*(y^*)$ are temperature-, velocity- profiles, volumetric airflow and mass transfer for domain with three openings.

3.2.2 Solution of the dimensionless model equations for rectangular domain with two openings

This sub- section (3.2.2) consists of two sub- sub sections (3.2.2.1) and (3.2.2.2), which intends to describe the solution methods of the dimensionless energy and momentum equations in order to predict temperature profiles and in other hands to predict the velocity profiles, volumetric airflow together with mass transfer across the openings in a cross ventilated rectangular domains with two openings.

3.2.2.1 Solution of the dimensionless energy equations for rectangular domain with two openings

This sub- sub section (3.2.2.1) intends to; describe the solution methods of the dimensionless energy in order to predict temperature profiles across the openings in a rectangular domain with two openings.

The D.E in (3.19) is a homogeneous differential equation, one need to define the corresponding auxiliary Equation associated with the D.E as

$$d^2 = 0, \tag{3.40}$$

where the roots of the equation (3.40) are $d_1 = d_2 = 0$

The solution to the D.E in equation (3.40) is,

$$\theta^*(y^*) = C_5 + C_6 y^*. \quad 3.41$$

where, C_5 and C_6 are arbitrary constants in equation (3.41).

The two constant which appear in equation (3.41) can be determined by prescribing the boundary condition for the temperature profile in equation (3.17), thus obtaining,

$$C_5 = -\theta_0\,, C_6 = 1. \quad 3.42$$

Substituting equation (3.42) into (3.41), yield the temperature profile as,

$$\theta^*(y^*) = \theta_2^*(y^*) = y^* - \theta_0. \quad 3.43$$

3.2.2.2 Solution of the dimensionless momentum equations for rectangular domain with two openings

This sub- subsection also consists of three (3) sub- sub subsections (3.2.2.2.1), (3.2.2.2.2), and (3.2.2.2.3), which intends to describes the solution methods of the dimensionless momentum equation in order to predicts velocity profiles together with volumetric airflow and mass transfer across the openings in a rectangular domain with two openings.

3.2.2.2.1 Velocity profiles across the opening in rectangular domain with two openings

This sub- sub subsection (3.2.2.2.1) intends to predict the dimensionless velocity profiles using the dimensionless momentum equation in (3.18) in which, the D.E becomes.

$$\frac{d^2U^*}{dy^{*2}} = -\frac{1}{Pr}(y^* - \theta_0)\,, \quad 3.44$$

Since the D.E in (3.44) is non homogeneous, one need to start with the corresponding homogeneous D.E associated with Equation (3.44) in order to obtain the complimentary solution,

$$\frac{d^2U^*}{dy^{*2}} = 0. \tag{3.45}$$

The corresponding auxiliary equation to equation (3.45) is given by,

$$f^2 = 0, \tag{3.46}$$

where, the roots of the Equation (3.46) are $f_1 = f_2 = 0$.

The complementary solution $U_{C_2}(y^*)$ of the D.E (3.46) is given by,

$$U_{C_2}(y^*) = C_7 + C_8 y^*, \tag{3.47}$$

where, C_7 and C_8 are arbitrary constant in equation (3.47).

By employing the variation of parameter methods, one can write the particular solution $U_{P_2}(y^*)$ of equation (3.44) as,

$$U_{P_2}(y^*) = V_3(y^*)y_3 + V_4(y^*)y_4\,, \tag{3.48}$$

where, $y_3 = 1$ $y_4 = y^*$, are known functions obtained from Equation (3.47) and V_3, V_4 are unknown functions of y^* which can be determined from Equation (3.48). In which,

$V_3 = \int \frac{-R_2 y_4^*}{W(y_3,y_4)} dy^*$, and $V_2 = \int \frac{R_2 y_3^*}{W(y_3,y_4)} dy^*$,

$$V_3(y^*) = \frac{1}{Pr}\int (y^* - \theta_0) y^*\, dy^*, \tag{3.49}$$

$$V_4(y^*) = -\frac{1}{Pr}\int (y^* - \theta_0)\, dy^*, \tag{3.50}$$

where, $R_2 = -\frac{1}{Pr}(y^* - \theta_0)$, and Wroskian is $W(y_3, y_4) = 1$.

Integrating equation (3.49) and (3.50) with respect to y^*, one obtains,

$$V_3(y^*) = \frac{1}{Pr}\left(\frac{y^{*3}}{3} - \theta_0 \frac{y^{*2}}{2}\right),$$

$$V_4(y^*) = -\frac{1}{Pr}\left(\frac{y^{*2}}{2} - \theta_0 y^*\right), \tag{3.51}$$

Substituting equation (3.51) into (3.48), one obtain the particular solution as,

$$U_{P_2}(y^*) = \frac{1}{Pr}\left(\frac{\theta_0 y^{*2}}{2} - \frac{y^{*3}}{6}\right). \tag{3.52}$$

The general solution of Equation (3.44) is given by,

$$U^*(y^*) = U_{P_2}(y^*) + U_{C_2}(y^*),$$

therefore, inserting equation (3.47) and (3.52) into $U^*(y^*)$, one obtains the general solution of equation (3.44) as,

$$U^*(y^*) = C_7 + C_8 y^* + \frac{1}{Pr}\left(\frac{\theta_0 y^{*2}}{2} - \frac{y^{*3}}{6}\right). \tag{3.53}$$

The two constant which appear in equation (3.53) can be determined by prescribing the boundary condition for the velocity field in equation (3.17), thus obtaining,

$$U^*(y^*) = U_2^*(y^*) = \frac{1}{Pr}\left(\frac{\theta_0 y^{*2}}{2} - \frac{y^{*3}}{6} - \left(\frac{3\theta_0 - 1}{6}\right) y^*\right), \tag{3.54}$$

where, $C_7 = 0, C_8 = -\frac{1}{Pr}\left(\frac{\theta_0}{2} - \frac{1}{6}\right)$.

3.2.2.2.2 Volumetric airflow in rectangular domain with two openings

This sub- sub subsection (3.2.2.2.2) intends to predict the volumetric airflow.

$$\text{Volumetric airflow} = Q_2^* = A_2^* c_d \int_{s=0}^{s=\frac{y^*}{2}} U_2^*(s) ds, \quad 3.55$$

where, s is any dummy variable.

By integrating equation with respect to y^* (3.55), one obtains the volumetric airflow as,

$$Q_2^*(y^*) = \frac{A_2^* c_d}{Pr}\left(\frac{\theta_0}{48} y^{*3} - \frac{1}{384} y^{*4} - \frac{(3\theta_0 - 1)}{48} y^{*2}\right). \quad 3.56$$

3.2.2.2.3 Mass transfer in rectangular domain with two openings

This sub- sub subsection (3.2.2.2.3) intends to predict the mass transfer in rectangular domain with two openings.

$$m_2^*(y^*) = \rho_0 Q_2^*(y^*). \quad 3.57$$

Substituting equation (3.56) into (3.57), one obtains the mass transfer as,

$$m_2^*(y^*) = \frac{A_2^* \rho_0 c_d}{Pr}\left(\frac{\theta_0}{48} y^{*3} - \frac{1}{384} y^{*4} - \frac{(3\theta_0 - 1)}{48} y^{*2}\right). \quad 3.58$$

where, A_2^* is the dimensionless total area of the openings, $\theta_2^*, U_2^*, Q_2^*, m_2^*(y^*)$ are temperature, and velocity- profiles together with volumetric airflow and mass transfer for domain with two openings.

CHAPTER FOUR

ANALYSES, AND DISCUSSION OF THE RESULTS OBTAINED FROM MODEL EQUATIONS AND KEY INTERVENTIONS WITH THE PREVIOUS STUDIES

4.0 PREAMBLE

This chapter consists of three (3) sections which intends to; (4.1) presents the analyses of results for predicted velocity, temperature profiles across the openings together with volumetric airflow and mass- transfer. The analyses of the results are done in order to see the effects of changes of parameters to the overall flow distributions, while keeping other operating conditions and parameters fixed. (4.2) discuss the results obtained from section (4.1), and lastly, (4.3) present the key interventions with the previous studies.

4.1 ANALYSES OF THE RESULTS OBTAINED FOR VELOCITY, TEMPERATURE PROFILES ACROSS THE OPENINGS TOGETHER WITH THE VOLUMETRIC AIRFLOW AND MASS TRANSFER FOR DOMAIN WITH OPENING ON VERTICAL WALL

This section (4.1) consists of two (2) sub- sections which intends to presents; (4.1.1) analyses of the results obtained for predicted velocity-, and temperature- profiles across the openings together with volumetric airflow and mass transfer in the domain with three openings, and (4.1.2) analyses of the results obtained for predicted velocity-, and temperature- profiles together with volumetric airflow and mass transfer in the domain with two openings. The

analyses are done in order to assess the overall behavior of the flow distributions and ascertain the best one for optimal natural ventilation.

4.1.1 Analyses of the results obtained for temperature -, and velocity profiles together with the volumetric airflow and mass transfer for domain with three openings

This sub section (4.1.1) also consists of four sub- subsections (4.1.1.1) , (4.1.1.2) , (4.1.1.3) and (4.1.1.4), that present the analyses of the results obtained in equations (3.23), (3.33), (3.35) and (3.39) for predicted temperature and velocity- profiles together with volumetric airflow and mass transfer in the domain with three openings. The parameters and other operating conditions in the study are shown in Table 4.1.

Table 4.1

Table 4.1 shows the dimensionless parameters and operating conditions used in the rectangular domain with three openings

$A^*_{u1} = A^*_{u2} = 0.7$	$x^*_{l1} = x^*_{u2} = 1.0$	$A^*_{u1} = A^*_{u1} = 0.35$	$y^*_u = 1.0$	$A^*_3 = 0.1633$
ρ_0 $= 1.1849 kg/m^3$	θ_0 $= 0.01, 0.10, 0.19$	c_d $= 0.6, 0.675, 0.75$	Pr $= 0.510, 0.710, 0.910$	

with dimensionless total area of the openings as,

$$A^*_3 = \frac{A^*_l A^*_{u1} A^*_{u2}}{\sqrt{A^{*2}_l + A^{*2}_{u1} + A^{*2}_{u2}}}$$

4.1.1.1 Analyses of the results obtained for temperature profiles in the domain with three openings: This sub- subsection (4.1.1.1) also consists of two sub- sub subsections

(4.1.1.1.1) and (4.1.1.1.2) that present the analyses of the results obtained in equations (3.23), for predicted temperature profiles. The effect of parameters and other operating conditions for temperature profiles using three (3) different values of effective thermal coefficient θ_0: 0.01, 0.10,0.19 and Prandtl number Pr: 0.510, 0.710, 0.910 are shown in Figure 4.1 and 4.2. The maximum values of θ_0 is between the range of 0.35~1 in the presence of internal heat source for fully mixed zone (Yugou, (2001)) and maximum value of $Pr = 0.71$ (Kays and Crawford (1993)).

4.1.1.1.1 Temperature profile using different values of effective thermal coefficient (θ_0) for domain with three openings

The result in equation (3.23) is plotted in Figure 4.1 using three different values of effective thermal coefficient as $\theta_0 = 0.01, 0.10,$ and 0.19.

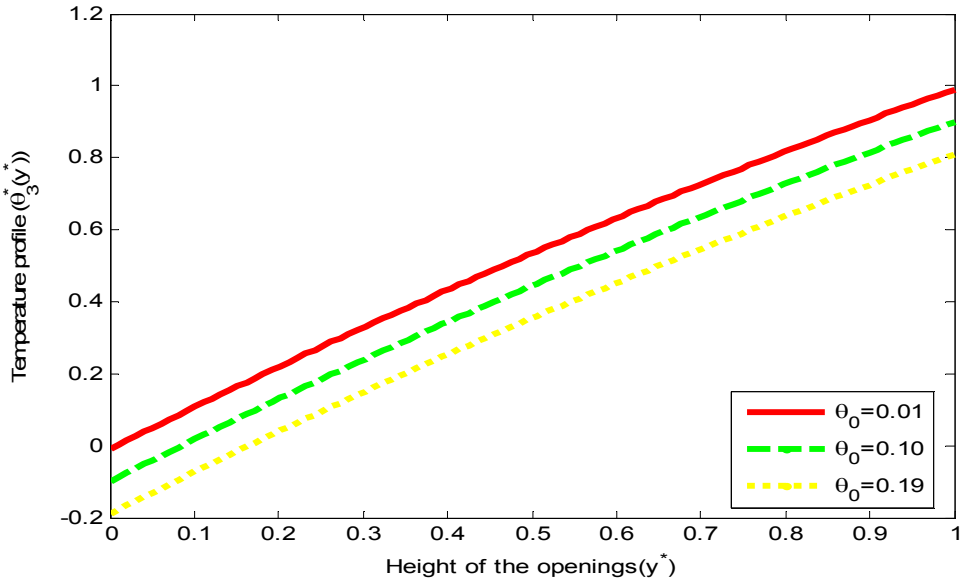

Figure 4.1: Temperature profiles θ_3^* versus $y^*$for different values of effective thermal coefficient θ_0 and fixed $v_0 = -0.5, Pr = 0.710$.

4.1.1.1.2 Temperature profile using different values of Prandtl number (Pr) for domain with three openings

The result in equation (3.23) is plotted in Figure 4.2 using three different values of Prandtl number as $Pr = 0.510,\ 0.710,$ and 0.910.

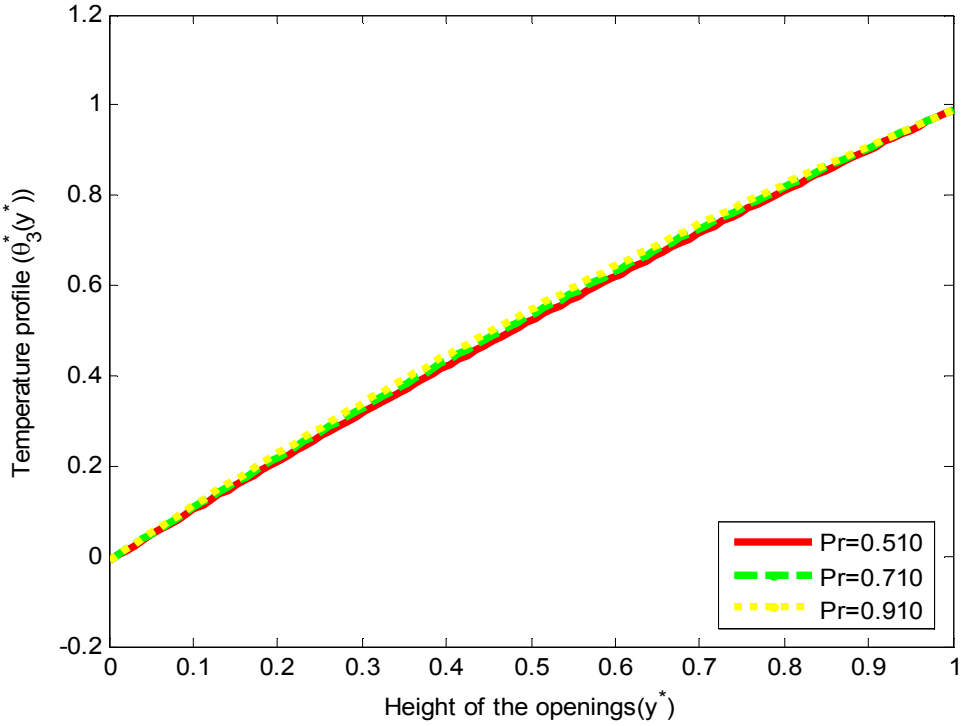

Figure 4.2: Temperature profiles θ_3^* versus $y^*$for different values of Prandtl number Pr and fixed $v_0 = -0.5, \theta_0 = 0.01$.

4.1.1.2 Analyses of the Results obtained for velocity profiles in the domain with three openings

This sub- subsection (4.1.1.2) consists of two sub- sub subsections (4.1.1.2.1) and (4.1.1.2.2) that present the analyses of the results obtained in equations (3.33), for predicted velocity

profiles. The effect of parameters and other operating conditions for the velocity profiles using three (3) different values of effective thermal coefficient θ_0: 0.01, 0.10,0.19 and Prandtl number Pr: 0.510, 0.710, 0.910 are shown in Figure 4.3 and 4.4.

4.1.1.2.1 Velocity profile using different values of effective thermal coefficient (θ_0) for domain with three openings

The result in equation (3.33) is plotted in Figure 4.3 using three different values of effective thermal coefficient as $\theta_0 = 0.01, 0.10,$ and 0.19.

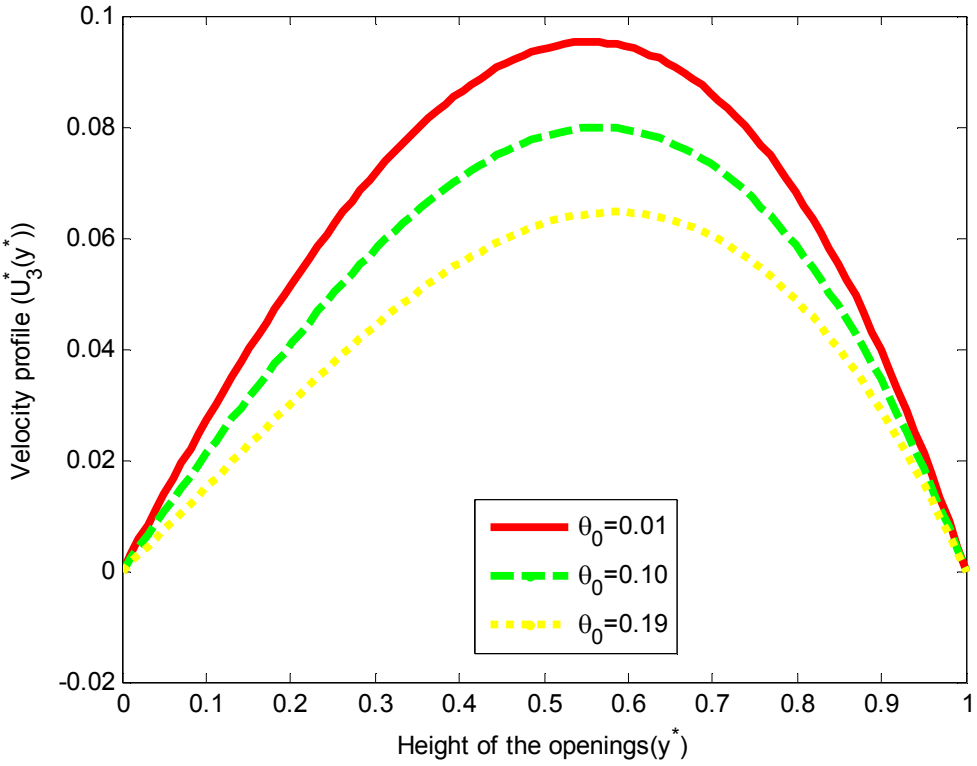

Figure 4.3: Velocity profiles U_3^* versus $y^*$for different values of effective thermal coefficient θ_0 and fixed $v_0 = -0.5, Pr = 0.710$.

4.1.1.2.2 Velocity profile using different values of Prandtl number (Pr) for domain with three openings

The result in equation (3.33) is plotted in Figure 4.4 using three different values of Prandtl number as $Pr = 0.510, 0.710, 0.910$.

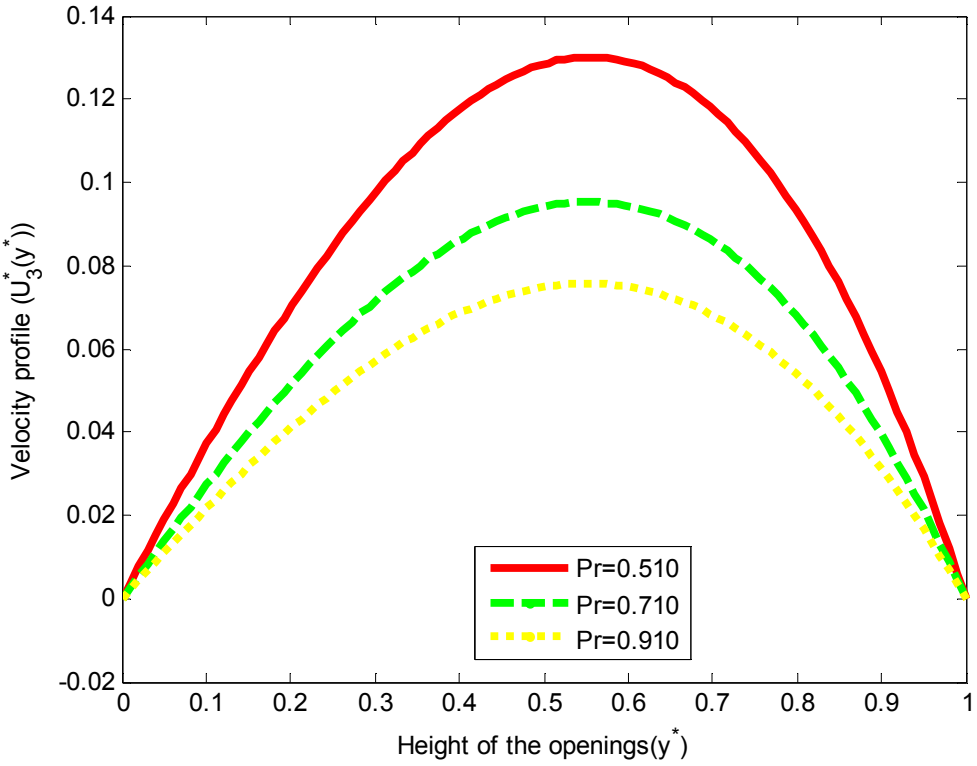

Figure 4.4: Velocity profiles U_3^* versus $y^*$for different values of Prandtl number Pr and fixed $v_0 = -0.5, \theta_0 = 0.01$.

4.1.1.3 Analyses of the Results obtained for volumetric airflow in the domain with three openings

This sub- subsection (4.1.1.3) consists of three sub- sub subsections (4.1.1.3.1), (4.1.1.3.2) and (4.1.1.3.3) that present the analyses of the results obtained in equations (3.35), for

predicted volumetric airflow. The effect of parameters and other operating conditions for the volumetric airflow using three (3) different values of effective thermal coefficient θ_0: 0.01, 0.10,0.19, Prandtl number Pr: 0.510, 0.710, 0.910 and c_d: 0.60, 0.675, 0.75 are shown in Figure 4.5, 4.6 and 4.7.

4.1.1.3.1 Volumetric airflow using different values of effective thermal coefficient (θ_0) for domain with three openings

The result in equation (3.35) is plotted in Figure 4.5 using three different values of effective thermal coefficient as $\theta_0 = 0.01, 0.10,$ and 0.19.

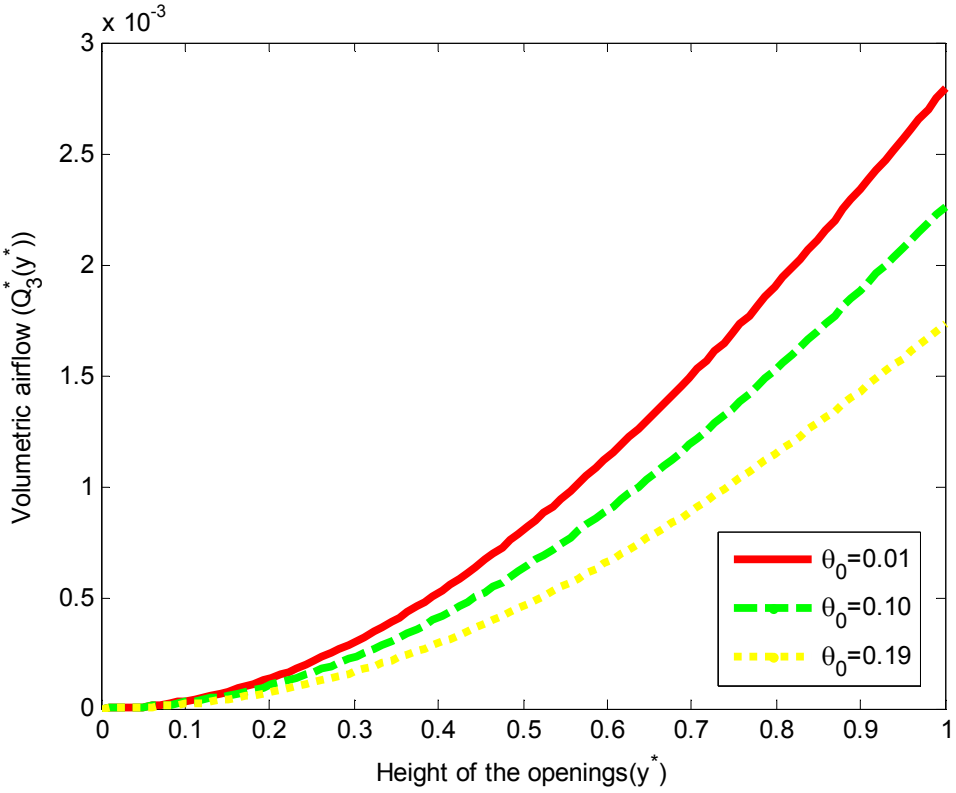

Figure 4.5: Volumetric airflow Q_3^* versus $y^*$for different values of effective thermal coefficient θ_0 and fixed $v_0 = -0.5, Pr = 0.710, A_3^* = 0.1633$.

4.1.1.3.2 Volumetric airflow using different values of Prandtl number (Pr) for domain with three openings

The result in equation (3.35) is plotted in Figure 4.6 using three different values of Prandtl number as $Pr = 0.510, 0.710,$ and 0.910.

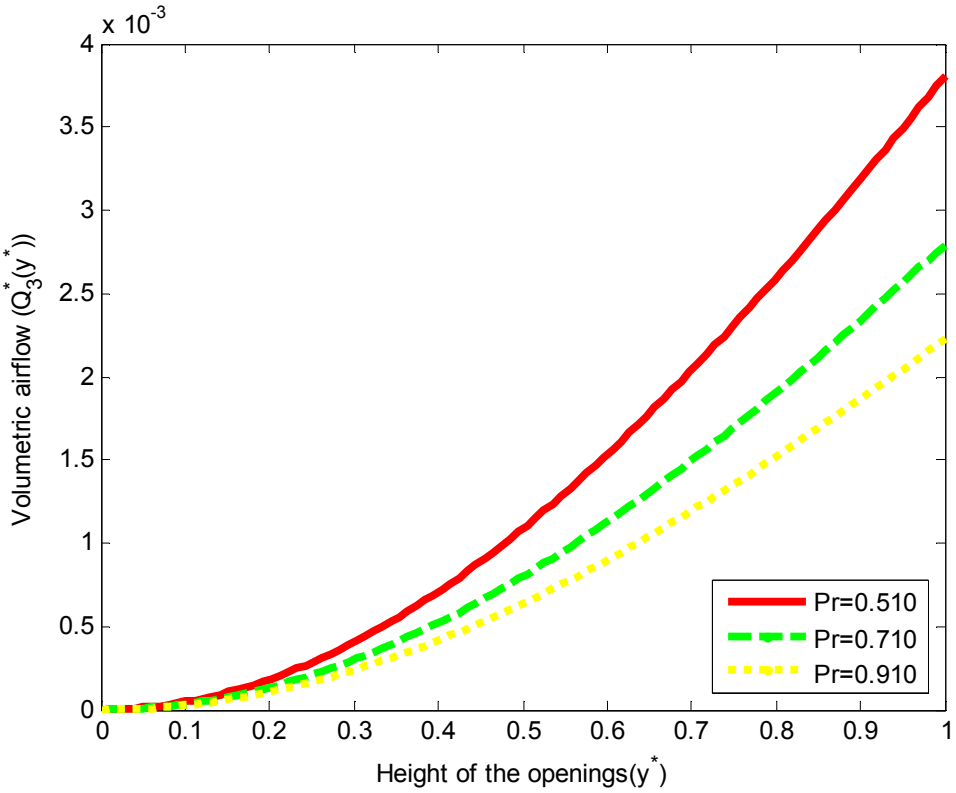

Figure 4.6: Volumetric airflow Q_3^* versus $y^*$for different values of Prandtl number Pr and fixed $v_0 = -0.5, \theta_0 = 0.01, c_d = 0.60,\ A_3^* = 0.1633$.

4.1.1.3.3 Volumetric airflow using different values of discharge coefficient (c_d) for domain with three openings

The result in equation (3.35) is plotted in Figure 4.7 using three different values of discharge coefficient as $c_d = 0.60,\ 0.675,$ and 0.75.

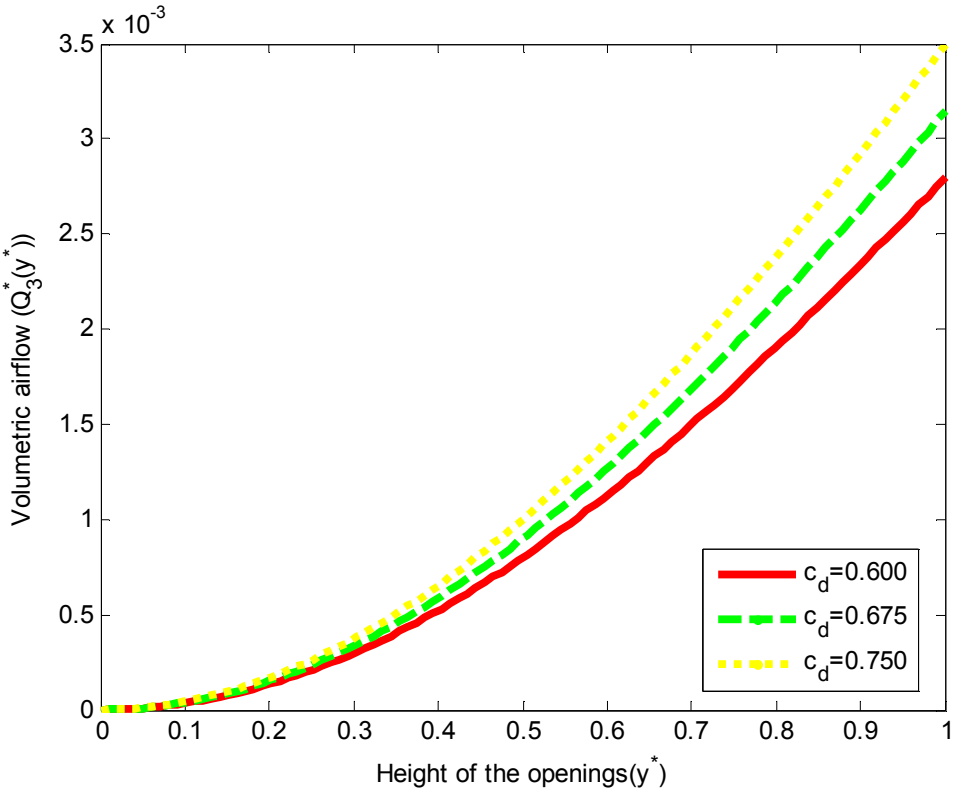

Figure 4.7: Volumetric airflow Q_3^* versus $y^*$for different values of discharge coefficient c_d and fixed $v_0 = -0.5, \theta_0 = 0.01, Pr = 0.710,\ A_3^* = 0.1633$.

4.1.1.4 Analyses of the Results obtained for mass transfer in the domain with three openings

This sub- subsection (4.1.1.4) consists of three sub- sub subsections (4.1.1.4.1), (4.1.1.4.2) and (4.1.1.4.3) that present the analyses of the results obtained in equations (3.39), for predicted mass transfer. The effect of parameters and other operating conditions for the dimensionless mass transfer using three (3) different values of effective thermal coefficient θ_0: 0.01, 0.10,0.19, Prandtl number Pr: 0.510, 0.710, 0.910 and c_d: 0.60, 0.675, 0.75 are shown in Figure 4.8, 4.9 and 4.10.

4.1.1.4.1 Mass transfer using different values of effective thermal coefficient (θ_0) for domain with three openings

The result in equation (3.39) is plotted in Figure 4.8 using three different values of effective thermal coefficient as $\theta_0 = 0.01, 0.10,$ and 0.19.

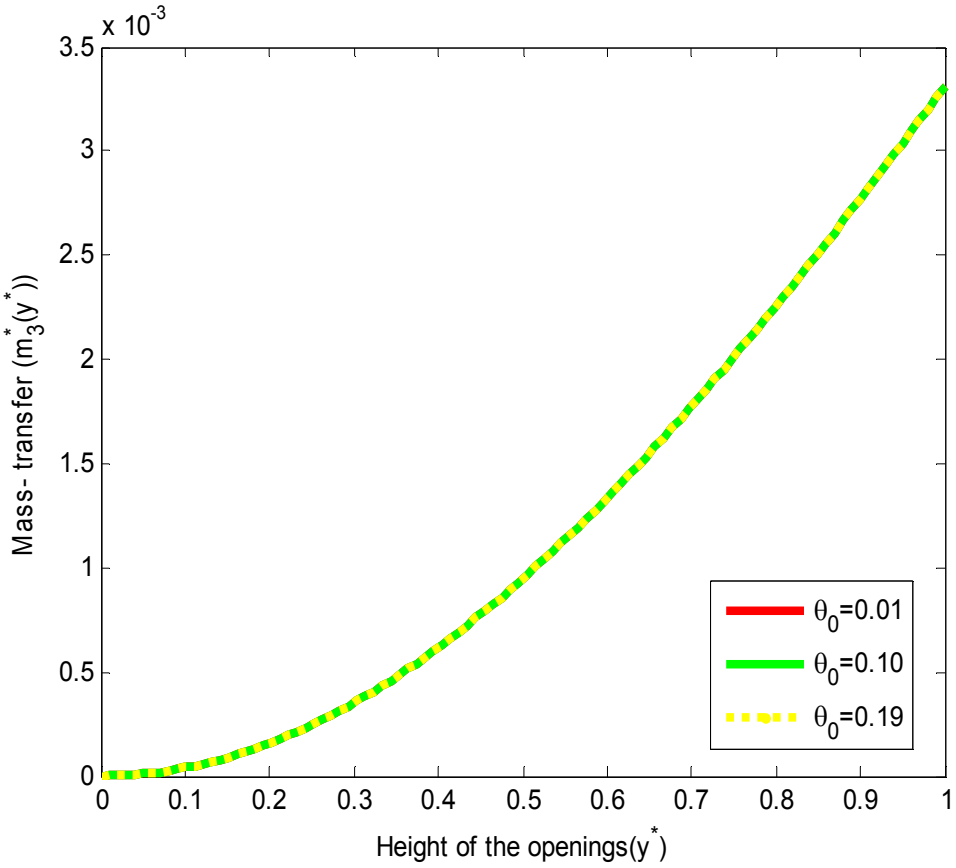

Figure 4.8: Mass transfer m_3^* versus $y^*$for different values of effective thermal coefficient θ_0 and fixed $v_0 = -0.5, Pr = 0.710, A_3^* = 0.1633, \rho_0 = 1.1849, c_d = 0.6$.

4.1.1.4.2 Mass transfer using different values of Prandtl number (Pr) for domain with three openings

The result in equation (3.39) is plotted in Figure 4.9 using three different values of Prandtl number as $Pr = 0.510, 0.710,$ and 0.910.

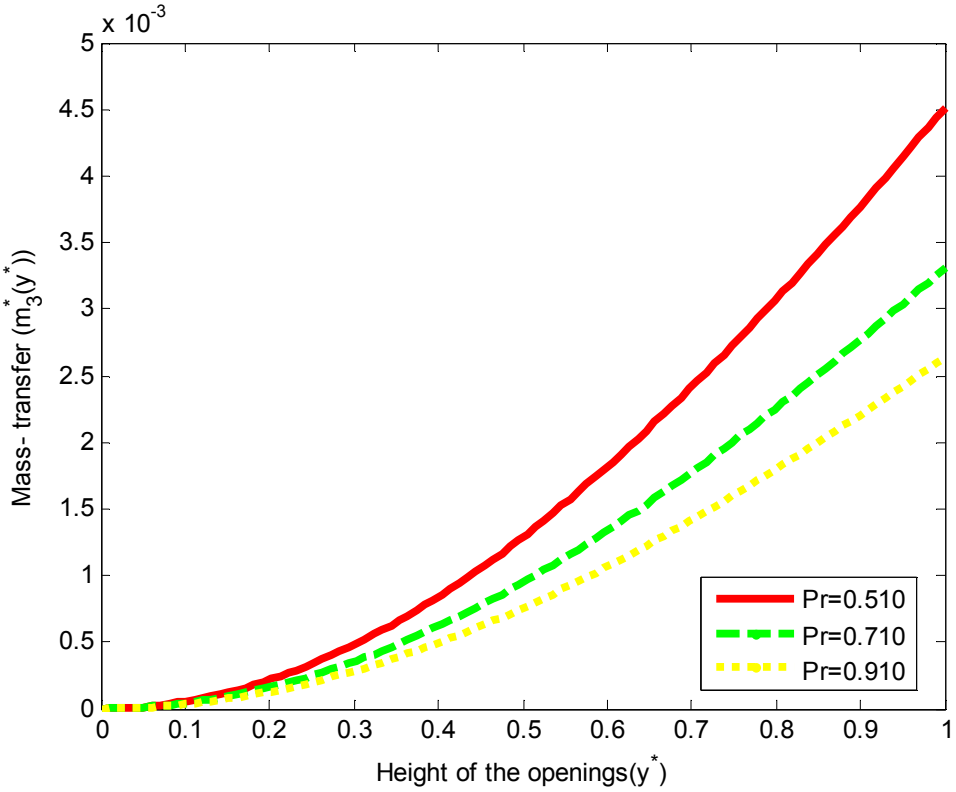

Figure 4.9: Mass transfer m_3^* versus $y^*$for different values of Prandtl number Pr and fixed $v_0 = -0.5, \theta_0 = 0.01, A_3^* = 0.1633, \rho_0 = 1.1849, c_d = 0.6$.

4.1.1.4.3 Mass transfer using different values of discharge coefficient (c_d) for domain with three openings

The result in equation (3.39) is plotted in Figure 4.10 using three different values of discharge coefficient as $c_d = 0.60,\ 0.675,$ and 0.75.

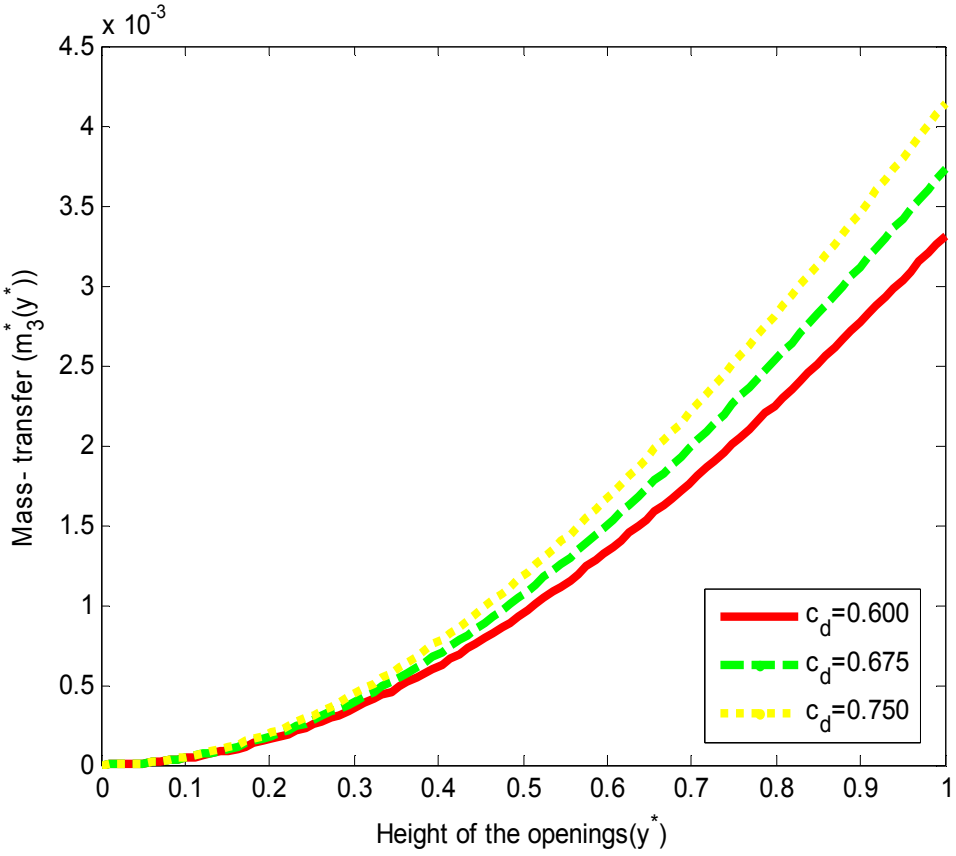

Figure 4.10: Mass transfer m_3^* versus y^* for different values of discharge coefficient c_d and fixed $v_0 = -0.5, Pr = 0.710, A_3^* = 0.1633, \rho_0 = 1.1849, \theta_0 = 0.01$.

4.1.2 Analyses of the Results obtained for temperature -, and velocity profiles together with the volumetric airflow and mass transfer for domain with two openings

This sub section (4.1.2) also consists of four sub- subsections (4.1.2.1) , (4.1.2.2) , (4.1.2.3) and (4.1.2.4) the present the analyses of the results obtained in equations (3.43), (3.54), (3.56) and (3.58) for predicted temperature-, and velocity- profiles together with volumetric airflow and mass transfer in the domain with two openings. The parameters and other operating conditions works in the study are shown in Table 4.2.

Table 4.2

Table 4.2 shows the dimensionless parameters and operating conditions used same as in Table 4.1.

$y^* = y_l^* = 1.0$	$x_l^* = x_u^* = 1.0$	$A_l^* = 0.35$	$y_u^* = 1.0$	$A_u^* = 0.7$
$A_2^* = 0.3131$				

where, dimensionless quantities for height, width and area of the openings are as follows,

$y^* = y_l^* = \frac{y}{L}$, $A_u^* = \frac{y_u x_u}{L^2}$, $A_l^* = \frac{y_l x_l}{L^2}$, $x_l^* = \frac{x_l}{L}$, $x_u^* = \frac{x_u}{L}$, $y_u^* = \frac{y_u}{L}$, and $A_2^* = \frac{A_l^* A_u^*}{\sqrt{A^{*2}l + A^{*2}u}}$

4.1.2.1 Analyses of the results obtained for temperature profiles in the domain with two openings

This sub- subsection (4.1.2.1) consists of the following sub- sub subsection (4.1.2.1.1), which intends to presents the analyses of the results obtained in equations (3.43), for predicted temperature profiles. The effect of parameters and other operating conditions for the temperature profiles using three (3) different values of effective thermal coefficient θ_0: 0.01, 0.10,0.19 is shown in Figure 4.11.

4.1.2.1.1 Temperature profile using different values of effective thermal coefficient (θ_0) for domain with two openings

The result in equation (3.43) is plotted in Figure 4.11 using three different values of effective thermal coefficient as $\theta_0 = 0.01, 0.10,$ and 0.19.

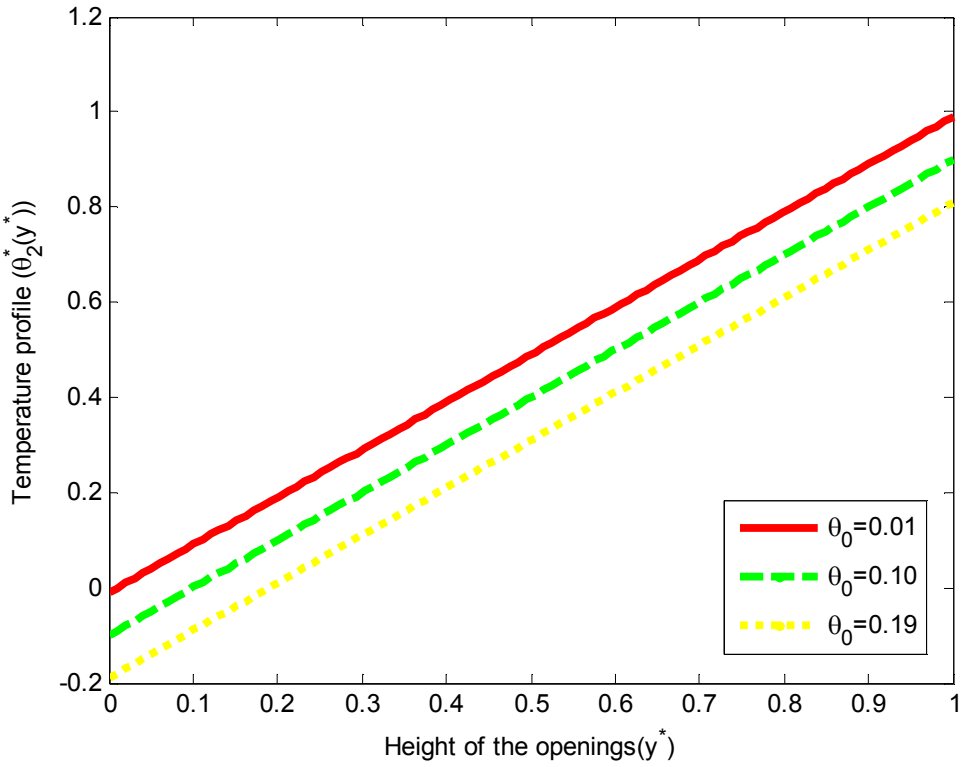

Figure 4.11: Temperature profiles θ_2^* versus $y^*$for different values of effective thermal coefficient θ_0.

4.1.2.2 Analyses of the results obtained for velocity profiles in the domain with two openings

This sub- subsection (4.1.2.2) consists of two sub- sub subsections (4.1.2.2.1) and (4.1.2.2.2) the present the analyses of the results obtained in equations (3.43), for predicted velocity profiles. The effect of parameters and other operating conditions for the velocity profiles using three (3) different values of effective thermal coefficient θ_0: 0.01, 0.10,0.19 and Prandtl number Pr: 0.510, 0.710, 0.910 are shown in Figure 4.12 and 4.13.

4.1.2.2.1 Velocity profile using different values of effective thermal coefficient (θ_0) for domain with two openings

The result in equation (3.54) is plotted in Figure 4.12 using three different values of effective thermal coefficient as $\theta_0 = 0.01, 0.10,$ and 0.19.

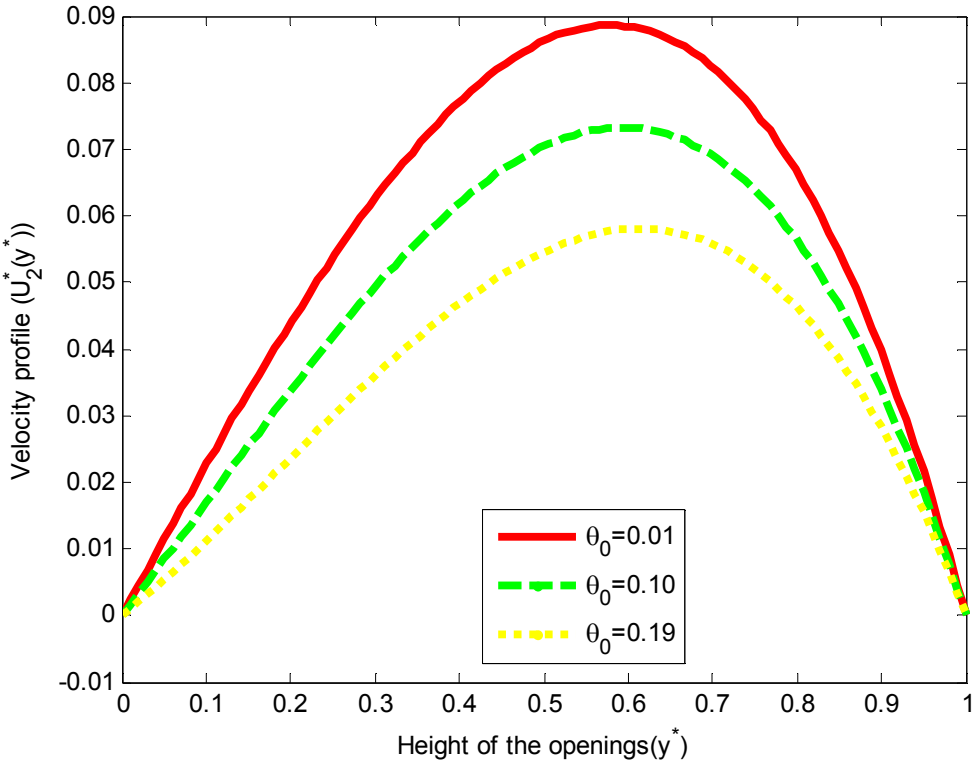

Figure 4.12: Velocity profiles U_2^* versus y^* for different values of effective thermal coefficient θ_0 and fixed $Pr = 0.710$.

4.1.1.2.2 Velocity profile using different values of Prandtl number (Pr) for domain with two openings

The result in equation (3.54) is plotted in Figure 4.13 using three different values of Prandtl number as $Pr = 0.510, 0.710, 0.910$.

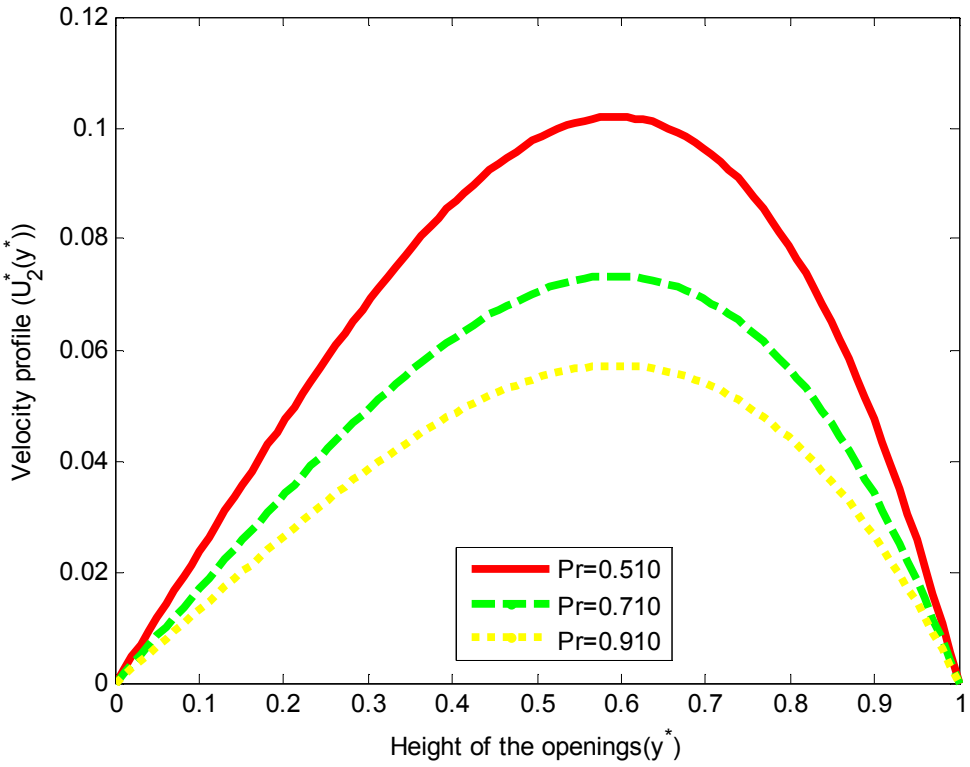

Figure 4.13: Velocity profiles U_2^* versus $y^*$for different values of Prandtl number Pr and fixed $\theta_0 = 0.01$.

4.1.2.3 Analyses of the results obtained for volumetric airflow in the domain with two openings

This sub- subsection (4.1.2.3) consists of three sub- sub subsections (4.1.2.3.1), (4.1.2.3.2) and (4.1.2.3.3) that present the analyses of the results obtained in equations (3.35), for predicted volumetric airflow. The effect of parameters and other operating conditions for the volumetric airflow using three (3) different values of effective thermal coefficient θ_0: 0.01, 0.10,0.19, Prandtl number Pr: 0.510, 0.710, 0.910 and c_d: 0.60, 0.675, 0.75 are shown in Figure 4.14, 4.15 and 4.16.

4.1.2.3.1 Volumetric airflow using different values of effective thermal coefficient (θ_0) for domain with two openings

The result in equation (3.56) is plotted in Figure 4.14 using three different values of effective thermal coefficient as $\theta_0 = 0.01, 0.10,$ and 0.19.

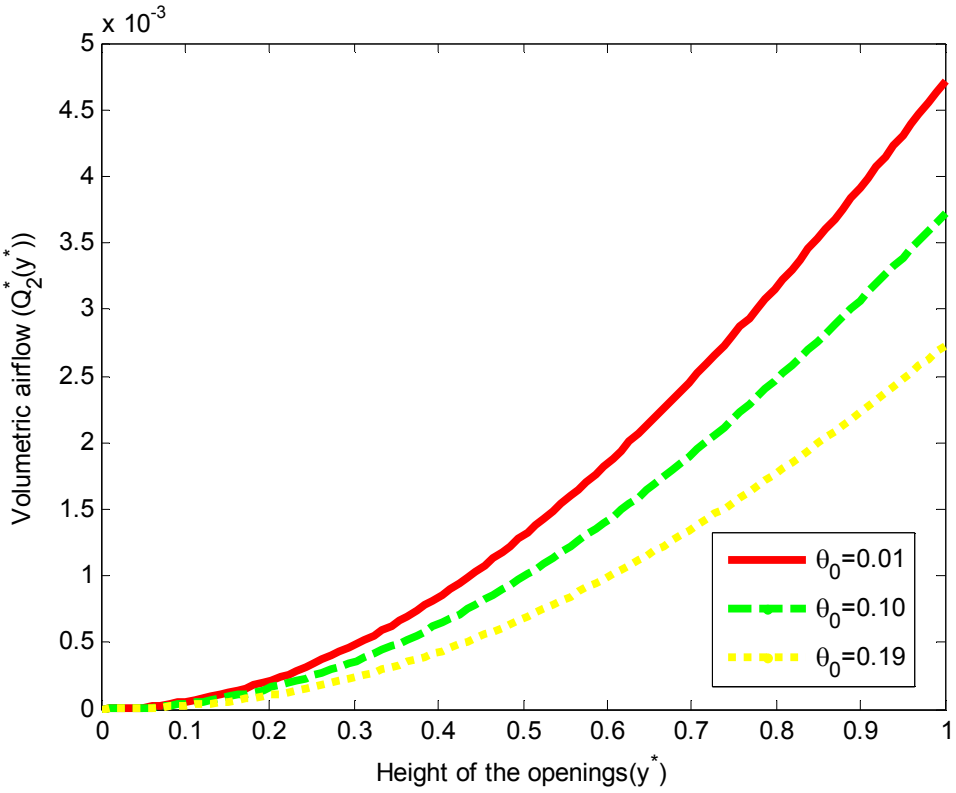

Figure 4.14: Volumetric airflow Q_2^* versus $y^*$for different values of effective thermal coefficient θ_0 and fixed $Pr = 0.710, A_2^* = 0.3131, c_d = 0.6$.

4.1.2.3.2 Volumetric airflow using different values of Prandtl number (Pr) for domain with two openings

The result in equation (3.35) is plotted in Figure 4.6 using three different values of Prandtl number as $Pr = 0.510, 0.710,$ and 0.910.

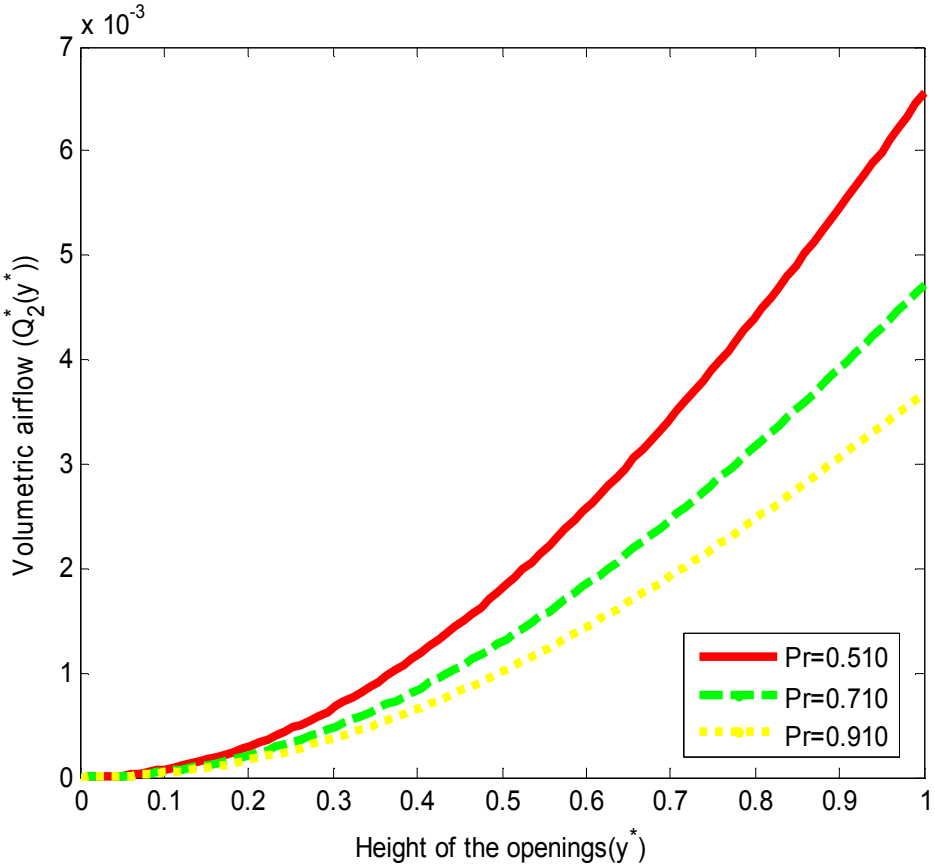

Figure 4.15: Volumetric airflow Q_2^* versus $y^*$for different values of Prandtl number Pr and fixed $\theta_0 = 0.01, c_d = 0.60,\ A_3^* = 0.1633.$

4.1.2.3.3 Volumetric airflow using different values of discharge coefficient (c_d) for domain with two openings

The result in equation (3.56) is plotted in Figure 4.16 using three different values of discharge coefficient as $c_d = 0.60,\ 0.675,$ and $0.75.$

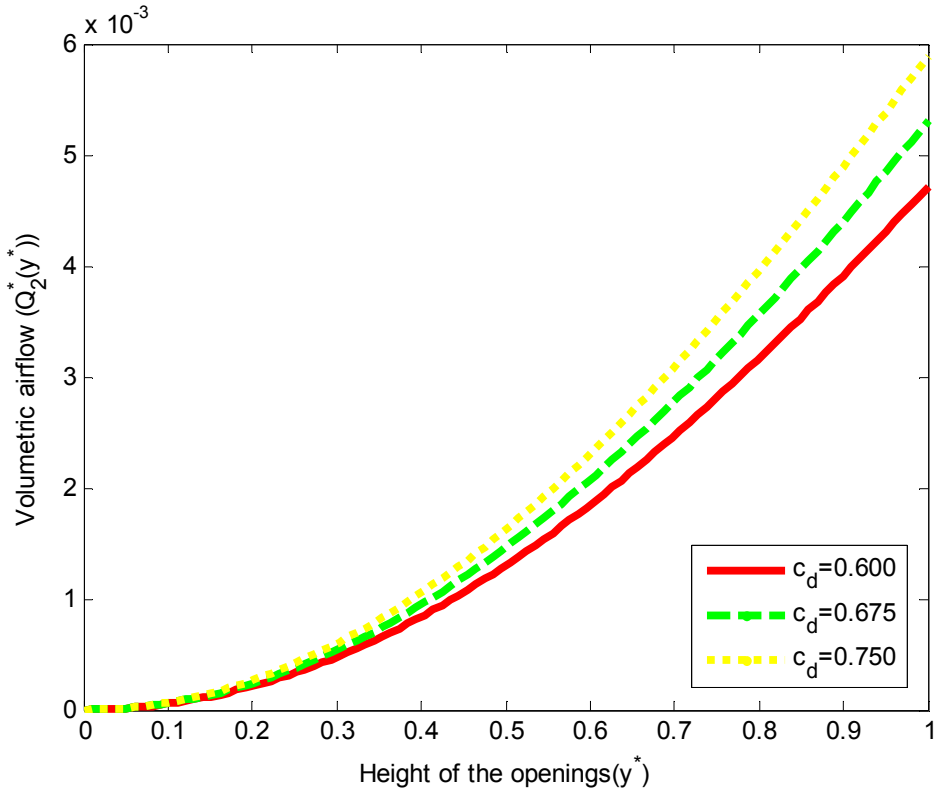

Figure 4.16: Volumetric airflow Q_2^* versus $y^*$for different values of discharge coefficient c_d and fixed $\theta_0 = 0.01, Pr = 0.710,\ A_2^* = 0.3131.$

4.1.2.4 Analyses of the results obtained for mass transfer in the domain with two openings

This sub- subsection (4.1.2.4) consists of three sub- sub subsections (4.1.2.4.1), (4.1.2.4.2) and (4.1.2.4.3) that present the analyses of the results obtained in equations (3.58), for predicted mass transfer. The effect of parameters and other operating conditions for the dimensionless mass transfer using three (3) different values of effective thermal coefficient θ_0: 0.01, 0.10,0.19, Prandtl number Pr: 0.510, 0.710, 0.910 and c_d: 0.60, 0.675, 0.75 are shown in Figure 4.17, 4.18 and 4.19.

4.1.2.4.1 Mass transfer using different values of effective thermal coefficient (θ_0) for domain with two openings

The result in equation (3.58) is plotted in Figure 4.17 using three different values of effective thermal coefficient as $\theta_0 = 0.01, 0.10,$ and 0.19.

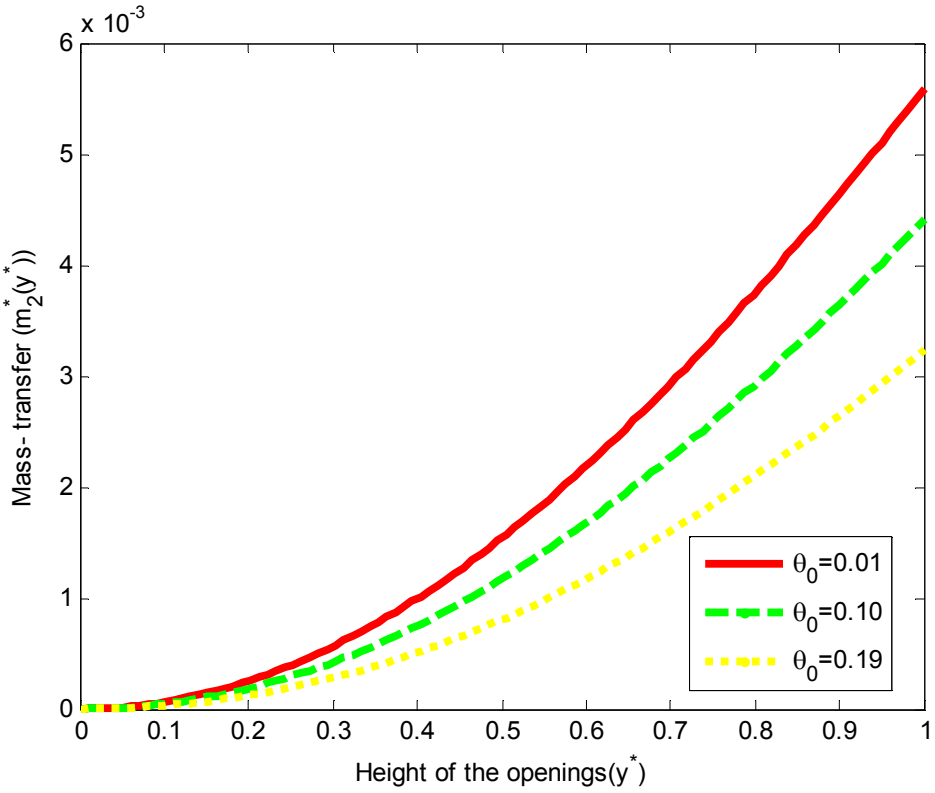

Figure 4.17: Mass transfer m_2^* versus $y^*$for different values of effective thermal coefficient θ_0 and fixed $Pr = 0.710, A_2^* = 0.3131, \rho_0 = 1.1849, c_d = 0.6$.

4.1.2.4.2 Mass transfer using different values of Prandtl number (Pr) for domain with two openings

The result in equation (3.58) is plotted in Figure 4.18 using three different values of Prandtl number as $Pr = 0.510, 0.710,$ and 0.910.

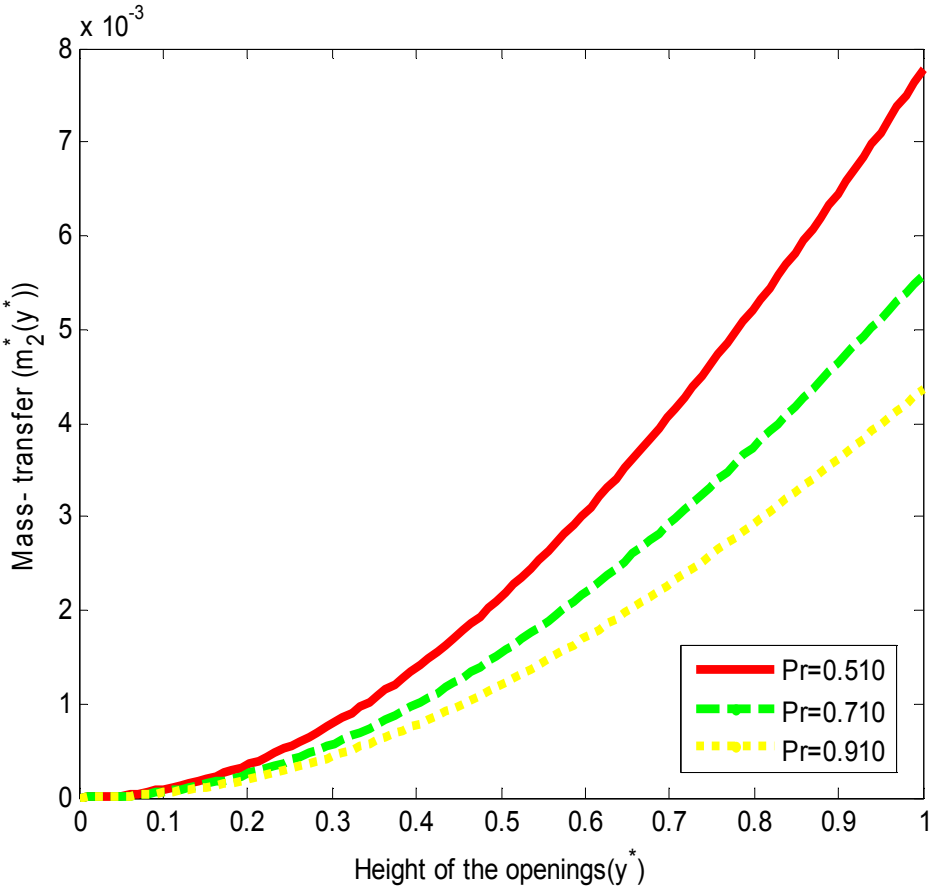

Figure 4.18: Mass transfer m_2^* versus $y^*$for different values of Prandtl number Pr and fixed $\theta_0 = 0.01, A_2^* = 0.3131, \rho_0 = 1.1849, c_d = 0.6$.

4.1.2.4.3 Mass transfer using different values of discharge coefficient (c_d) for domain with two openings

The result in equation (3.58) is plotted in Figure 4.19 using three different values of discharge coefficient as $c_d = 0.60,\ 0.675$, and 0.75.

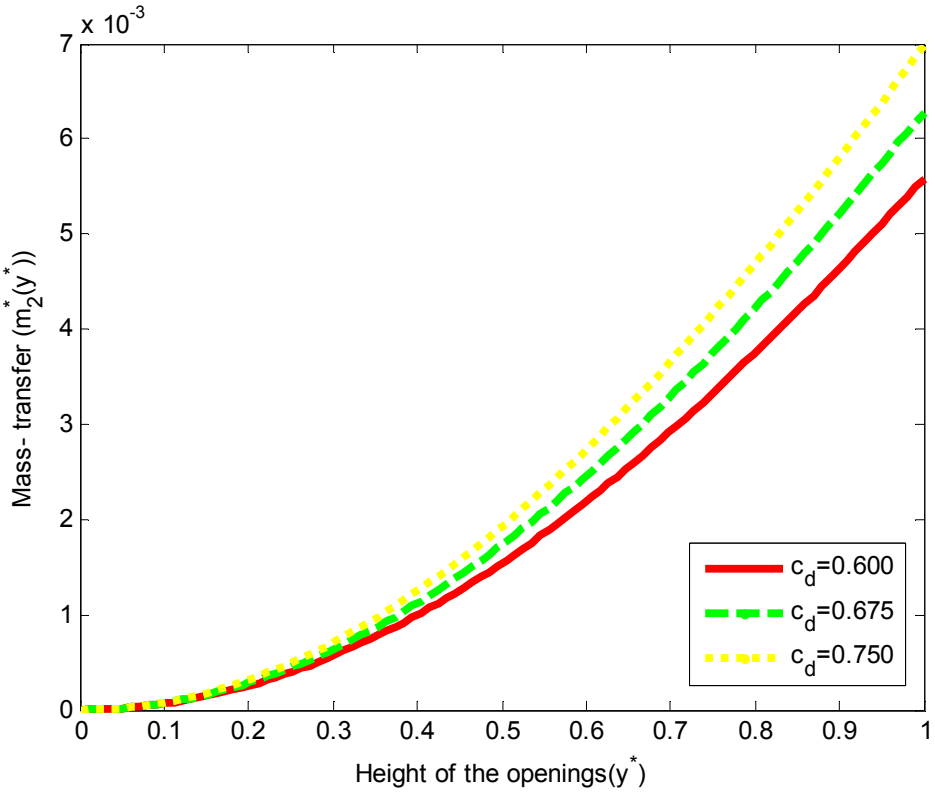

Figure 4.19: Mass transfer m_2^* versus y^* for different values of discharge coefficient c_d and fixed $Pr = 0.710, A_2^* = 0.3131, \rho_0 = 1.1849, \theta_0 = 0.01$.

4.2 DISCUSSION OF THE RESULTS OBTAINED FOR UN- STRATIFIED CROSS VENTILATED RECTANGULAR DOMAIN WITH OPENINGS ON VERTICAL WALLS

In this section (4.2) the main features of the results obtained from the previous section (4.1) will be discussed. The section (4.2) also consists of two (2) sub- sections which intends to; (4.2.1) discuss the analyses obtained for predicted velocity-, and temperature- profiles together with volumetric airflow and mass transfer in the domain with three openings, and

(4.2.2) discuss the analyses obtained for predicted velocity-, and temperature- profiles together with volumetric airflow and mass transfer in the domain with two openings.

4.2.1 Discussion of the results obtained from the analyses for predicted temperature, and velocity profiles together with the volumetric airflow and mass transfer in the domain with three openings

This sub section (4.2.1) intends to discuss the analyses obtained from the graphs depicted in Figure 4.1- 4.10.

Figure 4.1 depicts the effect of effective thermal coefficient θ_0 on temperature profiles θ_3^*. It is observed that the temperature profiles θ_3^* across the openings increases as effective thermal coefficient θ_0 decreases. The feature observed there is a linear temperature distribution. Due to the opposing flow in the upper openings in the domain, the effect of buoyancy forces are found to be strong. Maximum temperature θ_3^* is larger when $\theta_0 = 0.01$ and minimum when $\theta_0 = 0.19$. Therefore, the best value of effective thermal coefficient that provided thermal comfort in the domain is when $\theta_0 = 0.01$.

Figure 4.2 depicts the effect of Prandtl number Pr on temperature profiles θ_3^*. It is observed that temperature profiles across the openings increases as Prandtl number Pr increases. The feature observed is that, the lines of flow are almost linearly the same, due to the opposing flow in the upper opening, this lead to the minimal changes in temperature between interior and ambient, and therefore, the effect of buoyancy forces are also strong. Maximum temperature θ_3^* is larger when $Pr = 0.910$ and minimum when $Pr = 0.510$. Therefore, the temperature profiles θ_3^* is not within thermal comfort unless for the maximum value of Prandtl number $Pr = 0.910$.

Figure 4.3 depicts the effect of effective thermal coefficient θ_0 on velocity profiles U_3^*. It is observed that velocity profiles U_3^* across the openings increases as effective thermal coefficient θ_0 decreases. The feature observed is that, the flow starts from the floor with initial velocity $U_3^* = 0$, the formed a plume. The upward motion appears until the steady state flow of convection motion is reached. This fact depends on the pressure that lifted the air up to the neutral height $y^* = 0.5$, then drives the air out of the domain through the upper opening with an indirect velocity $v_0 = -0.5$. Positive buoyancy forces dominate, so that no back flows occur in this case. Maximum velocity U_3^* is larger when $\theta_0 = 0.01$ and minimum when $\theta_0 = 0.19$. Therefore, the best value of effective thermal coefficient θ_0 that gives effective ventilation in the domain is at minimal value of effective thermal coefficient $\theta_0 = 0.01$.

Figure 4.4 depicts the effect of Prandtl number Pr on velocity profiles U_3^*. It is observed that velocity profiles U_3^* across the openings increases as Prandtl number Pr decreases. The feature observed is that, the flow starts from the floor with initial velocity $U_3^* = 0$, the formed a plume. The upward motion appears until the steady state flow of convection motion is reached. This fact depends on the pressure that lifted the air up to the neutral height $y^* = 0.5$, then drives the air out of the domain through the upper opening with an indirect velocity of $v_0 = -0.5$. Positive buoyancy forces dominate, so that no back flows occur in this case. Maximum velocity U_3^* is larger when $Pr = 0.510$ and minimum when $Pr = 0.910$. Therefore, the best value of Prandtl number Pr that gives effective ventilation in the domain is at minimal value of Prandtl number $Pr = 0.510$.

Figure 4.5 depicts the effect of effective thermal coefficient θ_0 on volumetric airflow Q_3^*. It is observed that the volumetric airflow Q_3^* in the domain increases as effective thermal coefficient θ_0 decreases. The feature observed is due to the opposing flow in the upper opening, the effect of buoyancy is strong; this leads to the steady flow before it reached the maximal height. Maximum volumetric airflow Q_3^* is obtained when $\theta_0 = 0.01$ and minimum when $\theta_0 = 0.19$. Therefore, the best value of effective thermal coefficient for optimal ventilation in the domain is when $\theta_0 = 0.01$.

Figure 4.6 depicts the effect of Prandtl number Pr on volumetric airflow Q_3^*. It is observed that the volumetric airflow Q_3^* in the domain increases as Prandtl number Pr decreases. The feature observed due to the opposing flow in the upper opening, effect of buoyancy is strong; this leads to the steady flow before it reached the maximal height. Maximum volumetric airflow Q_3^* is larger when $Pr = 0.510$ and minimum when $Pr = 0.910$. Therefore, the best value of Prandtl number Pr for optimal ventilation in the domain is when $Pr = 0.510$.

Figure 4.7 depicts the effect of discharge coefficient c_d on volumetric airflow Q_3^*. It is observed that the volumetric airflow Q_3^* in the domain increases as discharge coefficient c_d increases. The feature observed due to the opposing flow in the upper openings, the effect of buoyancy is strong; this leads to the steady flow before it reached the maximal height. Maximum volumetric airflow Q_3^* is larger when $c_d = 0.75$ and minimum when $c_d = 0.60$. Therefore, the best value of discharge coefficient c_d for optimal ventilation in the domain is when $c_d = 0.75$.

Figure 4.8 depicts the effect of effective thermal coefficient θ_0 on mass transfer m_3^*. It is observed that the mass transfer m_3^* increases as effective thermal coefficient θ_0 decreases.

The feature observed is that mass transfer m_3^* is minimal due to the strong opposing flow in the upper openings. Maximum mass transfer m_3^* is larger when $\theta_0 = 0.01$ and minimum when $\theta_0 = 0.19$. Therefore, the best value of effective thermal coefficient for optimal ventilation in the domain is when $\theta_0 = 0.01$.

Figure 4.9 depicts the effect of Prandtl number Pr on mass transfer m_3^*. It is observed that the mass transfer m_3^* increases as Prandtl number Pr decreases. The feature observed is that, mass transfer m_3^* cannot easily remove when Prandtl number $Pr = 0.910$. Maximum mass transfer m_3^* is larger when $Pr = 0.510$ and minimum when $Pr = 0.910$. Therefore, the best value of Prandtl number Pr for optimal ventilation in the domain is when $Pr = 0.510$.

Figure 4.10 depicts the effect of discharge coefficient c_d on mass transfer m_3^*. It is observed that the mass transfer m_3^* increases as discharge coefficient c_d increases. The feature observed is that, mass transfer m_3^* cannot easily remove when $c_d = 0.60$. Maximum mass transfer m_3^* is larger when $c_d = 0.75$ and minimum when $c_d = 0.60$. Therefore, the best value of discharge coefficient c_d for optimal ventilation in the domain is when $c_d = 0.75$.

4.2.2 Discussion of the results obtained from the analyses for predicted temperature, and velocity profiles together with the volumetric airflow and mass transfer in the domain with two openings

This sub section (4.2.2) intends to discuss the analyses obtained from the graphs depicted in Figure 4.11- 4.19.

Figure 4.11 depicts the effect of effective thermal coefficient θ_0 on temperature profiles θ_2^*. It is observed that the temperature profiles θ_2^* across the openings increases as effective thermal coefficient θ_0 decreases. The feature observed is there is a linear temperature distributions,

due to the absence of opposing flow in the upper opening in the domain the effect of buoyancy forces is not strong. Maximum temperature θ_2^* is larger when $\theta_0 = 0.01$ and minimum when $\theta_0 = 0.19$. Therefore, the best value of effective thermal coefficient that provided thermal comfort in the domain is when $\theta_0 = 0.01$.

Figure 4.12 depicts the effect of effective thermal coefficient θ_0 on velocity profiles U_2^*. It is observed that the velocity profiles U_2^* across the openings increases as effective thermal coefficient θ_0 decreases. The feature observed is that, the flow starts from the floor with initial velocity $U_2^* = 0$, the formed a plume. The upward motion appears until the steady state of convection motion is reached. This fact depends on the pressure that lifted the air up to the neutral height $y^* = 0.5$, then drives the air out of the domain through the upper opening. Maximum velocity U_2^* is larger when $\theta_0 = 0.01$ and minimum when $\theta_0 = 0.19$. Therefore, the best value for effective thermal coefficient θ_0 that gives effective ventilation in the domain is when effective thermal coefficient $\theta_0 = 0.01$.

Figure 4.13 depicts the effect of Prandtl number Pr on velocity profiles U_2^*. It is observed that the velocity profiles U_2^* across the openings increases as Prandtl number Pr decreases. The feature observed is that, the flow starts from the floor with initial velocity $U_2^* = 0$, the formed a plume. The upward motion appears until the steady state flow of convection motion is reached. This fact depends on the pressure that lifted the air up to the neutral height $y^* = 0.5$, then drives the air out of the domain through the upper opening. Maximum velocity U_2^* is larger when $Pr = 0.510$ and minimum when $Pr = 0.910$. Therefore, the best value for Prandtl number Pr that gives effective ventilation in the domain is at minimal value of Prandtl number $Pr = 0.510$.

Figure 4.14 depicts the effect of effective thermal coefficient θ_0 on volumetric airflow Q_2^*. It is observed that the volumetric airflow Q_2^* in the domain increases as effective thermal coefficient θ_0 decreases. The feature observed due to the absence of opposing flow in the upper opening, the effect of buoyancy is not strong; this leads to the flow curves to reach the maximal height easily. Maximum volumetric airflow Q_2^* is larger when $\theta_0 = 0.01$ and minimum when $\theta_0 = 0.19$. Therefore, the best value of effective thermal coefficient for optimal ventilation in the domain is when $\theta_0 = 0.01$.

Figure 4.15 depicts the effect of Prandtl number Pr on volumetric airflow Q_2^*. It is observed that the volumetric airflow Q_2^* in the domain increases as Prandtl number Pr decreases. The feature observed due to the absence of opposing flow in the upper opening, the effect of buoyancy is not strong; this leads to the flow curves to reach the maximal height easily. Maximum volumetric airflow Q_2^* is larger when $Pr = 0.510$ and minimum when $Pr = 0.910$. Therefore, the best value of Prandtl number Pr for optimal ventilation in the domain is when $Pr = 0.510$.

Figure 4.16 depicts the effect of discharge coefficient c_d on volumetric airflow Q_2^*. It is observed that the volumetric airflow Q_2^* in the domain increases as discharge coefficient c_d increases. The feature observed due to the absence of opposing flow in the upper opening, the effect of buoyancy is not strong; this leads to the flow curves to reach the maximal height easily. Maximum volumetric airflow Q_2^* is larger when $c_d = 0.75$ and minimum when $c_d = 0.60$. Therefore, the best value of discharge coefficient c_d for optimal ventilation in the domain is when $c_d = 0.75$.

Figure 4.17 depicts the effect of effective thermal coefficient θ_0 on mass transfer m_2^*. It is observed that the mass transfer m_2^* increases as effective thermal coefficient θ_0 decreases.

The feature observed is that, mass transfer m_2^* can easily remove when $\theta_0 = 0.01$. Maximum mass transfer m_2^* is larger when $\theta_0 = 0.01$ and minimum when $\theta_0 = 0.19$. Therefore, the best value of effective thermal coefficient for optimal ventilation in the domain is when $\theta_0 = 0.01$.

Figure 4.18 depicts the effect of Prandtl number Pr on mass transfer m_2^*. It is observed that the mass transfer m_2^* increases as Prandtl number Pr decreases. The feature observed is that, mass transfer m_2^* can easily remove when Prandtl number $Pr = 0.510$. Maximum mass transfer m_2^* is larger when $Pr = 0.510$ and minimum when $Pr = 0.910$. Therefore, the best value of Prandtl number Pr for optimal ventilation in the domain is when $Pr = 0.510$.

Figure 4.19 depicts the effect of discharge coefficient c_d on mass transfer m_2^*. It is observed that the mass transfer m_2^* increases as discharge coefficient c_d increases. The feature observed is that, mass transfer m_2^* can easily remove when $c_d = 0.75$. Maximum mass transfer m_2^* is larger when $c_d = 0.75$ and minimum when $c_d = 0.60$. Therefore, the best value of discharge coefficient c_d for optimal ventilation in the domain is when $c_d = 0.75$.

4.3 KEY INTERVENTIONS

This section (4.3) consists of three (3) sub- sections which intends to presents; (4.3.1) developed study model for un- stratified cross- ventilated domain with opening on vertical walls with the predictions; (4.3.2) model from previous interventions with their predictions and (4.3.3) graphical comparison between developed and previous studies.

4.3.1 Developed study model for un- stratified cross- ventilated domain with openings on vertical walls

In the developed study, considerable research efforts have been made to presents new macroscopic ventilation models for steady flow in un- stratified cross ventilated rectangular domain with openings on vertical walls.

New model are obtained in equations (3.15) - (3.17), and (3.18) - (3.19) are only limited to cross ventilated domain with an equal height of openings on vertical wall. And have advances over the previous studies reported by Santamouris *et al* (1995), and Chow, (2010). The following are the contributions of the developed study;

1. In the developed study one dimensional Navier Stokes equation was used in developing the new ventilation model as in equations (3.15) – (3.17) and with the special case (3.18) – (3.19).

   $Pr\frac{d^2U^*}{dy^{*2}} + C\frac{dU^*}{dy^*} + \dot{\theta}^* = 0,$

   $\frac{d^2\dot{\theta}^*}{dy^{*2}} + C\frac{d\dot{\theta}^*}{dy^*} = 0,$

   $Pr\frac{d^2U^*}{dy^{*2}} + \theta^*(y^*) = 0,$

   $\frac{d^2\theta^*}{dy^{*2}} = 0,$

   together with the following dimensionless boundary conditions as,

   $0 \le y^* \le 1, U^*(y^* = 0) = 0, U^*(y^* = 1) = 0, \theta^*(y^* = 0) = -\theta_0, \theta^*(y^* = 1) = 1 - \theta_0.$

2. An approximation of reduced gravity is taken into account in order to maintain the thermal buoyancy effect in the domain envelopes.

3. Parameters such as, effective thermal coefficient and dimensionless group Prandtl number were also introduced.
4. Effects of changes of these parameters were also investigated in order see the effect to the overall flow distribution, which were believed to have significant effects on natural ventilation process in buildings.
5. Temperature profiles across the openings were also investigated.

4.3.1.1 Predictions

The model obtained from equation (3.15) - (3.17) and (3.18) – (3.19) resulted into the following equations (3.23), (3.33), (3.35), (3.39) and (3.43), (3.54), (3.56), (3.58),

$$\theta_3^*(y^*) = \frac{1-\theta_0\left(1-e^{v_0 Pr}\right)-e^{v_0 Pr y^*}}{1-e^{v_0 Pr}},$$

$$U_3^*(y^*) = \frac{1}{(v_0 Pr)^2\left(1-e^{v_0 Pr}\right)(1-e^{v_0})}\left[\left(1+\frac{Pr}{1-Pr}\right)\left(e^{v_0 Pr}-e^{v_0}-e^{v_0 y^*}(e^{v_0 Pr}-1)-\right.\right.$$

$$\left.e^{v_0 Pr y^*}(1-e^{v_0})\right)+\left(1-\theta_0(1-e^{v_0 Pr})\right)\left(-v_0 Pr-Pr(1-e^{v_0})+v_0 Pr e^{v_0 y^*}+\right.$$

$$\left.\left.(1-e^{v_0})(Pr+v_0 Pr y^*)\right)\right],$$

$$Q_3^*(y^*) = \frac{A_3^* c_d}{(v0Pr)^2(1-e^{v0Pr})(1-e^{v0})}\left[\left(1+\frac{Pr}{1-Pr}\right)\left[(e^{v_0 Pr}-e^{v_0})\frac{y^*}{2}-(e^{v_0 Pr}-1)\frac{e^{v_0\frac{y^*}{2}}}{v_0}-\right.\right.$$

$$\left.(1-e^{v_0})\frac{e^{v_0 Pr\frac{y^*}{2}}}{v_0 Pr}+\frac{(e^{v_0 Pr}-1)}{v_0}+\frac{(1-e^{v_0})}{v_0 Pr}\right]+\left(1-\theta_0(1-e^{v_0 Pr})\right)\left[-Pr\left(v_0+(1-e^{v_0})\right)\frac{y^*}{2}+\right.$$

$$\left.\left.Pre^{v_0\frac{y^*}{2}}+(1-e^{v_0})\left(Pr\frac{y^*}{2}+v_0 Pr\frac{y^{*2}}{8}\right)-Pr\right]\right],$$

$$m_3^*(y^*) = \frac{A^*{}_3\rho_0 c_d}{(v0Pr)^2(1-e^{v0Pr})(1-e^{v0})}\left[\left(1+\frac{Pr}{1-Pr}\right)\left[(e^{v_0Pr}-e^{v_0})\frac{y^*}{2}-(e^{v_0Pr}-1)\frac{e^{v_0\frac{y^*}{2}}}{v_0}-\right.\right.$$

$$\left.(1-e^{v_0})\frac{e^{v_0Pr\frac{y^*}{2}}}{v_0Pr}+\frac{(e^{v_0Pr}-1)}{v_0}+\frac{(1-e^{v_0})}{v_0Pr}\right]+\left(1-\theta_0(1-e^{v_0Pr})\right)\left[-Pr\left(v_0+(1-e^{v_0})\right)\frac{y^*}{2}+\right.$$

$$\left.\left.Pre^{v_0\frac{y^*}{2}}+(1-e^{v_0})\left(Pr\frac{y^*}{2}+v_0Pr\frac{y^{*2}}{8}\right)-Pr\right]\right],$$

$$\theta_2^*(y^*) = y^* - \theta_0,$$

$$U_2^*(y^*) = \frac{1}{Pr}\left(\frac{\theta_0 y^{*2}}{2}-\frac{y^{*3}}{6}-\left(\frac{3\theta_0-1}{6}\right)y^*\right),$$

$$Q_2^*(y^*) = \frac{A_2^* c_d}{Pr}\left(\frac{\theta_0}{48}y^{*3}-\frac{1}{384}y^{*4}-\frac{(3\theta_0-1)}{48}y^{*2}\right),$$

$$m_2^*(y^*) = \frac{A_2^*\rho_0 c_d}{Pr}\left(\frac{\theta_0}{48}y^{*3}-\frac{1}{384}y^{*4}-\frac{(3\theta_0-1)}{48}y^{*2}\right).$$

4.3.2 Previous interventions

Considerable research efforts have been made in the present study on understanding the airflow process through openings in building envelopes. In the literature on airflow process, a wealth of information is available and satisfactory means have been evolved for the estimation of the velocity distributions, volumetric airflow and mass transfer in buildings. In the previous interventions Bernoulli's equations were used in developing their ventilation models as follows,

4.3.2.1: Santamouris *et al* (1995) presented a macroscopic model that describes heat and mass- transfer through an openings by natural convection in a single sided ventilated building

using Bernoulli's equation for an in viscid fluid and obtained the model equations given by equation (2.23) as,

$\Delta T g Y_N = \frac{1}{2}\bar{T} v_M^2$,

with $v_1 = v_2 = 0$ at $Y_N = 0$ and $v_2 = 0$ at $Y_N = 1, Y_N = \frac{Y_x}{2}$.

4.3.2.1.1 Prediction

The model given in (2.23) predicted the following results as in (2.24) - (2.26),

$v_M(Y_N) = \sqrt{2g\frac{\Delta T}{\bar{T}} Y_N}$,

$Q_M = \frac{1}{3} c_d W Y_x^{1.5} \sqrt{g\frac{\Delta T}{\bar{T}}}$,

$m_M = \frac{2}{3} c_d \bar{\rho}\ W Y_x^{1.5} \sqrt{g\frac{\Delta T}{\bar{T}}}$

4.3.2.2: Chow, (2010) investigated volumetric airflow across vertical opening induced by room heat sources using a macroscopic model given by (Awbi and Nemri, (1990) and Awbi, (1990)), using Bernoulli's equation as in equation (2.7),

$\Delta T g H_w = \frac{1}{2} T_O v_C^2$,

with, $v_i = v_O = 0$ at $z = 0$ and $v_O = 0$ at $z = 1, z = \frac{H_w}{2}$.

4.3.2.2.1 Predictions

The model given in (2.11) predicted the following results as in (2.8) - (2.10),

$$v_C(H_w) = \sqrt{2gH_w\frac{\Delta T}{T_O}},$$

$$Q_C = \frac{1}{3}A_w c_d\sqrt{gH_w\frac{\Delta T}{T_O}},$$

$$m_C = \frac{1}{3}c_d A_w \rho_0\sqrt{\frac{gH_w\Delta T}{T_0}}.$$

4.3.3 Comparison between developed with the available previous studies

This sub- section (4.3.3) here intends to make comparison between developed with the available previous results in the domain with openings on vertical walls. The simulations of the results are depicted in Figures 4.20- 4.23 below for volumetric airflows together with mass transfers given as in equations (3.35), (3.39), and (3.56), (3.58) and (2.9) - (2.10), and (2.25) - (2.26).

Table 4.3 shows the experimental values of parameters and operating conditions used in comparisons between developed with the available previous studies.

$y^* = 1.0$	$v_0 = -0.5$	$A_2^* = 0.3131$	$A_3^* = 0.1633$	$\rho_0 = 1.1849$
$\theta_0 = 0.01$	$c_d = 0.6$	$Pr = 0.710$	$w = 0.7$	$\Delta T = 5$
$g = 10$	$\bar{T} = 298$	$T_0 = 298$	$c_{d1} = 0.064$	

Figure 4.20 - 4.23 shows the comparison between three different studies for volumetric airflows Q_M, Q_C with Q_3^*, Q_2^* and mass transfers m_M, m_C with m_3^*, m_2^*.

In Figure 4.20, $Q_M > Q_3^* > Q_C$ and 4.22, $Q_M > Q_2^* > Q_C$, the feature observed is that the of amount of air (volumetric airflow) in the domain for Santamouris, *et al* (1995) studies is higher than that of developed and Chow, (2010) studies. The physical reason behind this is that, Santamouris, *et al* (1995) in the research considered a domain that has two openings on the same vertical wall (Single- sided ventilated domain). As the air enter through the lower opening it will spread on the floor and then mixed with air that is inside, since there is uniformity of interior temperature the air have to accumulate for some period of time before reaching the neutral height then it will flow out to the ambient.

The developed study considered cross ventilated domain with openings on vertical walls in the absence of internal heat source. It means the effect of buoyancy forces is not strong enough that is why if the air enter through lower opening, since the domain is cross ventilated it means there is direct internal path between the openings the effect of buoyancy forces attracting the flow will not allow the air to accumulate much in the room. The air can easily reach the neutral height and then flow out to the ambient.

Chow, (2010) considered airflow process in cross ventilated building induced by internal heat source in the room. Since, there is internal heat source in the room it means effect of buoyancy forces is very strong. Effect of buoyancy forces attracting the flow will not allow air to accumulate much in the room. Frequently, the amount of air can easily reach the neutral height and then flow out to the ambient.

Figure 4.21 and 4.23 $m_M > m_3^* > m_C$ and 4.22 $m_M > m_2^* > m_C$, the feature observed is the amount of air that flows out from Santamouris, *et al.* (1995) studies is much higher than that of developed and Chow studies. The physical reason behind this is that Santamouris, *et al.* (1995) considered the domain in which all the openings are on the same vertical wall (single-sided), and the effect of buoyancy forces attracting the flow is negligible. So, the amount of air accumulated in the domain (see Figure 4.20 and (4.22)) is much higher than the one considered by developed and Chow studies.

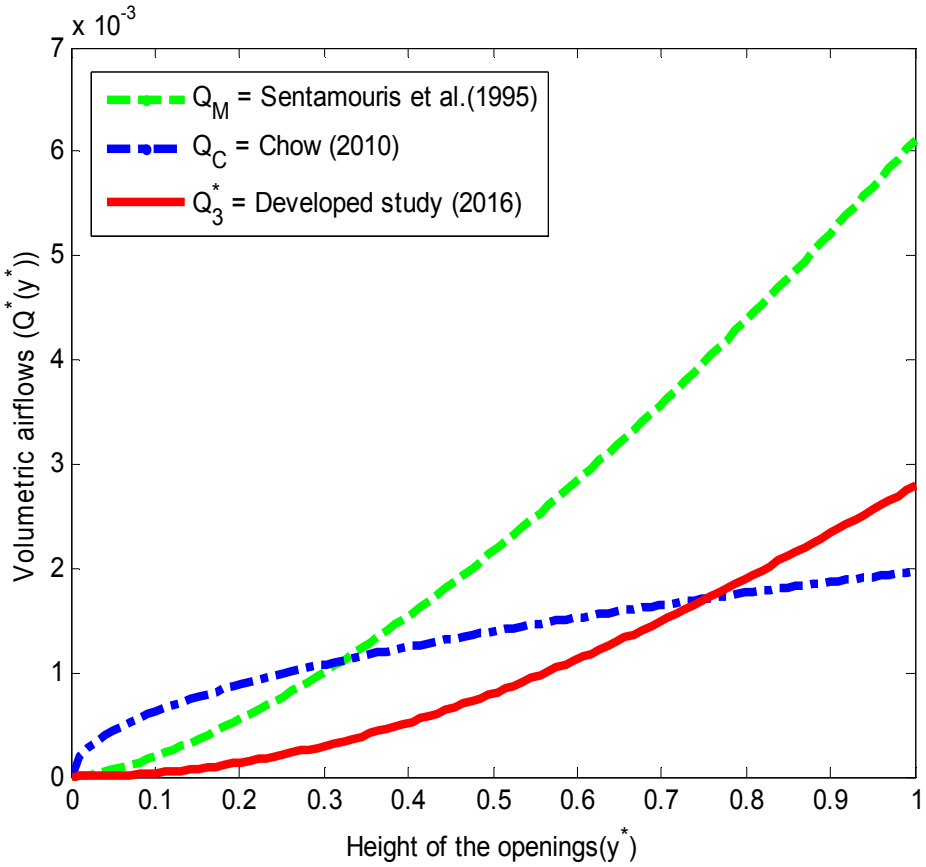

Figure 4.20: Comparison between Q_M, Q_C, with Q_3^* in rectangular domain with three openings

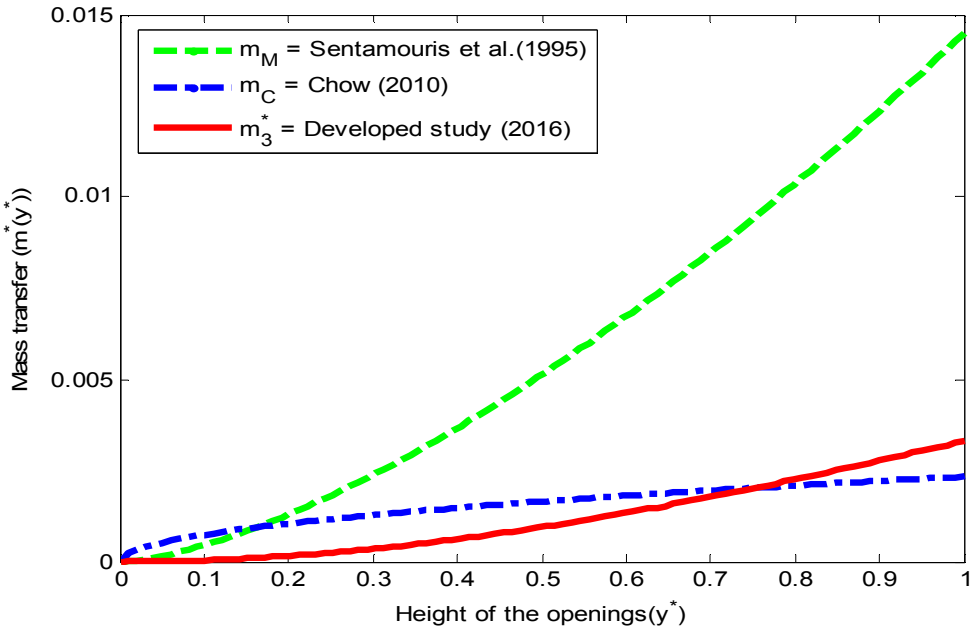

Figure 4.21: Comparison between m_M, m_C with m_3^* in rectangular domain with three openings.

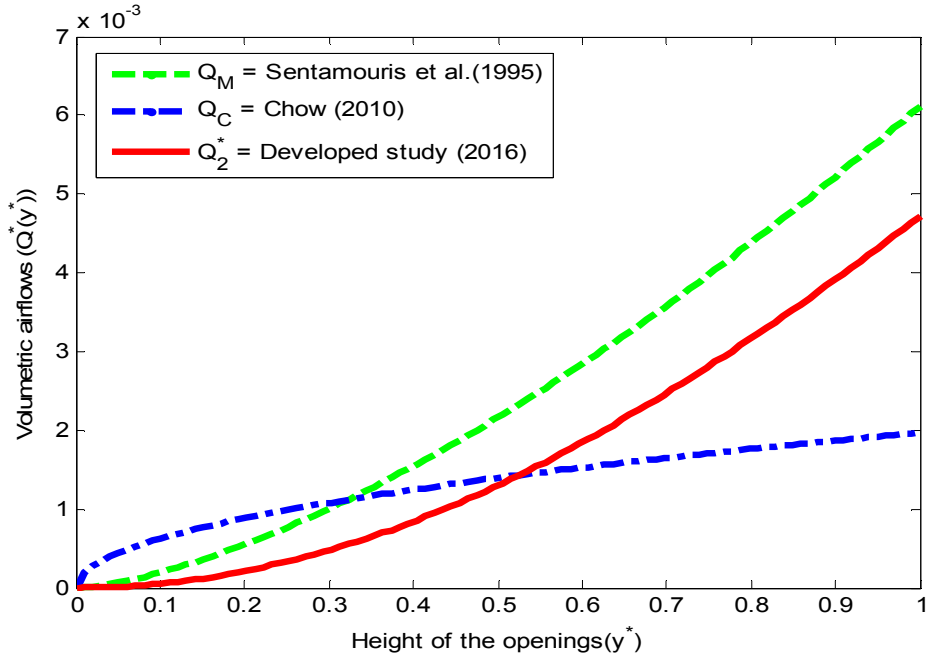

Figure 4.22: Comparison between Q_M, Q_C, with Q_2^* in rectangular domain with two openings

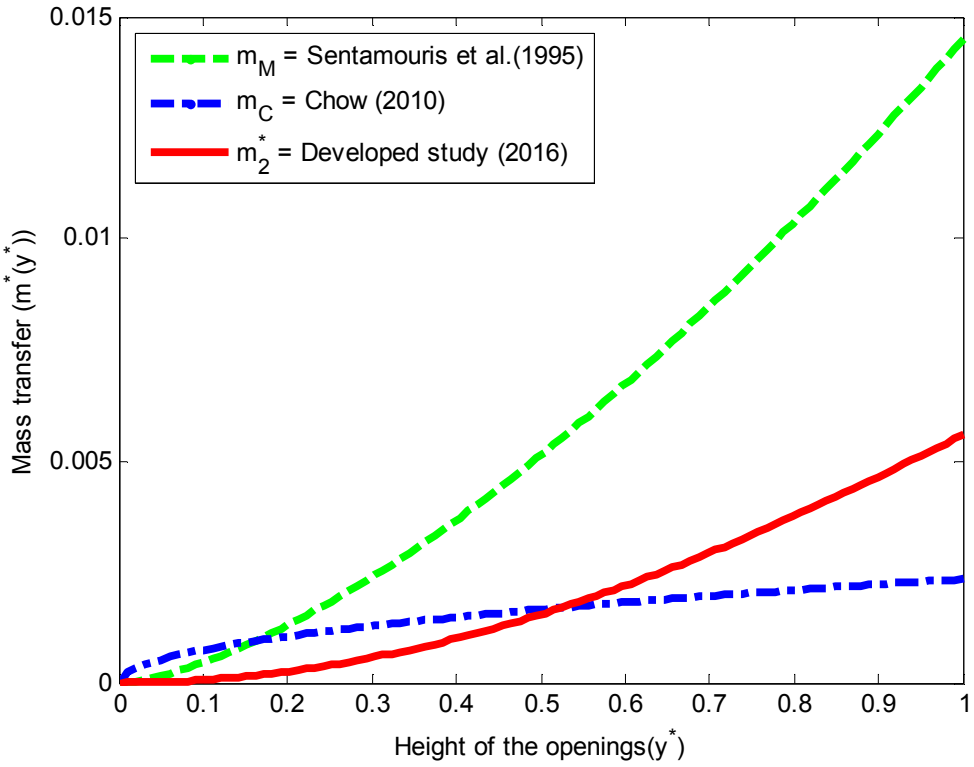

Figure 4.23: Comparison between m_M, m_C with m_2^* in rectangular domain with two opening.

CHAPTER FIVE

SUMMARY, CONCLUSION AND RECOMMENDATIONS

5.1 SUMMARY

Natural ventilation of building provides improvement of internal comfort and air quality conditions leading to a significant reduction of cooling energy consumption. Design of natural ventilation systems for many types of building is based on buoyancy forces. However, external wind flow can have significant effects on buoyancy- driven natural ventilation. In the proposed study, model of airflow process in un- stratified cross- ventilated rectangular domain with openings on vertical walls was presented. The study considered a uniform interior temperature, the assumption has enabled the simplification of the calculation of air flow process in the building. One dimensional Navier- Stokes equations was utilized to model the airflow process in the domain, in which approximation of reduced gravity was also invoked in order to maintain the effect of buoyancy forces in the domain envelope.

5.2 CONCLUSION

Considerable research efforts have been made in the developed study on understanding the airflow process through openings on vertical wall. In the literature on airflow process, a wealth of information is available and satisfactory means have been evolved for the estimation of the velocity profiles, volumetric airflow and mass transfer in domain envelopes, similar analytical procedures are available in the literature for a variety of combinations of boundary conditions, but not including the ones considered here.

In the developed study, the effect of various parameters on airflow process in un- stratified cross- ventilated rectangular domain with openings on vertical wall such as; discharge coefficient, effective thermal coefficient and Prandtl number has been studied, which were believed to have significant effects on natural ventilation process in the domain envelopes. Analytical results for the velocity, temperature profiles together with volumetric airflow and mass transfer are presented. MATLAB Codes were written to describe the asymptotic behavior of the results. Various parameters of airflow process; such as effective thermal coefficient (θ_0), Prandtl number (Pr), and discharge coefficient (c_d) were used to see the effect of changes of parameters to the overall flow distributions, and ascertain the best one for optimal natural ventilation. And comparison between developed with previous results in which, the behavior of parameters described in the domain for volumetric airflows and mass transfers have been presented graphically. Therefore, the expected aim and the set objectives for the study were achieved.

The following observations have been made from the developed study analyses as;

1- A decrease in effective thermal coefficient θ_0 results in increases in temperature profiles θ_2^* and θ_3^* across the openings. Maximum temperature θ_3^* is larger at $\theta_0 = 0.01$ and minimum at $\theta_0 = 0.19$. Temperatures profile θ_2^* and $\dot{\theta}_3^*$ are more sensitive at lower values of effective thermal coefficient θ_0. Therefore, the greater number of openings and the greater temperature difference between the inside and the outside, the stronger is the effect of the buoyancy.

2- An increase in Prandtl number Pr results in an increase in temperature profiles $\dot{\theta}_3^*$ across the openings. Maximum temperature θ_3^* is larger at $Pr = 0.910$ and minimum at $Pr = 0.510$. Therefore, the temperature profile θ_3^* is not within thermal comfort.

3- The velocity U_2^* and U_3^* increases more rapidly for lower values of effective thermal coefficient θ_0. Positive buoyancy forces dominate, so that no back flows occur in this case. Maximum velocities U_2^* and U_3^* are larger at $\theta_0 = 0.01$ and minimum at $\theta_0 = 0.19$.

4- An increase in Prandtl number Pr results in a decreases in velocity profiles U_2^* and U_3^* across the openings. Positive buoyancy forces dominate, so that no back flows occur in this case. Maximum velocity U_2^* and U_3^* is larger when $Pr = 0.510$ and minimum when $Pr = 0.910$. Therefore, velocity profiles U_2^* and U_3^*decreases more rapidly for higher values of Prandtl number Pr.

5- An increase in effective thermal coefficient θ_0 results in a decreases in volumetric airflows Q_2^* and Q_3^*. Due to the opposing flow in the upper opening, the effect of buoyancy is strong; this leads to the steady flow before it reached the maximal height in Figure 4.5. In Figure 4.14 due to the absence of opposing flow in the upper opening, the effect of buoyancy is not strong; this leads to the flow curves to reach the maximal height easily. Maximum volumetric airflow Q_2^* and Q_3^* are larger at $\theta_0 = 0.01$ and minimum at $\theta_0 = 0.19$.

6- The volumetric airflows Q_2^* and Q_3^* are more sensitive for lower values of Prandtl number Pr, in comparison with higher values of Pr. Due to the opposing flow in the upper opening, the effect of buoyancy is strong; this leads to the steady flow before it reached the maximal height in Figure 4.6. For Figure 4.15 due to the absence of opposing flow in the upper opening, the effect of buoyancy is not strong; this leads to the flow curves to reach the maximal height easily. Maximum volumetric airflow Q_2^* and Q_3^* are larger at $Pr = 0.510$ and minimum at $Pr = 0.910$.

7- The volumetric airflows Q_2^* and Q_3^* are more sensitive for higher values of discharge coefficients c_d, in comparison with lower values of c_d. Due to the opposing flow in the upper

opening, the effect of buoyancy is strong; this leads to the steady flow before it reached the maximal height in Figure 4.7. In Figure 4.16 due to the absence of opposing flow in the upper opening, the effect of buoyancy is not strong; this leads to the flow curves to reach the maximal height easily. Maximum volumetric airflow Q_2^* and Q_3^* are larger when $c_d = 0.75$ and minimum when $c_d = 0.60$.

8- An increase in effective thermal coefficient θ_0 results in a decreases in mass transfer m_2^* and m_3^*. Mass transfer m_2^* and m_3^* can easily remove from the domain at $\theta_0 = 0.01$. Maximum mass transfers for m_2^* and m_3^* are larger at $\theta_0 = 0.01$ and minimum at $\theta_0 = 0.19$. Therefore, mass transfer m_2^* and m_3^* are more sensitive for lower values of effective thermal coefficient θ_0, in comparison with higher values of θ_0.

9- An increase in Prandtl number Pr results in a decreases in mass transfer m_2^* and m_3^*. Mass transfer m_2^* and m_3^* can easily remove from the domain at $Pr = 0.710$. Maximum mass transfers for m_2^* and m_3^* are larger at $Pr = 0.710$ and minimum at $Pr = 0.910$. Therefore, mass transfer m_2^* and m_3^* are more sensitive for lower values of Pr.

10- An increase in discharge coefficient c_d results in increases in mass transfer m_2^* and m_3^*. Mass transfer m_2^* and m_3^* can easily remove from the domain at $c_d = 0.75$. Maximum mass transfers for m_2^* and m_3^* are larger at $c_d = 0.75$ and minimum at $c_d = 0.60$. Therefore, mass transfer m_2^* and m_3^* are more sensitive for higher values of c_d.

11- Orientation of the domain has a strong effect to the airflow around it.

12- Temperature distributions have a significant influence on the airflow.

13- Study gives the Architectures and designers a luxury to consider several design options in a minimum amount of time.

14- Flow is dominated by buoyancy effect, in some cases leads to the equally or uniformly distributed flow across the openings.

15- Lines of flow for velocity, temperature distributions together with volumetric airflow rate are approaching each other which show that the effect of buoyancy is minimized.

16- The position/ or location of the openings in the study give a more homogeneous temperature profiles in the domain envelopes in order to avoid overheating therefore, the temperature profiles in the domains are within comfortable conditions.

17- The mass- transfers are always higher than the volumetric airflow air in the domain.

To date there are few validated models for natural ventilation process on the basis of a theoretical approach. Our models are only valid for cross-ventilated domain with openings at the same height on vertical wall.

5.3 RECOMMENDATIONS

Based on the research conducted in this work, an issue for further research and development is pointed out below. More knowledge on this issue is essential to future practice and to the use of natural ventilation in buildings.

- The study did not factor-in the effect of pollution, noise, and room heat source, largely because of the complexity of ventilation process. Therefore, a possible extension of the study is to take cognizance of these parameters.

Lastly, we believe that our findings will help in developing a better understanding of natural ventilation process and help researchers to gain more insights into the phenomenon and therefore come up with more models.

REFERENCES

1. Andrew, A. and Gary, R. H. (2014). A simplified mathematical approach for modeling stack ventilation in multi-compartment buildings. *Building and Environment*, 71: 121- 130.

2. Angui, L., Phillip, J., Pingge, Z. and Liping, W. (2004). Heat transfer and natural ventilation of air flow rates from single sided heated solar chimney for building. *Journal of Asian Architecture and building Engineering*, 238: 233- 237.

3. Allocca, C., Qingyan, C. and Leon, R. G. (2003). Design analysis of single-sided natural ventilation. Building Technology. *Energy and Building*, 35(8): 785 - 795.

4. Awbi, H. B., and Nemri, M. M. (1990). Scale effect in room air-flow studies. *Energy and Buildings,* 14(3): 207- 210.

5. Awbi, H. B. (1996). Air movement on naturally-ventilated buildings. *Renewable Energy,* 8(1): 241- 247.

6. Britter, R. E., Hunt , J. C. R. and Mumford, J. C. (1979). The distortion of turbulence by a circular cylinder. *J. Fluid Mech.,* 92: 269- 301.

7. Brown, W. G. and Solvason, K. R. (1962a). Natural convection through rectangular opening in partition-I. *Int. J. Heat-Mass Transfer,* 5: 859- 868.

8. Brown, W. G. and Solvason, K. R. (1962b). Natural con-vection heat transfer through rectangular openings in partitions-II. *Int. J. Heat Mass Transf,* 5, 869 – 878.

9. Brown, W. G. and Solvason, K. R. (1963). Heat and moisture flow through openings by convection. *J. Am. Soc. Heat Vent. Air Cond. Eng.,* 5: 49- 54.

10. Buchanan, C. R., and Sherman, M. H. (2000). A Mathematical model for infiltration heat recovery. Energy performance of buildings group indoor environment department, environmental energy Technologies division, University of California. 1- 40.

11. Chow, C. L. (2010). Air flow rate across vertical opening induced by room heat sources. *International Journal on Architectural Science*, 8(1): 11- 16.

12. Colombari, M. and Balocco, C. (2005). Thermal behavior of interactive mechanically ventilated double glazed façade: Non- dimensional analysis. *Energy and Building,* 38: 1- 7.

13. Cooper, P. and Linden, P. F. (1995). Natural ventilation of an enclosure containing one positive and one negative source of buoyancy. Proc. 12 thAustralas. Fluid mechanics Conf.,Sydney Austrlia: 645- 648.

14. Cooper, P. and Linden, P. F. (1996). Natural ventilation of an enclosure containing two buoyancy sources. *J. Fluid mechanics,* 311: 153- 176.

15. Cui, Q. and Lihua, Z. (2010). Study on the Energy efficient potential of natural ventilation for residential building in Guangzhou. 2010 international conference on advances in energy eng, China: 312- 316.

16. Daniel, N. R. (2005). Mathematical modeling of wind forces. Department of theoretical and applied mechanics, University of Illinois at Urbana- Champaign. USA. 1 - 14.

17. Davies, G. M. J. and Linden, P. F. (1992). The effects of headwind on buoyancy- driven flow through a doorway. Proc. ROOMVENT'92, 3RD Int. Conf. Air distr. In rooms, Denmark: 419- 433.

18. Duan, S. and Yuguo, L. (2005). An example of solution multiplicity in a building with bi-directional flow openings. *Indoor Built Environment*, 14(5): 359– 69.

19. Emswiler, J. E. (1926). The neutral zone in ventilation. *Trans. Amer. Soc. Heat vents. Engrs.,* 32.

20. Fan, Y. (1995). CFD modeling of the air and contaminant distribution in rooms. *Energy and Building,* 23(1): 33- 39.

21. Fu, Y., Huang, C., Wang, X., Luo, X. and Liu, S. (2009). Study on the application of hybrid system in a large space building. 2009 international conference on energy and environment Tech., China: 365- 368.

22. Gan, G. (1995). Evaluation of room air distribution systems using CFD. *Energy and Building,* 23(2): 83- 93.

23. Gan, G. (2010). Simulation of buoyancy-driven natural ventilation of buildings-impact of computational domain. *Energy and building,* 42: 1290- 1300.

24. Gladstone, C., Woods, A., Philips, J. and Caulfied C. (1998). Experimental study of mixing in a closed room by doorway exchange flow. *Proc,* ROOMVENT'98. Stockholm, Sweden.

25. Gratia, E. and De Herde A. (2007). Greenhouse effect in double- skin façade. *Energy and Buildings,* 39: 199- 211.

26. Han, X., Yang, J., Zhang, X., Wang, X., Zhu, C. and Sui, X. (2011). Numerical study of natural ventilation in High- rise building. 2011 Third International conference on measuring Technology and mecharonics Automation, China: 732- 735.

27. Harral, B. B. and Boon, C. R. (1997). Comparison of predicted and measured airflow patterns in a mechanically ventilated livestock without animals. *J. Agric. Eng. Research,* 66(3): 221- 228.

28. Henry, S. C. and Leslie, N. K. (2009). Naturally ventilated and mixed-mode buildingsdPart I: Thermal modeling. *Building and Environment*, 44: 736– 749.

29. Hunt, G. R. and Linden, P. F. (2001). Steady-state flows in an enclosure ventilated by buoyancy forces assisted by wind. *J. Fluid Mech.,* 426: 355- 386.

30. Iain, S. W. and David, J. W. (1998). Field validation of Algebraic Equations for stack and wind-driven Air infiltration calculations. *ASHRAE HVAC & Research Journal*, 4(2): 1- 6.

31. Isabel, A. M., Helena, C. and Ricardo, D. P. (2011). Passive Systems for Buildings Using Buoyancy-Driven Airflows. *Recent Patents on Engineering,* 5: 23- 31.

32. Kays, W. M. and Crawford, M. E. (1993). Convective Heat and Mass Transfer, 3rd Ed., McGraw-Hill Int. Editions, New York (1993), 542 - 543.

33. Lee, I. B. and Short, T. (2000). Two- dimensional numerical simulation of natural ventilation in a multi- span greenhouse. *Trans. ASAE,* 43(3): 745- 753.

34. Liang, C. J. L. (2012). *Predicting wind driven cross ventilation in buildings with small openings*. (Doctoral thesis). University of Texas, USA.

35. Liddament, M. W. (1991). A review of building air flow simulation. *Tech. Note AIVC 33*. Air infiltration and ventilation centre, Coventry, UK 1991.

36. Linden, P. F., Lane- Serff, G. F. and Smeed, D. A. (1990). Emptying filling spaces: the fluid mechanics of natural ventilation. *Journal of Fluid Mechanics,* 212: 309- 335.

37. Linden, P. F. (1999). The Fluid Mechanics of Natural ventilation. *Annu. Rev. Fluid Mech.,* 31(1): 201 - 238.

38. Luo, Z., Zhao, J., Gao, J. and He, L. (2007). Estimating natural ventilation potential considering both thermal comfort and IQA issues. *Build. Environ.,* 42: 2289- 2298.

39. Mahajan, B. M. (987). Measurements of air velocity components of natural convective inter- zonal airflow. *J. Solar Energy Eng.,* 109: 276- 283.

40. Mostafa, R. and Imam, A. (2009). The effect of a vertical vent on single-sided displacement ventilation. Department of Mech. Eng. University of Mohaghegh Ardabili, Iran, 1- 10.

41. Murakami, S. and Kato, S. (1989). Numerical and experimental study on room air flow-3-D predictions using the K – ε turbulence model. *Building and Environment,* 24(1): 85-97.

42. Omar, A. S. and Mohamed, G. B. (2008). Using CFD to investigate ventilation characteristics of vaults as wind- inducing devices in building. *Applied Energy,* 85: 1126-1140.

43. Park C., Augenbroe G., Messadi T., Thitisawat N. and Sadegh M. N. (2004). Calibration of a lump simulation model for double- skin façade system. *Energy and Building,* 36: 1117- 1130.

44. Praphanpong, S., Umphisak, T. and Wirapan, S. (2009). Investigation of Buoyancy Air Flow inside Solar Chimney using CFD Technique. Department of Mech. Eng. University of Warinchumrab,Ubonratchathani Thailand. 1- 5.

45. Ramesh, S., Bala R. D. (2010). Integration of Natural Ventilation by Thermal Buoyancy in Solar Thermal Modeling for Conservation of Thermal Energy in Vernacular Buildings in India. 2010 International Conference on Environmental Engineering and Applications (ICEEA 2010). 291- 294.

46. Riffat, S. B. (1989). A study of heat and mass- transfer through a doorway in a traditional house. *ASHRAE Trans.,*: 548- 589.

47. Roberto, F. (2010). Experimental and Numerical analysis of heat transfer and airflow on an interactive building façade". *Energy and Buildings,* 42(1): 23- 28.

48. Saelens, D., Carmeliet, j. and Hens, H. (2003). Energy performance assessment of multiple skin façade. *HVAC and Research,* 9(2): 167- 186.

49. Santamouris , M., Argiriou, A., Asimakopoulos, D., Klitsikas, N. Dounis, A. (1995). Heat and Mass- transfer through large openings by natural convection. *Energy and Buildings,* 23: 1- 8.

50. Schmidt, E. (1961). Heat transfer by natural convection. International Heat Transfer Conference. University of Colorado. Published by ASME 1961.

51. Sun, H., Stowell, R. R., Keener, H. M. and Michel Jr. F. C. (2002). Two- dimensional computational fluid dynamics modeling of air velocity and Ammonia distribution in a High- Rise ™ Hog building. *2002 American Society of Agricultural Engineering (ASAE),*: 1-5.

52. Tine, S. L. (2003). The 4th international Symposium on HVAC Beijing, China, October 9- 11, 2003. 159- 163.

53. Tong, Y. (2004). CFD and Field Testing of a naturally ventilated Full-scale Building. (Doctoral thesis) University of Nottingham, UK. May 2004.

54. Vandaele, L. and Wouters, P. (1990). Models for ventilation and infiltration- an overview. *IEA Rep.,*: 230- 246.

55. Van der maas, J., Roulet, C. A. and Hertig, J. A. (1989). Some aspect of gravity driven air flow through large apertures in buildings. *ASHRAE Trans.,* 95(3): 573- 583.

56. Van der maas, J. (ed.) (1992). Airflow through large opening. *International Energy Agency*,: 319- 328.

57. Van Hooff, T. and Blocken, B. (2013). CFD evaluation of natural ventilation of indoor environments by the concentration decay method: CO_2 gas dispersion from a semi-enclosed stadium. *Building and Environment*, 61: 1- 17.

58. Wei, Y., Guoqiang, Z., Wei, Y. and Xiao, W. (2010). Natural ventilation potential model considering solution multiplicity, window opening percentage, air velocity and humidity in china. *Building and Environment*, 45: 338- 344.

59. Wilson, D. J. and Keil, D. E. (1990). Gravity-driven coun-terflow through an open door in a sealed room. *Building and Environment,* 25: 379– 388.

60. Xin, W., Chen, H. and Weiwu, C. (2009). Mathematical modeling and experimental study on vertical temperature distribution of hybrid ventilation in an atrium building. *Energy and Buildings*, (41): 907– 914.

61. Yi, J. and Qingyan, C. (2003). Buoyancy-driven single-sided natural ventilation in buildings with large openings. *International Journal of Heat and Mass transfer,* 46: 973-988.

62. Yi, J., Camille, A. and Qingyan, C. (2004). Validation of CFD Simulations for Natural Ventilation. *International Journal of Ventilation,* 2(4): 359- 370.

63. Yugou, L. (1999). Analysis Methods For Natural And Hybrid Ventilation—An IEA ECB ANNEX35 Literature Review ISHVAC, 1999, 12– 29.

64. Yugou, L. and Delsante, A. (2001). Natural ventilation induced by combined wind and thermal forces. *Building and Environment,* 36(1): 59 - 71.

65. Yunlong, L. and Alfred, M. (2003). Numerical modeling of airflow over the Ahmed Body. Air and climate group, Zurich, Switzerland: 1- 10.

66. Zollner, A., Winter, E. R. F. and Viskanta, R. (2002). Experimental studies of combined heat transfer in turbulent mixed convection fluid flow in double- skin façades. *Int. J. of Heat and mass transfer,*45: 4401- 4408.

APPENDICES

Appendix A: Basic definition of terms

A.1 Ventilation Process/ Ventilation Systems

A.1.1 Ventilation Process

People spend 90% of their time live and work in buildings. Building ventilation provides the required amount of fresh air into a building under specific weather and environmental conditions. The process includes supplying air to and removing it from enclosures, distributing and circulating the air therein, or preventing indoor contamination.

Ventilation, whether mechanical or natural, may be used for:

- Air Quality control: to control building air quality, by diluting internally-generated air contaminants with cleaner outdoor air.
- Direct Advective Cooling: to directly cool building interiors by replacing or diluting warm indoor air with cooler outdoor air when conditions are favorable.
- Indirect Night Cooling: to indirectly cool building interiors by pre-cooling thermally massive components of the building fabric or a thermal mass system with cool nighttime outdoor air.

A.1.2 Types of Ventilation

A.1.2.1 Natural Ventilation: Is the process of supplying and removing air through an indoor space by natural means. Natural ventilation also has the potential to provide good indoor air quality, thermal comfort for occupants, and can also save energy and reduced CO_2 emission.

A.1.2.1.1 Types of Natural Ventilation

I. Wind-driven ventilation: Wind – driven ventilation is the one which the flow is provided by wind.

II. Buoyancy-driven (stack) ventilation: Stack –driven ventilation is the one in which the flow is provided by temperature differences between the ambient and the interior of the building.

A.1.2.2 Mechanical Ventilation: Is the process of supplying and removing air through an indoor space by electrical equipments such as fans, air conditioners and so on.

A.1.2.3 Hybrid Ventilation: Is the type of ventilation in which the flow is caused by combined natural and mechanical ventilations.

A.2 Natural Ventilation System: Buildings can use various types of natural ventilation and their combinations, namely displacement ventilation, cross ventilation, single-sided ventilation and mixing ventilation. A greater understanding of the relationship between the driving forces and indoor environmental conditions would increase designer confidence in generating natural ventilation design solutions.

A.2.1 Single- Sided Ventilation System: Is one of the more common forms of natural ventilation and occurs when all the openings are on the same external wall. Exchange of air takes place by wind turbulence, by outward openings interacting with the local external airstream and by local stack/buoyancy effects. Buoyancy effect can also introduce air flow into the space at low level and flow out at high level of a single opening.

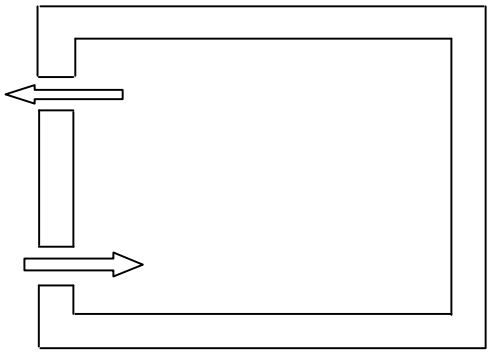

Figure A.1: Schematic Single-sided ventilation (Wind driven effect).

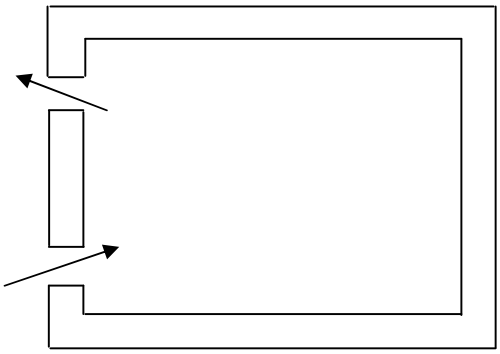

Figure A.2: Schematic Single-sided ventilation (Buoyancy- driven effect).

A.2.2 Cross-Ventilation System: cross-ventilation occurs when the inflow and outflow openings in external walls have a clear internal path between them.

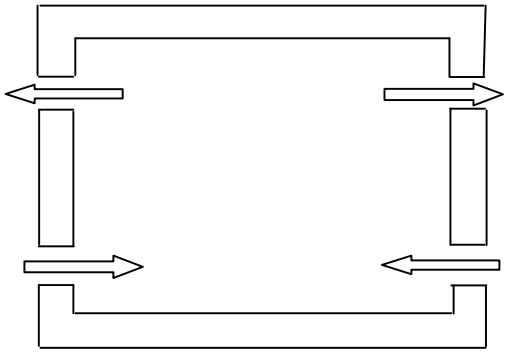

Figure A.3: Schematic of cross ventilation (Wind driven effect).

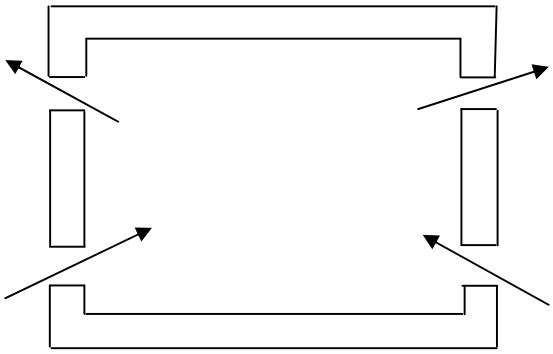

Figure A.4: Schematic of cross ventilation (Buoyancy effect).

A.2.3 Mixing Ventilation: If the air in the space is warm compared to the environment, then a single opening at the top of the space will allow exchange of warm air outwards and cool air inward. The incoming cool air will descend as a turbulent plume that will tend to mix the air within the space. This type of ventilation is known as mixing ventilation and is characterized by a relatively uniform interior temperature distribution.

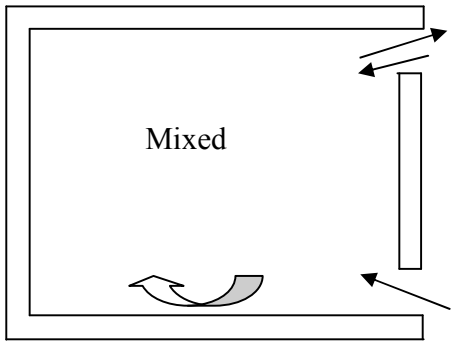

Figure A.5: Schematic of mixing ventilation.

A.2.4 Displacement Ventilation: If two vents are open, one near the top of the space and the second near the bottom of the space, warm air flow out through the upper opening and cool air enters the lower opening. A stable density interface forms between the warm, upper layer and the cooler, incoming air. This form of ventilation is known as displacement ventilation. It

is characterized, in contrast to mixing ventilation; by large temperature variations within the space.

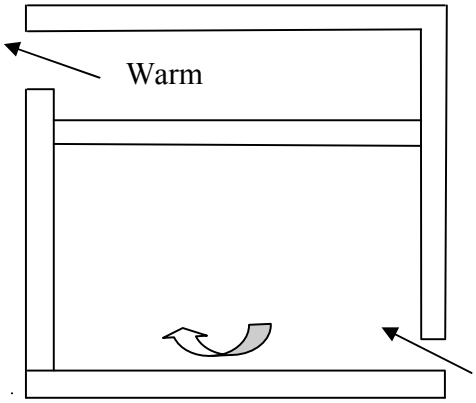

Figure A.6: Schematic of displacement ventilation.

A.3 Simple-Zone: Simple-zone building is a type of building in which a building is represented by a single one zone (without partition).

A.4 Multiple-Zones (Complex) Building: Multiple-zone building is a type of building in which a building is represented by a number of zones (with partitions). Zones are interconnected by flow paths, such as cracks, windows, doors and shafts.

A.5 Neutral Level: The neutral level is defined as the height that separates lower and upper openings: air flows out through openings above the neutral level (upper openings) and in through openings below the neutral level (lower openings).

A.6 Computational Fluid Dynamics (CFD): Computational fluid dynamics (CFD) offers detailed information about indoor flow patterns, air movement, temperature and local draught distribution in buildings, so it has unique advantages as an efficient and cost-effective tool

for optimum design in a complex built environment or CFD is the numerical analysis and simulation of fluid flow processes.

A.7 CFD Simulation: CFD simulations are used to design, investigate the operation of the different building systems and to determine the performance under various conditions.

A.8 CFD Solution: CFD solutions are the numerical approximation of the governing equations of fluid flow in space and time.

A.9 Macro and Microscopic model: Macroscopic model is Simple, usually in formula or graphical form. The model normally applied to a structure that can be described by a single, well mixed zone. The major application for this model type is on the single-family house with no internal partitions. Microscopic model is usually Predict flow field in details. The model normally applied to a structure that can be described by multi- zones buildings. The major application for this model type is on a building with internal partitions.

A.10 Absolute pressure: Absolute pressure P_0 is the point where the building air pressure is everywhere equal.

A.11 Reduced gravity: The buoyancy force is most conveniently described in terms of a reduced gravity g'which is the fractional change in density which is generated by temperature differences.

A.12 Fluid: A fluid is a substance that continually deforms (flows) under an applied shear stress. Fluids are a subset of the phases of matter and include liquids, gases, plasmas and, to some extent, plastic solids

Fluid mechanics can be divided into fluid statics, the study of fluids at rest; fluid kinematics, the study of fluids in motion; and fluid dynamics, the study of the effect of forces on fluid motion.

A.13 Compressible/Incompressible Fluid: A compressible fluid is one in which the fluid density changes when it is subjected to high pressure-gradients. And incompressible fluid is one in which the fluid density does not changes when it is subjected to high pressure-gradients. For gasses, changes in density are accompanied by changes in temperature, and this complicates considerably the analysis of compressible flow.

A.14 Boundary layer region/ in viscid region: Boundary layer region is the region where the viscous effects and the velocity changes are significant and the in viscid region is the region in which the frictional effects are negligible and the velocity remains essentially constant.

A.15 Pressure gradient: the pressure gradient (typically of air, more generally of any fluid) is a physical quantity that describes which direction and at what rate the pressure changes the most rapidly around a particular location.

A.16 Prandtl number: is a measure of relative thickness of the velocity and thermal boundary Layer

$$Pr = \frac{molecular\ diffusivity\ of\ momentum}{molecular\ diffusivity\ of\ heat} = \frac{v}{\alpha} = \frac{\mu C_p}{k}$$

A.17 Viscosity: is a measure of fluid resistance to flow, and is a strong function of temperature.

A.18 In viscid Fluid: Is an ideal fluid that has very negligible effect of viscosity.

A.19 Un- stratified Building: A building is said to be un- stratified if there is no internal partitions within the building envelope.

Appendix B: MATLAB Scripts

B.1 Effect of changes of effective thermal coefficient to temperature profiles in domain with three openings

```
shg
y=linspace(0.0,1.0,100);v0=-0.5;Pr=0.710;
bb=linspace(0.01,0.19,3);
n=length(bb);
C=[1 0 0;0 1 0;1 1 0];
for i=1:n
    theta0=bb(i);
    CC=C(i,:);
x1=v0*Pr;
x2=x1*y;
x3=exp(x1);
x4=exp(x2);
x5=(1-x3);
x6=theta0*x5;
x7=(1-x6-x4);
x8=x7/x5;
theta=x8;
plot(y,theta,'linewidth',3.0,'color',CC)
```

```
hold on
end
hold off
xlabel('Height of the openings(y^*)')
ylabel('Temperature profile (\theta^*_3(y^*))')
legend('\theta_0=0.01','\theta_0=0.10','\theta_0=0.19')
```

B.1 Effect of changes of Prandtl number to temperature profiles in domain with three openings

```
shg
y=linspace(0.0,1.0,100);v0=-0.5;theta0=0.01;
bb=linspace(0.510,0.910,3);
n=length(bb);
C=[1 0 0;0 1 0;1 1 0];
for i=1:n
    Pr=bb(i);
    CC=C(i,:);
x1=v0*Pr;
x2=x1*y;
x3=exp(x1);
x4=exp(x2);
x5=(1-x3);
x6=theta0*x5;
x7=(1-x6-x4);
x8=x7/x5;
```

```
theta=x8;
plot(y,theta,'linewidth',3.0,'color',CC)
hold on
end
hold off
xlabel('Height of the openings(y^*)')
ylabel('Temperature profile (\theta^*_3(y^*))')
legend('Pr=0.510','Pr=0.710','Pr=0.910')
```

B.3 Effect of changes of effective thermal coefficient to velocity profiles in domain with three openings

```
shg
y=linspace(0.0,1.0,100);v0=-0.5;Pr=0.710;
bb=linspace(0.01,0.19,3);
n=length(bb);
C=[1 0 0;0 1 0;1 1 0];
for i=1:n
    theta0=bb(i);
    CC=C(i,:);
x1=v0;
x2=x1*Pr;
x3=x2.^2;
x4=exp(x1);
x5=exp(x2);
x6=x2*y;
```

```
x7=x1*y;

x8=exp(x6);

x9=exp(x7);

x10=(x5-1);

x11=-x10;

x12=(1-x4);

x13=(1-Pr);

x14=Pr/x13;

x15=(1+x14);

x16=x3*x11*x12;

x17=1/x16;

x18=x9*x10;

x19=x8*x12;

x20=theta0*x11;

x21=(1-x20);

x22=Pr*x12;

x23=x2*x9;

x24=(Pr+x6);

x25=x12*x24;

x26=(x5-x4-x18-x19);

x27=x15*x26;

x28=(-x2-x22+x23+x25);

x29=x21*x28;

x30=(x27+x29);
```

```
x31=x17*x30;

U=x31;

plot(y,U,'linewidth',3.0,'color',CC)

hold on

end

hold off

xlabel('Height of the openings(y^*)')

ylabel('Velocity profile (U^*_3(y^*))')

legend('\theta_0=0.01','\theta_0=0.10','\theta_0=0.19')
```

B.4 Effect of changes of Prandtl number to velocity profiles in domain with three openings

```
shg

y=linspace(0.0,1.0,100);v0=-0.5;theta0=0.01;

bb=linspace(0.510,0.910,3);

n=length(bb);

C=[1 0 0;0 1 0;1 1 0];

for i=1:n

    Pr=bb(i);

    CC=C(i,:);

x1=v0;

x2=x1*Pr;

x3=x2.^2;

x4=exp(x1);

x5=exp(x2);
```

```
x6=x2*y;

x7=x1*y;

x8=exp(x6);

x9=exp(x7);

x10=(x5-1);

x11=-x10;

x12=(1-x4);

x13=(1-Pr);

x14=Pr/x13;

x15=(1+x14);

x16=x3*x11*x12;

x17=1/x16;

x18=x9*x10;

x19=x8*x12;

x20=theta0*x11;

x21=(1-x20);

x22=Pr*x12;

x23=x2*x9;

x24=(Pr+x6);

x25=x12*x24;

x26=(x5-x4-x18-x19);

x27=x15*x26;

x28=(-x2-x22+x23+x25);

x29=x21*x28;
```

```
x30=(x27+x29);

x31=x17*x30;

U=x31;

plot(y,U,'linewidth',3.0,'color',CC)

hold on

end

hold off

xlabel('Height of the openings(y^*)')

ylabel('Velocity profile (U^*_3(y^*))')

legend('Pr=0.510','Pr=0.710','Pr=0.910')
```

B.5 Effect of changes of effective thermal coefficient to volumetric airflow in domain with three openings

```
shg

y=linspace(0.0,1.0,100);v0=-0.5;Pr=0.710;A=0.1633;cd=0.6;

bb=linspace(0.01,0.19,3);

n=length(bb);

C=[1 0 0;0 1 0;1 1 0];

for i=1:n

    theta0=bb(i);

    CC=C(i,:);

x1=v0;

x2=x1*Pr;

x3=x2.^2;

x4=exp(x1);
```

```
x5=exp(x2);

x6=y/2;

x7=x2*x6;

x8=x1*x6;

x9=exp(x7);

x10=exp(x8);

x11=(1-x5);

x12=-x11;

x13=(1-x4);

x14=A*cd;

x15=(1-Pr);

x16=Pr/x15;

x17=(x5-x4);

x18=(1+x16);

x19=x12/x1;

x20=x13/x2;

x21=theta0*x11;

x22=(1-x21);

x23=(x1+x13);

x24=Pr*x10;

x25=Pr*x6;

x26=y.^2;

x27=x26/8;

x28=x3*x11*x13;
```

```
x29=x14/x28;

x30=x17*x6;

x31=x19*x10;

x32=x20*x9;

x33=x23*x6;

x34=Pr*x33;

x35=x2*x27;

x36=(x25+x35);

x37=x13*x36;

x38=(x30-x31-x32+x19+x20);

x39=x18*x38;

x40=(-x34+x24+x37-Pr);

x41=x22*x40;

x42=(x39+x41);

x43=x29*x42;

Q=x43;

plot(y,Q,'linewidth',3.0,'color',CC)

hold on

end

hold off

xlabel('Height of the openings(y^*)')

ylabel('Volumetric airflow (Q^*_3(y^*))')

legend('\theta_0=0.01','\theta_0=0.10','\theta_0=0.19')
```

B.6 Effect of changes of Prandtl number to volumetric airflow in domain with three openings

```
shg
y=linspace(0.0,1.0,100);v0=-0.5;theta0=0.01;A=0.1633;cd=0.6;
bb=linspace(0.510,0.910,3);
n=length(bb);
C=[1 0 0;0 1 0;1 1 0];
for i=1:n
    Pr=bb(i);
    CC=C(i,:);
x1=v0;
x2=x1*Pr;
x3=x2.^2;
x4=exp(x1);
x5=exp(x2);
x6=y/2;
x7=x2*x6;
x8=x1*x6;
x9=exp(x7);
x10=exp(x8);
x11=(1-x5);
x12=-x11;
x13=(1-x4);
x14=A*cd;
```

```
x15=(1-Pr);

x16=Pr/x15;

x17=(x5-x4);

x18=(1+x16);

x19=x12/x1;

x20=x13/x2;

x21=theta0*x11;

x22=(1-x21);

x23=(x1+x13);

x24=Pr*x10;

x25=Pr*x6;

x26=y.^2;

x27=x26/8;

x28=x3*x11*x13;

x29=x14/x28;

x30=x17*x6;

x31=x19*x10;

x32=x20*x9;

x33=x23*x6;

x34=Pr*x33;

x35=x2*x27;

x36=(x25+x35);

x37=x13*x36;

x38=(x30-x31-x32+x19+x20);
```

```
x39=x18*x38;

x40=(-x34+x24+x37-Pr);

x41=x22*x40;

x42=(x39+x41);

x43=x29*x42;

Q=x43;

plot(y,Q,'linewidth',3.0,'color',CC)

hold on

end

hold off

xlabel('Height of the openings(y^*)')

ylabel('Volumetric airflow (Q^*_3(y^*))')

legend('Pr=0.510','Pr=0.710','Pr=0.910')
```

B.7 Effect of changes of discharge coefficient to volumetric airflow in domain with three openings

```
shg

y=linspace(0.0,1.0,100);v0=-0.5;Pr=0.710;A=0.1633;theta0=0.01;

bb=linspace(0.6,0.75,3);

n=length(bb);

C=[1 0 0;0 1 0;1 1 0];

for i=1:n

    cd=bb(i);

    CC=C(i,:);
```

```
x1=v0;

x2=x1*Pr;

x3=x2.^2;

x4=exp(x1);

x5=exp(x2);

x6=y/2;

x7=x2*x6;

x8=x1*x6;

x9=exp(x7);

x10=exp(x8);

x11=(1-x5);

x12=-x11;

x13=(1-x4);

x14=A*cd;

x15=(1-Pr);

x16=Pr/x15;

x17=(x5-x4);

x18=(1+x16);

x19=x12/x1;

x20=x13/x2;

x21=theta0*x11;

x22=(1-x21);

x23=(x1+x13);

x24=Pr*x10;
```

```
x25=Pr*x6;

x26=y.^2;

x27=x26/8;

x28=x3*x11*x13;

x29=x14/x28;

x30=x17*x6;

x31=x19*x10;

x32=x20*x9;

x33=x23*x6;

x34=Pr*x33;

x35=x2*x27;

x36=(x25+x35);

x37=x13*x36;

x38=(x30-x31-x32+x19+x20);

x39=x18*x38;

x40=(-x34+x24+x37-Pr);

x41=x22*x40;

x42=(x39+x41);

x43=x29*x42;

Q=x43;

plot(y,Q,'linewidth',3.0,'color',CC)

hold on

end

hold off
```

```
xlabel('Height of the openings(y^*)')

ylabel('Volumetric airflow (Q^*_3(y^*))')

legend('c_d=0.600','c_d=0.675','c_d=0.750')
```

B.8 Effect of changes of effective thermal coefficient to mass transfer in domain with three openings

```
shg

y=linspace(0.0,1.0,100);v0=-

0.5;Pr=0.710;A=0.1633;cd=0.6;ro=1.1849;

bb=linspace(0.01,0.19,3);

n=length(bb);

C=[1 0 0;0 1 0;1 1 0];

for i=1:n

    t0=bb(i);

    CC=C(i,:);

x1=v0;

x2=x1*Pr;

x3=x2.^2;

x4=exp(x1);

x5=exp(x2);

x6=y/2;

x7=x2*x6;

x8=x1*x6;

x9=exp(x7);

x10=exp(x8);
```

```
x11=(1-x5);

x12=-x11;

x13=(1-x4);

x14=A*cd*ro;

x15=(1-Pr);

x16=Pr/x15;

x17=(x5-x4);

x18=(1+x16);

x19=x12/x1;

x20=x13/x2;

x21=theta0*x11;

x22=(1-x21);

x23=(x1+x13);

x24=Pr*x10;

x25=Pr*x6;

x26=y.^2;

x27=x26/8;

x28=x3*x11*x13;

x29=x14/x28;

x30=x17*x6;

x31=x19*x10;

x32=x20*x9;

x33=x23*x6;

x34=Pr*x33;
```

```
x35=x2*x27;

x36=(x25+x35);

x37=x13*x36;

x38=(x30-x31-x32+x19+x20);

x39=x18*x38;

x40=(-x34+x24+x37-Pr);

x41=x22*x40;

x42=(x39+x41);

x43=x29*x42;

m=x43;

plot(y,m,'linewidth',3.0,'color',CC)

hold on

end

hold off

xlabel('Height of the openings(y^*)')

ylabel('Mass- transfer (m^*_3(y^*))')

legend('\theta_0=0.01','\theta_0=0.10','\theta_0=0.19')
```

B.9 Effect of changes of Prandtl number to mass transfer in domain with three openings

```
shg

y=linspace(0.0,1.0,100);v0=-

0.5;theta0=0.01;A=0.1633;cd=0.6;ro=1.1849;

bb=linspace(0.510,0.910,3);

n=length(bb);
```

```
C=[1 0 0;0 1 0;1 1 0];
for i=1:n
    Pr=bb(i);
    CC=C(i,:);
x1=v0;
x2=x1*Pr;
x3=x2.^2;
x4=exp(x1);
x5=exp(x2);
x6=y/2;
x7=x2*x6;
x8=x1*x6;
x9=exp(x7);
x10=exp(x8);
x11=(1-x5);
x12=-x11;
x13=(1-x4);
x14=A*cd*ro;
x15=(1-Pr);
x16=Pr/x15;
x17=(x5-x4);
x18=(1+x16);
x19=x12/x1;
x20=x13/x2;
```

```
x21=theta0*x11;

x22=(1-x21);

x23=(x1+x13);

x24=Pr*x10;

x25=Pr*x6;

x26=y.^2;

x27=x26/8;

x28=x3*x11*x13;

x29=x14/x28;

x30=x17*x6;

x31=x19*x10;

x32=x20*x9;

x33=x23*x6;

x34=Pr*x33;

x35=x2*x27;

x36=(x25+x35);

x37=x13*x36;

x38=(x30-x31-x32+x19+x20);

x39=x18*x38;

x40=(-x34+x24+x37-Pr);

x41=x22*x40;

x42=(x39+x41);

x43=x29*x42;

m=x43;
```

```
plot(y,m,'linewidth',3.0,'color',CC)
hold on
end
hold off
xlabel('Height of the openings(y^*)')
ylabel('Mass- transfer (m^*_3(y^*))')
legend('Pr=0.510','Pr=0.710','Pr=0.910')
```

B.10 Effect of changes of discharge coefficient to mass transfer in domain with three openings

```
shg
y=linspace(0.0,1.0,100);v0=-
0.5;Pr=0.710;A=0.1633;theta0=0.01;ro=1.1849;
bb=linspace(0.6,0.75,3);
n=length(bb);
C=[1 0 0;0 1 0;1 1 0];
for i=1:n
    cd=bb(i);
    CC=C(i,:);
x1=v0;
x2=x1*Pr;
x3=x2.^2;
x4=exp(x1);
x5=exp(x2);
x6=y/2;
```

```
x7=x2*x6;

x8=x1*x6;

x9=exp(x7);

x10=exp(x8);

x11=(1-x5);

x12=-x11;

x13=(1-x4);

x14=A*cd*ro;

x15=(1-Pr);

x16=Pr/x15;

x17=(x5-x4);

x18=(1+x16);

x19=x12/x1;

x20=x13/x2;

x21=theta0*x11;

x22=(1-x21);

x23=(x1+x13);

x24=Pr*x10;

x25=Pr*x6;

x26=y.^2;

x27=x26/8;

x28=x3*x11*x13;

x29=x14/x28;

x30=x17*x6;
```

```
x31=x19*x10;

x32=x20*x9;

x33=x23*x6;

x34=Pr*x33;

x35=x2*x27;

x36=(x25+x35);

x37=x13*x36;

x38=(x30-x31-x32+x19+x20);

x39=x18*x38;

x40=(-x34+x24+x37-Pr);

x41=x22*x40;

x42=(x39+x41);

x43=x29*x42;

m=x43;

plot(y,m,'linewidth',3.0,'color',CC)

hold on

end

hold off

xlabel('Height of the openings(y^*)')

ylabel('Mass- transfer (m^*_3(y^*))')

legend('c_d=0.600','c_d=0.675','c_d=0.750')
```

B.11 Effect of changes of effective thermal coefficient to temperature profiles in domain with two openings

```
shg
y=linspace(0.0,1.0,100);
bb=linspace(0.01,0.19,3);
n=length(bb);
C=[1 0 0;0 1 0;1 1 0];
for i=1:n
    theta0=bb(i);
    CC=C(i,:);
x1=theta0;
x2=(y-x1);
theta=x2;
plot(y,theta,'linewidth',3.0,'color',CC)
hold on
end
hold off
xlabel('Height of the openings(y^*)')
ylabel('Temperature profile (\theta^*_2(y^*))')
legend('\theta_0=0.01','\theta_0=0.10','\theta_0=0.19')
```

B.12 Effect of changes of effective thermal coefficient to velocity profiles in domain with two openings

```
shg
y=linspace(0.0,1.0,100);Pr=0.710;
bb=linspace(0.01,0.19,3);
n=length(bb);
C=[1 0 0;0 1 0;1 1 0];
for i=1:n
    theta0=bb(i);
    CC=C(i,:);
x1=Pr;
x2=1/x1;
x3=y.^2;
x4=y.^3;
x5=theta0/2;
x6=x5*x3;
x7=x4/6;
x8=3*theta0;
x9=(x8-1);
x10=x9/6;
x11=x10*y;
x12=(x6-x7-x11);
x13=x2*x12;
U=x13;
```

```
plot(y,U,'linewidth',3.0,'color',CC)
hold on
end
hold off
xlabel('Height of the openings(y^*)')
ylabel('Velocity profile (U^*_2(y^*))')
legend('\theta_0=0.01','\theta_0=0.10','\theta_0=0.19')
```

B.13 Effect of changes of Prandtl number to velocity profiles in domain with two openings

```
shg
y=linspace(0.0,1.0,100);theta0=0.01;
bb=linspace(0.510,0.910,3);
n=length(bb);
C=[1 0 0;0 1 0;1 1 0];
for i=1:n
    Pr=bb(i);
    CC=C(i,:);
x1=Pr;
x2=1/x1;
x3=y.^2;
x4=y.^3;
x5=theta0/2;
x6=x5*x3;
x7=x4/6;
```

```
x8=3*theta0;

x9=(x8-1);

x10=x9/6;

x11=x10*y;

x12=(x6-x7-x11);

x13=x2*x12;

U=x13;

plot(y,U,'linewidth',3.0,'color',CC)

hold on

end

hold off

xlabel('Height of the openings(y^*)')

ylabel('Velocity profile (U^*_2(y^*))')

legend('Pr=0.510','Pr=0.710','Pr=0.910')
```

B.14 Effect of changes of effective thermal coefficient to volumetric airflow in domain with two openings

```
shg

y=linspace(0.0,1.0,100);Pr=0.710;A=0.3131;cd=0.6;

bb=linspace(0.01,0.19,3);

n=length(bb);

C=[1 0 0;0 1 0;1 1 0];

for i=1:n

    theta0=bb(i);

    CC=C(i,:);
```

```
x1=Pr;

x2=A*cd;

x3=x2/x1;

x4=y.^3;

x5=y.^4;

x6=y.^2;

x7=theta0/48;

x8=x7*x4;

x9=1/384;

x10=x9*x5;

x11=3*theta0;

x12=(x11-1);

x13=x12/48;

x14=x13*x6;

x15=(x8-x10-x14);

x16=x3*x15;

Q=x16;

plot(y,Q,'linewidth',3.0,'color',CC)

hold on

end

hold off

xlabel('Height of the openings(y^*)')

ylabel('Volumetric airflow (Q^*_2(y^*))')

legend('\theta_0=0.01','\theta_0=0.10','\theta_0=0.19')
```

B. 15 Effect of changes of Prandtl number to volumetric airflow in domain with two openings

```
shg
y=linspace(0.0,1.0,100);theta0=0.01;A=0.3131;cd=0.6;
bb=linspace(0.510,0.910,3);
n=length(bb);
C=[1 0 0;0 1 0;1 1 0];
for i=1:n
    Pr=bb(i);
    CC=C(i,:);
x1=Pr;
x2=A*cd;
x3=x2/x1;
x4=y.^3;
x5=y.^4;
x6=y.^2;
x7=theta0/48;
x8=x7*x4;
x9=1/384;
x10=x9*x5;
x11=3*theta0;
x12=(x11-1);
x13=x12/48;
x14=x13*x6;
```

```
x15=(x8-x10-x14);

x16=x3*x15;

Q=x16;

plot(y,Q,'linewidth',3.0,'color',CC)

hold on

end

hold off

xlabel('Height of the openings(y^*)')

ylabel('Volumetric airflow (Q^*_2(y^*))')

legend('Pr=0.510','Pr=0.710','Pr=0.910')
```

B.16 Effect of changes of discharge coefficient to volumetric airflow in domain with three openings

```
shg

y=linspace(0.0,1.0,100);Pr=0.710;A=0.3131;theta0=0.01;

bb=linspace(0.6,0.75,3);

n=length(bb);

C=[1 0 0;0 1 0;1 1 0];

for i=1:n

    cd=bb(i);

    CC=C(i,:);

x1=Pr;

x2=A*cd;

x3=x2/x1;

x4=y.^3;
```

```
x5=y.^4;

x6=y.^2;

x7=theta0/48;

x8=x7*x4;

x9=1/384;

x10=x9*x5;

x11=3*theta0;

x12=(x11-1);

x13=x12/48;

x14=x13*x6;

x15=(x8-x10-x14);

x16=x3*x15;

Q=x16;

plot(y,Q,'linewidth',3.0,'color',CC)

hold on

end

hold off

xlabel('Height of the openings(y^*)')

ylabel('Volumetric airflow (Q^*_2(y^*))')

legend('c_d=0.600','c_d=0.675','c_d=0.750')
```

B.17 Effect of changes of effective thermal coefficient to mass transfer in domain with two openings

```
shg
y=linspace(0.0,1.0,100);Pr=0.710;A=0.3131;cd=0.6;ro=1.1849;
bb=linspace(0.01,0.19,3);
n=length(bb);
C=[1 0 0;0 1 0;1 1 0];
for i=1:n
    theta0=bb(i);
    CC=C(i,:);
x1=Pr;
x2=A*cd*ro;
x3=x2/x1;
x4=y.^3;
x5=y.^4;
x6=y.^2;
x7=theta0/48;
x8=x7*x4;
x9=1/384;
x10=x9*x5;
x11=3*theta0;
x12=(x11-1);
x13=x12/48;
x14=x13*x6;
```

```
x15=(x8-x10-x14);

x16=x3*x15;

m=x16;

plot(y,m,'linewidth',3.0,'color',CC)

hold on

end

hold off

xlabel('Height of the openings(y^*)')

ylabel('Mass- transfer (m^*_2(y^*))')

legend('\theta_0=0.01','\theta_0=0.10','\theta_0=0.19')
```

B.18 Effect of changes of Prandtl number to mass transfer in domain with three openings

```
shg

y=linspace(0.0,1.0,100);theta0=0.01;A=0.3131;cd=0.6;ro=1.1849;

bb=linspace(0.510,0.910,3);

n=length(bb);

C=[1 0 0;0 1 0;1 1 0];

for i=1:n

    Pr=bb(i);

    CC=C(i,:);

x1=Pr;

x2=A*cd*ro;

x3=x2/x1;

x4=y.^3;
```

```
x5=y.^4;

x6=y.^2;

x7=theta0/48;

x8=x7*x4;

x9=1/384;

x10=x9*x5;

x11=3*theta0;

x12=(x11-1);

x13=x12/48;

x14=x13*x6;

x15=(x8-x10-x14);

x16=x3*x15;

m=x16;

plot(y,m,'linewidth',3.0,'color',CC)

hold on

end

hold off

xlabel('Height of the openings(y^*)')

ylabel('Mass- transfer (m^*_2(y^*))')

legend('Pr=0.510','Pr=0.710','Pr=0.910')
```

B.19 Effect of changes of discharge coefficient to mass transfer in domain with two openings

```
shg
y=linspace(0.0,1.0,100);Pr=0.710;A=0.3131;theta0=0.01;ro=1.184
9;
bb=linspace(0.6,0.75,3);
n=length(bb);
C=[1 0 0;0 1 0;1 1 0];
for i=1:n
    cd=bb(i);
    CC=C(i,:);
x1=Pr;
x2=A*cd*ro;
x3=x2/x1;
x4=y.^3;
x5=y.^4;
x6=y.^2;
x7=theta0/48;
x8=x7*x4;
x9=1/384;
x10=x9*x5;
x11=3*theta0;
x12=(x11-1);
x13=x12/48;
```

```
x14=x13*x6;

x15=(x8-x10-x14);

x16=x3*x15;

m=x16;

plot(y,m,'linewidth',3.0,'color',CC)

hold on

end

hold off

xlabel('Height of the openings(y^*)')

ylabel('Mass- transfer (m^*_2(y^*))')

legend('c_d=0.600','c_d=0.675','c_d=0.750')
```

B.20 Comparison of developed with previous studies for volumetric airflow in domain with three openings

```
shg

y=linspace(0,1,100);w=0.7;DT=5;g=10;T̄=298;cd=0.6;cd1=0.064;A3=

0.1633;T0=293;Pr=0.710;theta0=0.01;v0=-0.5;

C=[1 0 0;0 1 0;];

x1=1/3;

x2=x1*w*cd1;

x3=y.^(1.5);

x4=x2*x3;

x5=DT;

x6=x5/T̄;

x7=g*x6;
```

```
x8=sqrt(x7);

x9=x4*x8;

QM=x9;

x1=1/3;

x2=A3*cd1*x1;

x3=g*y;

x4=DT;

x5=x4/T0;

x6=x3*x5;

x7=sqrt(x6);

x8=x2*x7;

QC=x8;

x1=v0;

x2=x1*Pr;

x3=x2.^2;

x4=exp(x1);

x5=exp(x2);

x6=y/2;

x7=x2*x6;

x8=x1*x6;

x9=exp(x7);

x10=exp(x8);

x11=(1-x5);

x12=-x11;
```

```
x13=(1-x4);

x14=A3*cd;

x15=(1-Pr);

x16=Pr/x15;

x17=(x5-x4);

x18=(1+x16);

x19=x12/x1;

x20=x13/x2;

x21=theta0*x11;

x22=(1-x21);

x23=(x1+x13);

x24=Pr*x10;

x25=Pr*x6;

x26=y.^2;

x27=x26/8;

x28=x3*x11*x13;

x29=x14/x28;

x30=x17*x6;

x31=x19*x10;

x32=x20*x9;

x33=x23*x6;

x34=Pr*x33;

x35=x2*x27;

x36=(x25+x35);
```

```
x37=x13*x36;

x38=(x30-x31-x32+x19+x20);

x39=x18*x38;

x40=(-x34+x24+x37-Pr);

x41=x22*x40;

x42=(x39+x41);

x43=x29*x42;

Q3=x43;

plot(y,QM,'g',y,QC,'b',y,Q3,'r','linewidth',3)

hold on

xlabel('Height of the openings(y^*)')

ylabel('Volumetric airflows (Q^*(y^*))')

legend('Q_M = Sentamouris et al.(1995)','Q_C = Chow

(2010)','Q_3^* = Developed study (2016)' )
```

B.21 Comparison of developed with previous studies for mass transfer in domain with three openings

```
shg

y=linspace(0,1,100);w=0.7;DT=5;g=10;T̄=298;cd=0.6; cd1=0.064;

A3=0.1633;T0=293;Pr=0.710;theta0=0.01;ro=1.1849;v0=-0.5;

C=[1 0 0;0 1 0;];

x1=2/3;

x2=x1*w*cd1*ro;

x3=y.^(1.5);

x4=x2*x3;
```

```
x5=DT;

x6=x5/T̄;

x7=g*x6;

x8=sqrt(x7);

x9=x4*x8;

mM=x9;

x1=1/3;

x2=A3*cd1*x1*ro;

x3=g*y;

x4=DT;

x5=x4/T0;

x6=x3*x5;

x7=sqrt(x6);

x8=x2*x7;

mC=x8;

x1=v0;

x2=x1*Pr;

x3=x2.^2;

x4=exp(x1);

x5=exp(x2);

x6=y/2;

x7=x2*x6;

x8=x1*x6;

x9=exp(x7);
```

```
x10=exp(x8);

x11=(1-x5);

x12=-x11;

x13=(1-x4);

x14=A3*cd*ro;

x15=(1-Pr);

x16=Pr/x15;

x17=(x5-x4);

x18=(1+x16);

x19=x12/x1;

x20=x13/x2;

x21=theta0*x11;

x22=(1-x21);

x23=(x1+x13);

x24=Pr*x10;

x25=Pr*x6;

x26=y.^2;

x27=x26/8;

x28=x3*x11*x13;

x29=x14/x28;

x30=x17*x6;

x31=x19*x10;

x32=x20*x9;

x33=x23*x6;
```

```
x34=Pr*x33;

x35=x2*x27;

x36=(x25+x35);

x37=x13*x36;

x38=(x30-x31-x32+x19+x20);

x39=x18*x38;

x40=(-x34+x24+x37-Pr);

x41=x22*x40;

x42=(x39+x41);

x43=x29*x42;

m3=x43;

plot(y,mM,'g',y,mC,'b',y,m3,'r','linewidth',3)

hold on

xlabel('Height of the openings(y^*)')

ylabel('Mass transfer (m^*(y^*))')

legend('m_M = Sentamouris et al.(1995)','m_C = Chow'

(2010),'m_3^* = Developed study (2016)' )
```

B.22 Comparison of developed with previous studies for volumetric airflow in domain with two openings

```
shg

y=linspace(0,1,100);w=0.7;DT=5;g=10;T̄=298;cd=0.6; cd1=0.064;

A2=0.3131;T0=293;Pr=0.710;theta0=0.01;

C=[1 0 0;0 1 0;];

x1=1/3;
```

```
x2=x1*w*cd1;

x3=y.^(1.5);

x4=x2*x3;

x5=DT;

x6=x5/T̄;

x7=g*x6;

x8=sqrt(x7);

x9=x4*x8;

QM=x9;

x1=1/3;

x2=A2*cd1*x1;

x3=g*y;

x4=DT;

x5=x4/T0;

x6=x3*x5;

x7=sqrt(x6);

x8=x2*x7;

QC=x8;

x1=Pr;

x2=A2*cd;

x3=x2/x1;

x4=y.^3;

x5=y.^4;

x6=y.^2;
```

```
x7=theta0/48;

x8=x7*x4;

x9=1/384;

x10=x9*x5;

x11=3*theta0;

x12=(x11-1);

x13=x12/48;

x14=x13*x6;

x15=(x8-x10-x14);

x16=x3*x15;

Q2=x16;

plot(y,QM,'g',y,QC,'b',y,Q2,'r','linewidth',3)

hold on

xlabel('Height of the openings(y^*)')

ylabel('Volumetric airflows (Q^*(y^*))')

legend('Q_M = Sentamouris et al.(1995)','Q_C = Chow

(2010)','Q_2^* = Developed study (2016)' )
```

B.23 Comparison of developed with previous studies for mass transfer in domain with two openings

```
shg

y=linspace(0,1,100);w=0.7;DT=5;g=10;T̄=298;cd=0.6; cd1=0.064;

A2=0.3131;T0=293;Pr=0.710;theta0=0.01;ro=1.1849;

C=[1 0 0;0 1 0;];

x1=2/3;
```

```
x2=x1*w*cd1*ro;

x3=y.^(1.5);

x4=x2*x3;

x5=DT;

x6=x5/T̄;

x7=g*x6;

x8=sqrt(x7);

x9=x4*x8;

mM=x9;

x1=1/3;

x2=A2*cd1*x1*ro;

x3=g*y;

x4=DT;

x5=x4/T0;

x6=x3*x5;

x7=sqrt(x6);

x8=x2*x7;

mC=x8;

x1=Pr;

x2=A2*cd*ro;

x3=x2/x1;

x4=y.^3;

x5=y.^4;

x6=y.^2;
```

```
x7=theta0/48;

x8=x7*x4;

x9=1/384;

x10=x9*x5;

x11=3*theta0;

x12=(x11-1);

x13=x12/48;

x14=x13*x6;

x15=(x8-x10-x14);

x16=x3*x15;

m2=x16;

plot(y,mM,'g',y,mC,'b',y,m2,'r','linewidth',3)

hold on

xlabel('Height of the openings(y^*)')

ylabel('Mass transfer (m^*(y^*))')

legend('m_M = Sentamouris et al.(1995)','m_C = Chow

(2010)','m_2^* = Developed study (2016)' )
```